MONITORING DEPTH OF ANESTHESIA THROUGH MEASUREMENT OF PHASE COUPLING AMONG SPONTANEOUS EEG RHYTHMS

by

SEYED MORTAZA MOUSAVI

MS, in Anesthesia, Shiraz University, Iran, 1990

Submitted to the Institute of Biomedical Engineering
in partial fulfillment of the requirements
for the degree of
Doctor
of
Philosophy

Boğaziçi University
2014

ACKNOWLEDGMENTS

First of all, I would like to express my deepest gratitude to my thesis advisor Prof. *Ahmet Ademoglu* for providing me the opportunity for this thesis,for introducing me the interesting world of signal processing and his support during all these years. Professor *Tamer Demiralp* is acknowledged for his great patience in familiarizing me with the odd-looking waveforms called EEG.Being a witness of his scientific methodology and interests gave invaluable insights during my doctoral research.

Especially, I wish to express my gratitude to Professor *Yekta Ulgen* for more things that I have learned from his scientific lectures and his guidance and contributions on me.Associate Prof. Dr. *Mahrokh .G. Shayesteh* deserves many thanks for encouraging me to do my best to develop this work and solving some signal processing analysis.

Assistant professor *Guray Gurkan* for his helps during the first year of beginning of my thesis and *Hashem Kalbkhani* PhD candidate of Telecommunication for his cooperation at providing some processing codes and statistical analysis,are appreciated too.

Last but not least, I would like to say a big "Thank you" to my spouse for her patience, understanding, continuous reliance and support at all times. Without their encouragement and motivation, it would have been impossible for me to finish this work. I feel very grateful also for having a lot of beloved friends such as Dr Hassan Khorsandi and family who helped me pass through hard times with much ease. This work is dedicated to my spouse Rogi and my sons, Mohsen and Ehsan.

ABSTRACT

MONITORING DEPTH OF ANESTHESIA THROUGH MEASUREMENT OF PHASE COUPLING AMONG SPONTANEOUS EEG RHYTHMS

Awareness during general anesthesia for its serious psychological effects on patients and some juristically problems for anesthetists has been an important challenge during past decades. Monitoring depth of anesthesia is a fundamental solution to this problem. Induction of anesthesia alter frequency and mean of amplitudes of the electroencephalogram (EEG), and its phase couplings. By increasing the anesthetic drug dose, the mean frequency of the signal decreases and its amplitude increases and theta or delta waves appear. In this study, we analyze EEG changes for phase coupling between delta and alpha sub-bands using a new algorithm for depth of general anesthesia (DOA) measurement based on complex wavelet transform in patients anesthetized through total intravenous anesthesia (TIVA) by Propofol. By taking bispectral index (BIS) values as reference we calculate entropy and histogram of modulated signals.Entropies correspond to different BIS intervals using Mann-Whitney U test show that they have different continuous distributions. The results demonstrate that there is a phase coupling between 3-4 Hz in delta and 8-9 Hz in alpha sub-bands and these changes are shown better at the channel (T_7) of EEG. Moreover, when BIS values increase, the entropy value of modulated signal also increases and vice versa.Measuring phase coupling between delta and alpha sub-bands of EEG signals through Morlet continuous complex wavelet transform analysis reveals the depth of anesthesia level.The method can be used to measure depth of general anesthesia to prevent awareness of the patients during anesthesia.

Keywords: Depth of anesthesia, Awareness, Complex wavelet transform, Modulated Signal, Phase Coupling, EEG Waves, Entropy Measurement.

ÖZET

SÜREGİDEN EEG SALINIMLARI ARASINDAKİ FAZ BAĞLANIM ÖLÇÜMLERİYLE ANESTEZİ DERİNLİĞİNİN İZLENMESİ

Son yıllarda, genel anestezi sırasında (farkındalık) uyanık olma hali hastalarda ciddi psikolojik etkilere ve anestezi uzmanlarıile hukuki sorunlara neden olmaktadır. Anestezi derinliğni izlemek bu sorunun temel çözümüdür. Anestezinin başlamasıile EEG'nin frekansı, ortalama genliği ve faz bağlanımı değişir. Vücuda verilen anestezik maddenin dozunun artırılmasıile beraber sinyalin ortalama frekansı azalır, genliği artar, delta ve teta dalgaları görülür. Bu araştırmada, EEG değişimlerini, delta ve alfa alt bant dalgaları nın faz bağlanımlarını damardan uygulanan Propofol ile genel anestezi altındaki hastalarda araştırarak, anestezi derinliğiyle ilişkisini, karışık dalgacık dönüşüm sinyal analiz yöntemi ile inceledik. BIS indisini referans alarak module sinyallerin sıklık dağılımını ve dağısını hesapladık. Mann-Whitney U istatistiksel analiz yöntem ile çeşitli BIS indis aralıklarına uygun dağıdeğerleri analiz edildiğinde, bu verilerin farklı kesintisiz dağılımlar gösterdiğini gözlemledik. Sonuçlar, delta (3-4 Hz) ve alfa (8-9 Hz) aralıklarında faz bağlanımı olduğunu göstermektedir. Bu EEG değişimleri en iyi kanal T_7 gözlemlenmektedir. Morlet karışık dalgacık dönüşümü, delta ve alfa alt bantlarının faz bağlanımını ölçerek hastada anestezi derinliğini belirlememize imkan sağlamaktadır. Bu yöntem genel anestezi derinliğini ölçmede kullanılarak , hastaların anestezi halinde uyanıklığı önlenebilir.

Anahtar Sözcükler: Anestezi Derinliği, Uyanıklık, Karmaşık Dalgacık Dönüşümü, Kiplenmiş İşaret, Faz Bağlanımı, EEG Dalgaları, Dağı ölçümü

TABLE OF CONTENTS

LIST OF FIGURES

LIST OF TABLES

LIST OF SYMBOLS

α	alpha
β	beta
δ	delta
$>$	Greater
$\int$	Integral
log	Logarithm
ψ	Mother wavelet
p	Probability
Σ	Sigma
$<$	Smaller
t	Time
θ	theta
χ	Variable
W	Wavelet

LIST OF ABBREVIATIONS

AEP	Auditory Evoked Potential
ASA	American society of Anesthesiology
BAEP	Brainstem auditory evoked potential
BIS	Bispectral index
BS	Burst suppression
BSR	Burst suppression rate
CNS	Central nervous system
CSI	Cerebral state index
CSM	Cerebral State Monitor
CWT	Continuous wavelet transform
DOA	Depth of general anesthesia
EEG	Electroencephalogram
FD	Fast delta
FEMG	Frontal's electromyography
GA	General anesthesia
GABA	γ-amino butyric acid
LLAEP	Long latency auditory Evoked Potential
MLAEP	Mid-latency auditory-evoked responses
MS	Modulated signal
OP	Operation
PDF	Probability density function
Pre-Op	Pre-operation
Pt	Patients
PTSD	Post–traumatic stress disorder
RBR	Relative β ratio
RE	Response entropy
REM	Rapid Eye movement
SD	Slow delta

SE	State entropy
SQL	Signal Quality index
STFT	Short-time Fourier transform
TIVA	Total intravenous anesthesia
USA	United states of America
VSD	Very slow delta
WT	Wavelet transforms

1. INTRODUCTION

1.1 Motivation and Objectives

Awareness during general anesthesia is probably the most helpless and terrifying feeling in the world. It occurs when one is supposed to be completely asleep under full general anesthesia, but the brain is not asleep at all.Your body is almost always fully paralyzed; you have a tube down your throat; and you can't speak, breathe, or move or do anything to alert the doctors that you are awake, in other word awareness"occurs when "a patient becomes conscious during a procedure performed under general anesthesia and subsequently has recall of these events," with "recall" being limited to explicit memory only.It is a severe after-effect with potential long-term psychological outcomes such as post–traumatic stress disorder, repetitive nightmares, anxiety and irritability [1, 2].

In the United States, the incidence of intraoperative awareness is 0.1% to 0.2% of patients undergoing general anesthesia [2]. In Europe, a large prospective trial investigated conscious awareness in 11,785 patients who underwent general anesthesia [3]. The incidence of intraoperative awareness with explicit recall was 0.1% without the use of neuromuscular blocking agents. With the use of these agents, it was 0.18%.

Monitoring depth of anesthesia (DOA) is a fundamental solution to this problem.Because accurate evaluation of DOA helps precise drug delivering to the patients, thus preventing awareness or excessive depth of anesthesia and improving patients' outcomes [4, 5].

There are numerous approaches and devices to assess DOA based on clinical sign or brain electrical activity monitoring. According to the studies, determination of DOA based on electroencephalogram (EEG) parameter can be more informative than those just work based on simple vital signs, because central nervous system (CNS) is

the final target of general anesthetic drugs [6].

Some of commercially available depth of anesthesia monitors that work based on EEG are: Bispectral index (BIS), Narcotrend, Entropy, and Auditory Evoked Potential(AEP)monitors. These devices are not still exactly accurate and cases of alertness are reported even with them [7, 8]. BIS monitor is used as standard equipment for general anesthesia monitoring which is commonly used in comparison with other DOA monitors because of its presence in clinical practice for over two decades, though it does not necessarily mean that the BIS monitor is superior to others. In the last decade the BIS monitor has undergone meticulous testing, which has shown several drawbacks [9, 10]. Therefore, the problem of constructing an ideal DOA monitor is still unsolved. That is why we did the present research.

By considering about 0.2% incidence of awareness and it‘s complications in the united states of America (USA) and multiplying this incidence rate by 22 million anesthesia cases annually in the USA [2], we can find out the magnitude of the problem. Finding solution to this problem can be a great motivation to do of this study.

In this dissertation, we aimed to develop methods for monitoring depth of anesthesia precisely and prevent awareness and its squeals.For this reason we investigated modulation in spontaneous EEG between α and δ bands sub-bands to evaluate the depth of Propofol anesthesia by a new algorithm based on the Morlet continuous complex wavelet transform in order to overcome the limitations of other monitoring approaches such as the Fourier transform and short time Fourier transform.

1.2 Thesis contribution

There are various EEG based types of DOA approaches to prevent awareness and maintain safety for patients and anesthesiologist and help them to pay little money.The work presented in this thesis focused on developing an EEG signal analysis method to provide the EEG data with the least artifact and time delay.

Up to now most of EEG analyzing methods was used are based on Fourier or Short time Fourier transform signal processing approaches which in these methods the signals are assumed stationary and proceeding continued, whereas the EEG signals are non-stationary. To solve this problem we proposed to use Morlet continuous complex wavelet transform. In addition, it is helpful in finding hidden frequency information in the signal and enables a 3-d representation of the signal amplitude, frequency, and time.

Achieving the before mentioned aims will help precisely drug delivering to the patients, results in earlier recovery, reduced post anesthesia care unit stay, a reduction in the incidence of intraoperative awareness and improving patients' outcomes.

2. BACKGROUND

2.1 Anesthesia

Many surgical procedures would not be possible without the patient entering a state of general anesthesia (GA). The essential features of a successful general anesthesia, displayed by the patient, are a reversible loss of consciousness with a lack of movement, a lack of awareness, unresponsiveness to painful stimuli and a lack of recall of the surgical intervention [11,12]. But traditionally anesthesia means the condition of blocked pain feeling or temporarily taken away. It is tempted by drugs and reversible state of amnesia, analgesia, loss of responsiveness, loss of skeletal muscle reflexes, or all simultaneously. This allows patients to undergo surgery and other procedures without apprehension and pain. An alternative definition is a "reversible lack of awareness," including a total lack of awareness (e.g. a general anesthetic) or a lack of awareness of a part of the body such as a spinal anesthetic [1].

Types of anesthesia include local anesthesia, regional anesthesia, general anesthesia, and dissociative anesthesia. Local anesthesia inhibits sensory perception within a specific location on the body, such as a tooth or the urinary bladder. Regional anesthesia renders a larger area of the body insensate by blocking transmission of nerve impulses between a part of the body and the spinal cord [1].

General anesthesia is a reversible state characterized by unconsciousness, analgesia, muscle relaxation, and depression of reflexes which is achieved by the administration of anesthetic agents. It is a balance between the amount of anesthetic drugs administered and the state of stimulation of the patient. As the intensity of surgical stimulation varies during a surgical procedure, so does the requirement of anesthetic agents. The organ system effects of anesthetic drugs may limit the amount that can be given safely. This would, at occasions, create a critical imbalance between anesthetic requirement and anesthetic drug administration resulting in varying depth of anesthesia [13].

2.2 Awareness during anesthesia

The term "awareness" during anesthesia, as used in the anesthesia literature, implies that during a period of intended general anesthesia, the brain is aroused by stimuli that are stored in memory for future explicit recall. The term "explicit" distinguishes conscious memory, which is the intentional recollection of previous experiences, from "implicit" memory, which refers to changes in performance or behavior that are produced by prior experiences that do not require intentional or conscious recollection. Thus, patients who experience awareness are recalling occurrences during a state of inadequate anesthesia [2].

Awareness is a serious complication with potential long-term psychological consequences. Significant psychological outcomes e.g. nightmares, flashbacks, and post–traumatic stress disorder (PTSD) with Characteristic symptoms include anxiety and irritability, insomnia, repetitive nightmares, depression, a preoccupation with death [14] are common after an episode of intraoperative awareness, and affected patients may remain severely disabled for extended periods of time.However, in some circumstances, intraoperative awareness may be unavoidable to achieve other critically important anesthetic goals.

The risk of intraoperative awareness varies among countries, depending on their anesthetic practices.In the study of Moerman,70% of patients who had experienced awareness during general anesthesia had unpleasant after-effects and 6% of patients had needed psychotherapeutic help [15]. Shwender and co-workers showed that 48.9% of patients had after-effects, anxiety (55.0%) and nightmares (52.4%) being the most common ones. PTSD was found in 14.3% [16].

2.3 Causes of awareness

When a patient experiences awareness during anesthesia, usually it is caused by overly light anesthesia, increased anesthetic requirement, or malfunction or misuse of the anesthetic delivery system. In a recent review of published cases of awareness in the literature [17] overly light anesthesia accounted for 87% of the cases, increased anesthetic requirements for 7%, malfunction of the anesthesia delivery system for 5%, and misuse of the anesthesia delivery system for 4%.Overly light anesthesia is the most common cause of awareness. The majority of cases of awareness and recall seem to be due to preventable problems in the anesthetic apparatus and administration of anesthesia.

Awareness is important for anesthetist because his/her core business is to make sure that patients are properly and safely anesthetized, and avoiding awareness is part of his/her contract with the patient. Awareness has its own anesthetist's and patient's perspective. In anesthetist point of view, it puts effect on professional issues, feeling of guilt, adverse publicity and litigation. Cases of awareness represent between 2% (ASA (American society of Anesthesiology) Closed Claims Analysis) [18] to 2.2% (British data) of claims against anesthesiologists. In the USA, the median payment for such cases is $ 81,000 although recently, there have been several cases in which much larger claims have been settled [13, 18].

2.4 Management of Awareness through monitoring DOA

As overly light anesthesia is the most common cause of awareness,anesthesiologists use a variety of different indicators to measure depth of anesthesia, many of which rely upon monitoring more accurately the changes in normal physiological variables. DOA or depth of hypnosis refers to a continuum of progressive central nervous system depression and decreased responsiveness to stimulation. Based on following classification [19], there are various ways to measure or monitor DOA based on clinical/conventional mon-

itoring and/or brain electrical activity monitoring with their special drawbacks.

A. Subjective methods and conventional monitoring

1. Autonomic response
2. Patient Response to Surgical Stimulus

B. Brain electrical activity monitoring

1. Electroencephalogram and derived indices
   - Bispectral index
   - Entropy
   - Narcotrend index
   - Patient state index
   - Cerebral state index
2. Evoked potentials
   - Auditory evoked potentials

2.4.1 Subjective methods and conventional monitoring

Assessment DOA is necessary to anesthetic practice. Prior to the use of muscle relaxants, maintaining the appropriate depth of anesthesia was a balance betweenabolishing movement to pain whilst maintaining adequate respiration. With the absence of movement on incision it was safe to assume that the patient was not aware, however with the use of muscle relaxants it became necessary to be certain that the administered concentration of anesthetic agent was adequate to prevent awareness [19].

It is essential to continuously monitor patients' respiration and autonomic parameters during anesthesia because the signs of awareness are generated through sympathetic activation. Tachycardia, hypertension, sweating, pupillary dilatation, lacrimation and sweating are often used as clinical signs of an inadequate level of anesthesia

secondary to sympathetic. However they must be taken into context with the surgical procedure and the anesthetic technique, as cardiovascular parameters alone are poor predictors of the hypnotic state. Tachycardia secondary to anti-cholinergic drugs like atropine make the heart rate uninterpretable and beta- adrenergic blocking drugs, opiates and regional anesthetic techniques will reduce the sympathetic nervous system response to pain [20]. Traditional clinical monitoring modalities during anesthesia and the most commonly used conventional monitoring systems include ASA standard monitoring as well as end-tidal anesthetic analyzer are ineffective in preventing awareness. Although variations in these parameters can be associated with variations in the level of anesthesia, many studies have demonstrated that they are not completely reliable. Accurate monitoring of the level of consciousness and the potential awareness of an anesthetized patient require different techniques. No clinical trials or other comparative studies were found that examine the effect of clinical techniques or conventional monitoring on the incidence of intraoperative awareness [21]. With the emergence of new anesthetic techniques such as total intravenous anesthesia (TIVA), the use of potent opiate analgesics, newer volatile agents and more complicated regional nerve blocks, a means of measuring DOA is necessary. It began as the continuous clinical monitoring of patients as the analysis of neurophysiologic parameters derived from the EEG.

2.4.2 Brain electrical activity monitoring

CNS is the main target of anesthetic drugs, so EEG based monitoring seems to be more acceptable than subjective methods.EEG signals are the signatures of neural activities.They are produced by a summation of excitatory and inhibitory postsynaptic potentials produced in cortical gray matter of brain and they may represent complex irregular signals that may provide information about underlying neural activities in the brain [22]. They are captured by multiple-electrode EEG machines either from inside the brain, over the cortex under the skull, or certain locations over the scalp, and can be recorded indifferent formats.The EEGs recorded from the head, have small amplitude of about 100μV. The frequency range of these brain waves is from 0.5 to 100 Hz, and

their features are highly dependent on the degree of activity of the brain cortex [23]. Mostly, in normal people, the brain waves may be organized as the following classes [24] and also presented in Table 2.1 [12] and Figure 2.1 [25]:

1. The Delta(δ) waves include EEG waves below 3.5 Hz. They appear in deep sleep or coma, in childhood and in serious brain physical disease.

2. The Theta (θ) waves have frequencies between 4 and 7 Hz. These waves appear chiefly during the childhood, but they also occur during emotional stress in some adults. These waves are recorded in the parietal region.

3. The Alpha (α)waves occur at a frequency range between 8-13 Hz, which are seen in all normal people when their brain is awake in a quiet and resting state. They are usually recorded in the occipital region.

4. The Beta(β) waves have low amplitude and high frequency range between 13-30 Hz. They are affected by cerebral activity and can be recorded from frontal and parietal regions.

Table 2.1
Basic characteristics of EEG wave bands

EEG bands	**Frequency (Hz)**	**Amplitude (mV)**	**Generator of brain**
$\boldsymbol{\alpha}$ **(alpha)**	8-13	20-60	Thalamus
$\boldsymbol{\beta}$**(beta)**	13-30	2-20	Cortex
$\boldsymbol{\gamma}$ **(gamma)**	30-70	3-5	thalamus
$\boldsymbol{\delta}$ **(delta)**	0.5-4	20-200	thalamus
$\boldsymbol{\theta}$ **(theta)**	4-7	20-100	hippocampus and neocortex

General anesthetics act on different targets, i.e., receptors, for example γ-amino butyric acid (GABA) type A, nicotinic acetylcholine, and glutamate receptors (e.g., N-methyl-D-aspartate receptors) in the brain, as well as glycine receptors in the spinal cord [26, 27]. A clear distinction has to be made between the actions of general anesthetics and the mechanism of general anesthesia. The actions of general anesthetics

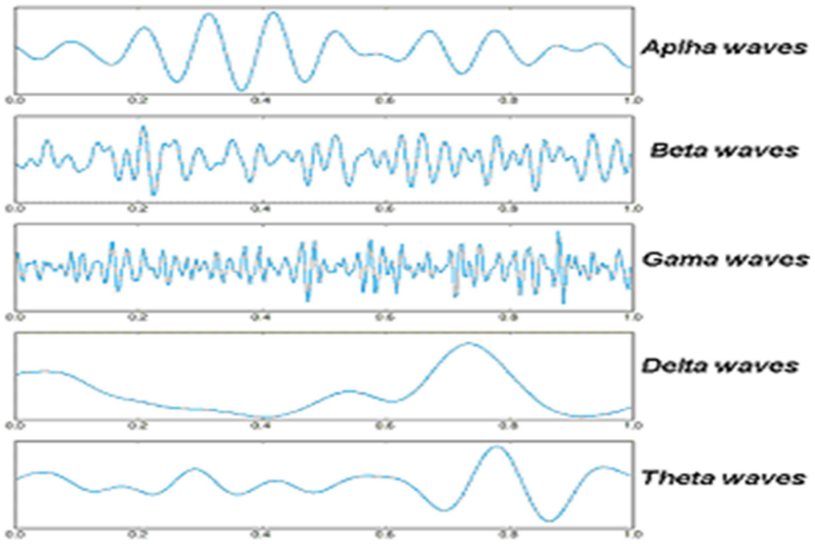

Figure 2.1 Example of different types of normal EEG rhythms

on the brain receptors are well known; the process by which these actions translate into general anesthesia (i.e., the mechanism of general anesthesia) is not well understood [28]. Distinct anesthetic properties are correlated with distinct sites in the CNS; for example, loss of consciousness is associated with the cerebral cortex, loss of memory with the limbic system and immobility and analgesia with spinal cord effects [28]. General anesthetic modulates the activity of several CNS structures including the spinal cord, brain stem, pons, thalamic nuclei and specific regions of the brain cortex (2.2). The effects of general anesthetics on the brain, which lead to loss of consciousness, are best understood at the level of the cortex and the thalamus.

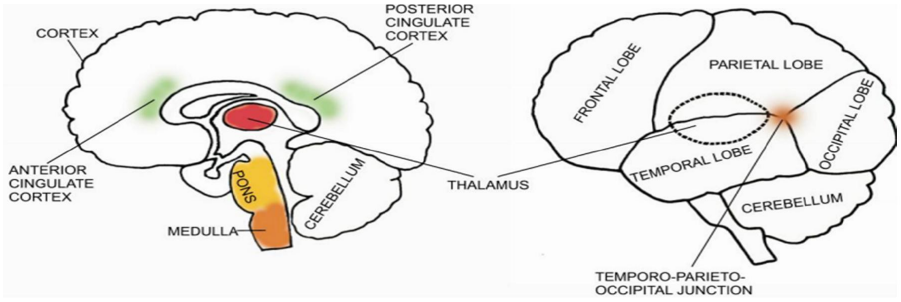

Figure 2.2 Key regions (shaded in color) in the central nervous system that contribute to the state of consciousness.

The shift from alertness to a state of GA is associated by considerable changes in the brain's spontaneous EEG activity [29]. The induction of anesthesia using most part of volatile and intravenous hypnotic drugs as the Propofol and the barbiturates

in variable doses alters frequency and mean of the amplitudes of the EEG signal. Interpreting the EEG during anesthesia attempts to monitor the effects of anesthetic agents in suppressing cerebral electrical activity. Low doses activate mainly β band and decreases EEG mean power in α band. By increasing the dose, the mean frequency of the signal decreases and its amplitude increases then θ or δ waves appear. In other words, by deepening anesthesia, the EEG becomes more regular before disappearing into an isoelectric activity in very deep anesthesia. Finally low voltage high frequency awareness pattern of EEG is changed to the slow-wave EEG of deep sleep, and then an EEG burst-suppression pattern. In moderate to deep anesthesia states, the EEG is ruled by totally sound slow wave's activities in the delta frequency range [30, 31].

As the CNS is the main target of anesthetic drugs, EEG based indexes seem to be more informative due to considering the factor of pain (burst pattern) to calculate DOA rather than those indices that just work based on simple vital signs [32].

Both spontaneous EEG and mid-latency auditory-evoked responses (MLAEP) offer information about the hypnotic state of the patient. Spontaneous EEG is of different types, like traditional EEG measures, BIS Index, Entropy,Patient State Index, Cerebral state index,Narcotrend Index, and Auditory evoked potentials [7].

2.4.2.1 BIS index. It was first introduced in 1992 by Aspect Medical Systems. The main component of the BIS monitor is the bispectral analysis, which evaluates the phase relations from a single channel EEG signal measured from the patient's forehead. The BIS monitor generates a dimensionless number on a continuous scale of 0-100, with 100 representing normal cortical electrical activity,40 to 60 is suitable range for general anesthesia and 0 indicating cortical electrical silence [33] (Figure 2.3).

EEG signal measured from the patient's forehead. is an empirically derived index that is dependent on a measure of the "coherence" among components of EEG and quantifies the phase relationships among the underlying sine wave components of the EEG and with the power and frequency information calculates a single numerical

variable. In other word, it is a complex index because it seems to be constructed based on a combination of features in time domain (burst suppression ratio), frequency domain (relative β ratio (RBR) and spectral edge frequency (SEF95)), and higher order spectral sub-parameters (sync-fast-slow) [34].

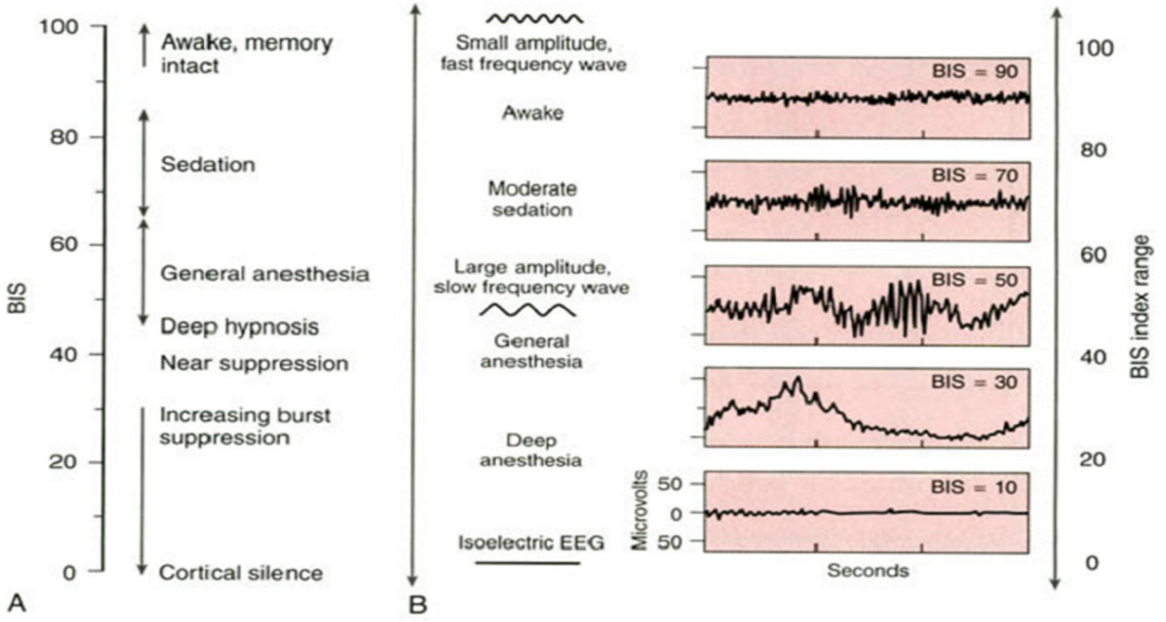

Figure 2.3 A, Clinical correlations of the bispectral index (BIS). Maintaining the BIS value of 45 to 60 during general anesthesia appears to ensure unconsciousness with a hypnotic/opioid anesthetic technique while providing for rapid emergence. B, Changes on the electroencephalogram (EEG) observed with increasing depth of anesthesia.

BIS monitor is used as standard equipment for general anesthesia monitoring which is commonly used in comparison with other DOA monitors because of its presence in clinical practice for over two decades, though it does not necessarily mean that the BIS monitor is superior to others.

The emerging data suggests that BIS monitoring is effective in reducing the incidence of awareness. When anesthesia was guided with BIS, a 77% reduction in the incidence of awareness was found. Myles and colleagues found in a double blind study of patients at high risk for awareness, that BIS guided anesthesia resulted in an 82% reduction in the incidence of awareness [35]. Moreover, a BIS guided titration can reduce anesthetic drug up to 30% during the maintenance period [35], which results in a lower drug usage, faster recovery and, finally, improves the quality of the anesthetic

process.

Although BIS is one of the most popular EEG-based DOA indices, the measurement of DOA is still an unsolved problem due to observation of some conflicts between the BIS index and other clinical signs during orthopedic and neurosurgical operations.

In the last decade, it has been shown that BIS has some limitations in terms of high dependence on the type of anesthetic agents [36]. Another shortcoming of BIS is that the reported index is determined after each 10 seconds, which might be long in crucial circumstances. Moreover, BIS value crosses the defined anesthetic levels repeatedly during painful surgeries. In other words, BIS suffers from a significant lack of robustness sensitivity, and specificity [37,38].

2.4.2.2 Narcotrend monitor. In Narcotrend after artifact analysis a multivariate statistical algorithm transforms the raw EEG data finally resulting in a 6-letter classification of the depth of anesthesia. After artifact exclusion and Fourier transformation, the original electronic algorithm classified the raw frontal EEG according to the following system:A (awake),B (sedated), C (light anesthesia), D (general anesthesia), E (general anesthesia with deep hypnosis), F (general anesthesia with increasing burst suppression). The system included a series of sub-classifications resulting in a total of 14 possible sub-stages:A, B0–2, C0–2, D0–2, E0–1, and F0–1. Additionally, in analogy with BIS, the newer versions of the monitor also display the index value (0–100).No clinical trials or other comparative studies were found that examine the impact of NarcotrendÂ® monitoring on the incidence of intraoperative awareness [39].

2.4.2.3 Patient state analyzer . The derivation of Patient State Index (PSI) is based on the observation that there are reversible spatial changes in power distribution of quantitative EEG at loss and return of consciousness. The PSI algorithm is calculated via a proprietary algorithm by a high-resolution 4-channel EEG monitor after advanced artifact rejection. The algorithm relies on EEG power, frequency and

phase information from anterior-posterior relationships of the brain as well as coherence between bilateral brain regions.The PSI has a range of 0–100, the decreasing values indicating decreasing levels of consciousness or increasing levels of sedation, similar to BIS, entropy, and Narcotrend®. It is constructed using stepwise, discriminant analysis based on multivariate combinations of quantitative EEG variables, derived after Fourier transformation of the raw EEG signal, and found to be sensitive to changes in the levelof anesthesia. PSI is a clinically validated measure of the effect of anesthesia and sedation and has been designed specifically for intra-operative and intensive care use to monitor patient sedation and drug effect. No clinical trials or other comparative studies were found that examine the impact of PSI monitoring on the incidence of intraoperative awareness [21].

2.4.2.4 Cerebral State Monitor (CSM). The Cerebral State Monitor is a hand held device that analyzes a single channel EEG and presents a cerebral state index (CSI) scaled from 0 to 100. In addition, it also provides EEG suppression percentage and a measure of EMG activity (75–85 Hz). The EEG waveform is derived from the signal recorded between the frontal and mastoid electrodes. The frequency content is 2-35 Hz. The performance of the CSI is based on the analysis of the frequency content of the EEG signal.The energy of the EEG is evaluated in specific frequency bands. These are used to define two energy ratios calledα andβ. The CSM is a portable, wireless monitor that uses fuzzy logic to calculate the cerebral state index (CSI). Firstly, one channel EEG signal ispre-processed and then processed by an artifact detection and removal algorithm. The pre-processed signal is then used to calculate three parameters in frequency domain: (a) α ratio, (b)βratio and (c)α- β ratio. Additionally, the burst suppression (BS) analysis is applied to calculate the burst (BSR). Afterwards, all parameters are fed to a fuzzy logic inference system to calculate the CSI. Finally the CSM displays the CSI, BSR and EMG values The CSI is a unit-less scale from 0 to 100, where 0 indicates a flat EEG and 100 indicate EEG activity corresponding to the awaked state [21].

2.4.2.5 Entropy. Entropy monitoring is based on acquisition and processing of raw EEG and Frontal's electromyography(FEMG) signals by using the Entropy algorithm. Entropy describes the irregularity, complexity, or unpredictability characteristics of a signal. It is a property of a physical system or data string consisting of a great number of elements. By adding the measurement of the cortical electrical activity, the clinician can assess the effect of anesthetics more comprehensively. EEG recordings change from irregular to more regular patterns when anesthesia deepens. Entropy of the signal has been shown to drop when a patient falls asleep and increase again when the patient wakes up. Similarly, FEMG quiets down as deeper parts of the brain are increasingly saturated with anesthetics. A single sine wave represents a completely predictable signal (entropy = 0), whereas noise from a random number generator represents entropy = 1. Entropy is independent of absolute scales such as the amplitude or the frequency of the signal. The commercially available Datex-Ohmeda module calculates entropy over time windows of variable duration and reports two separate entropy values. State entropy (SE) is an index ranging from 0 to 91 (awake), computed over the frequency range from 0.8 to 32 Hz, reflecting cortical state of the patient. Response entropy (RE) is an index ranging from 0 to 100 (awake), computed over a frequency range from 0.8 to 47 Hz, containing the higher EMG-dominated frequencies, and will thus also respond to the increased EMG activity resulting from inadequate analgesia. Noxious stimulation increases the difference between RE and SE, however, it is reported that an increase in the difference does not always indicate inadequate analgesia and should be interpreted carefully during anesthesia [40]. No clinical trials or other comparative studies were found that examine the impact of entropy monitoring on the incidence of intra operative awareness [21].

2.4.2.6 Auditory evoked potential (AEP). The AEP is defined as the passage of electrical activity from the cochlea to the cortex. A basic requirement for AEP analysis is a functional auditory system. Auditory stimuli with a defined frequency and intensity are presented – usually via headphones. According to latencies (time from stimulus to response), the AEP is separated into three parts: *an early component* (brainstem auditory evoked potential, *BAEP*; latencies <10 ms), *a middle latency*

component (middle latency AEP, *MLAEP*; latencies 10–50 ms) marked by the waves N0, P0, Na, Pa and Nb, are thought to originate from the primary auditory cortex, and *late components* (long latency AEP, *LLAEP*; >50 ms),consists of waves P1, N1, P2 and N2(Figure 2.4). It reflects the neural activity of the frontal cortex and association areas.Repeated stimuli are given as clicks (BAEP and MLAEP) or as a sound of defined characteristics (MLAEP, LLAEP). Usually, the AEP are recorded from vertex electrodes with a reference to mastoids. The AEP window of this monitor shows the BAEP and MLAEP. The BAEP is presented as a smoothed curve;therefore, typically only wave V can be detected. The AEP technology actively measures the brain's reaction to acoustic stimuli. It's the natural choice for measuring patient consciousness under anesthetic because hearing is the MLAEP in the primary auditory cortex of the temporal lobe, and LLAEP in the auditory association fields of the frontal lobe. Basic analysis of the AEP requires identification of peaks and troughs. Visual analysis is based on the presence, latency (time from stimulus to peak), and amplitudes (μV) of these peaks and troughs. The BAEP is relatively resistant to the effects of anesthesia, whereas the LLAEP disappears with subanesthetic concentrations. During anesthesia, the MLAEP shows characteristic changes (increase of latency, decrease of amplitude). The use of MLAEP as a monitor of anesthesia accounts for the high priority of acoustic perception, which has an alarming function for the individual. This is supported by the fact that recall of auditory perception is the symptom that is most frequently described by patients with awareness under anesthesia [15, 41].

AEP amplitudes are even lower than EEG amplitudes. Therefore the signal must be amplified. This makes it susceptible to artifacts. Particularly in the environment of the operating room, low signal quality may become a problem [42]. As with the EEG, impedances should be kept low. An additional problem arises from the technique itself: the AEP is generated by averaging numerous sweeps, i.e., numerous responses to repeated stimuli. This averaging procedure requires some time. Depending on signal quality, between 30 seconds and 2 minutes are required to generate a valid AEP. In dynamic phases of anesthesia, this time interval may be too long, i.e. anesthetic depth may have changed before signal averaging has been completed.

2.5 Pitfalls and limitations of an anesthesia index

Currently available indices are based on a probabilistic approach. Therefore, an index value provides a probability and is not 100% reliable. Thus an index does not allow a clear separation of "consciousness" from "unconsciousness." Details of calculation are unclear, and therefore the clinical user has little chance to identify reasons for erroneous index values. All indices require an (unknown) time to calculate the index value. This time delay is not constant for an index and depends not only on the EEG interval required for index calculation but also on the signal quality and artifact algorithms [40].

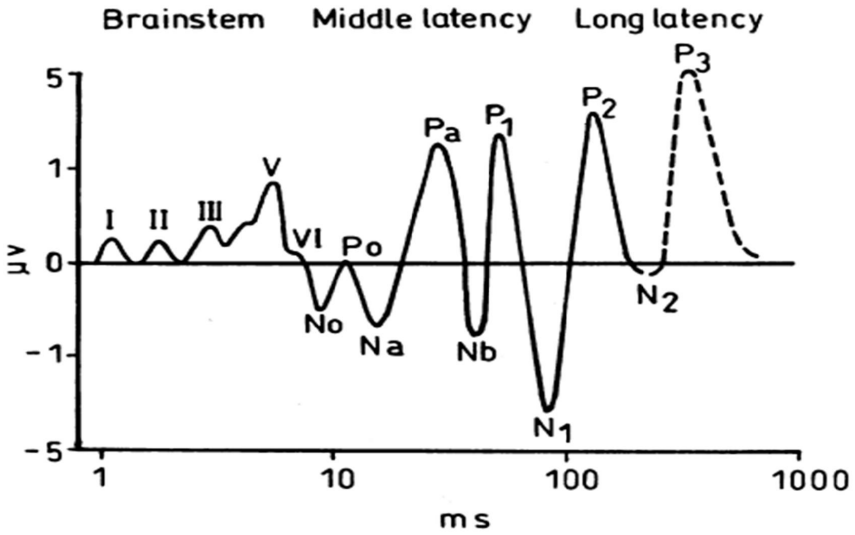

Figure 2.4 Diagrammatic representation of the transient auditory evoked response. The symbols above the waves represent the standard electrophysiological nomenclature. P3 or P300 component represents the events-related potential at 300 ms after stimulation.

The use of high-frequency signal components bears the risk that the indicated anesthetic depth is not based on parameters of the primary target organ, i.e., the brain (EEG), but rather on the surrogate parameter activity of frontal muscle (MEMG). This implies that a patient who is awake and paralyzed may be classified as unconscious [43].

With all of these possible pitfalls, the anesthesiologist should not use an index value to save drugs or time, but to obtain another parameter that presents additional information about anesthetic depth and the level of consciousness under anesthesia. The use of an index in the context of – and not in competition with – all parameters

may provide valuable additional information about the main target organ of anesthesia. In the future, it would be helpful to shift from a probabilistic to a mechanism-focused approach for anesthesia brain monitoring.

2.6 EEG bases of DOA and literature review

As mentioned, there are numerous methods and devices to assess DOA based on clinical sign or brain electrical activity monitoring. According to the studies, determining DOA based on EEG parameter can be more informative than those just work based on simple vital signs, because CNS is the final target of general anesthetic drugs [6].

Some of commercially available DOA monitors that work based on EEG are BIS, Narcotrend, Entropy, and Auditory Evoked Potential monitors. These devices are not still exactly accurate and cases of alertness are reported even with them [7, 8]. BIS monitor is used as standard equipment for general anesthesia monitoring which is commonly used in comparison with other DOA monitors because of its presence in clinical practice for over two decades, though it does not necessarily mean that the BIS monitor is superior to others. In the last decade the BIS monitor has undergone meticulous testing, which has shown several drawbacks [9, 10]. Therefore, the problem of constructing an ideal DOA monitor is still unsolved. That is why we did the present research.

The EEG reflects the combination of synaptic activity of excitatory and inhibitory post-synaptic potentials produced by cortical neurons. The shift from alertness to a state of general anesthesia is associated by considerable changes in the brain's spontaneous EEG activity [29] .

General anesthetic drugs are thought to block consciousness by depressing the central nervous system. Some of the resultant changes in the brain's spontaneous electrical activity are manifest in the EEG. Anesthesia related changes in the EEG are well

studied [44] and have some commonality with natural sleep processes [45]. In general, the low-voltage, high-frequency pattern of wakefulness transits to high-amplitude, low frequency waves, and finally to the burst suppression[1] pattern as anesthetic drug concentration increases [46, 47]. As yet, the physiological mechanisms that underlie EEG activity during anesthesia remain largely unclear. The effects of general anesthetics on the cerebral cortex and the thalamus [12] cause a multitude of different EEG oscillations [48]. Evidence from intracellular recordings in animals [49, 50] and EEG studies in humans [51, 52] indicate that the cortically generated slow oscillation (1 Hz) has the ability to trigger and group a variety of faster brain rhythms. The two classical slow rhythms (δ: 1–4 Hz and spindle: 7– 15 Hz) are predominant in non-rapid eye movement sleep, whereas the two fast oscillations (β: 20–30 Hz and γ: 30– 60 Hz) [48] are more commonly a feature of wakefulness and rapid eye movement sleep. However, it is unresolved as to whether the modulation of higher-frequency brain activities by slow oscillations is correlated with the level of unconsciousness when induced by general anesthesia [53]. Scalp EEG shows that delta band may include different types of activities. Benoit et al. presented that the slow and fast delta components differently correlate with alpha and beta frequency bands using the scalp EEG power spectra during non-Rapid Eye movement(REM) sleep [54]. They chose 0.7-2 Hz interval as slow delta and 2-4 Hz interval as fast delta.

Steriade et al. [48, 50] by studying on neural activities revealed that slow oscillation ($<$ 1 Hz) has the ability to activate and cluster cortical network firing, which correspond to higher frequency EEG activities from delta to gamma (30-60 Hz).

Molaee-Ardekani et al. showed that phase of modulation related to various delta sub-bands as very slow, slow, fast, narrow, cumulative slow 1 and cumulative slow 2 deltas with alpha waves had different correlations with depth of anesthesia, and finally they implied that a fast delta sub-band was the best choice among various delta sub-bands to correlate with brain activities, and their phase difference change with DOA [53]. Summary of anesthetics effects of on EEG include:

[1]Burst suppression is an electroencephalography (EEG) pattern that is characterized by periods of high-voltage electrical activity alternating with periods of no activity in the brain.

a. Decrease at 25-50 Hz band (upper β and γ bands)
b. Increase at slow waves (θ and δ bands)
c. Great increase in the signal strength which obtained from frontal region
d. Decrease at frequency coupling between frontal and parietal regions

In this study, we used a new algorithm based on the Morlet continuous complex wavelet transform for modulation in spontaneous EEG between α and δ bands partitioned as small as one Hz to evaluate the depth of Propofol anesthesia in order to overcome the limitations of the Fourier transform and short time Fourier transform which are used in algorithms of most of present DOA monitoring devices.

3. METHOD AND MATERIALS

We used a new algorithm based on the Morlet continuous complex wavelet transform to calculate modulation in spontaneous EEG between α and δ sub-bands partitioned as small as one Hz to evaluate the depth of general anesthesia in order to prevent awareness according to following stages.

3.1 Data recording protocol

After approval of the Institutional Research Ethics Committee,EEGs of 24 patients scheduled for elective gynecological surgeries in Capa medical faculty hospital's operating rooms in Istanbul were investigated initially and the 6 patients, aged 26-72 years old, who had analyzable EEGs were selected randomly.All of selected patients were in ASA I and II physical status classification and free of neurological diseases.

Written informed consent was obtained from all patients. In order to prepare patients psychologically and preventing unnecessary delay on schedule of surgery the patients preparation period to take EEG recording was started about one hours before the beginning of surgical operation in Pre-Op(pre-operation) period then spontaneous EEG were taken for 300 seconds. Then the patients were transferred to operating room and before starting the OP (operation) period, in EEG recording step, BIS device was attached.

In operating room Propofol was injected 30 seconds after the beginning of the induction period of EEG recordings and lasts as a main anesthetic in all patents accompanied by Remifentanyl (Ultiva) during surgery and Rocuronium Bromide (Esmeron). Spontaneous EEG recording was done during maintenance and emergence periods of anesthesia. At 10 minute intervals before cessation of anesthetic agent and wakening up, a long recording was done. The first and end of operation, spontaneous EEG recorded was the longest ones.

The duration of spontaneous EEG and BIS data recorded during surgery for patients (Pt.) are as:**1**.Pt.12 (90 min), **2**. Pt.13 (140 min), **3**. Pt.14 (52 min), **4**. Pt.17 (140 min), **5**. pt.23 (175min), **6**. Pt.24 (105 min)**.**

EEG electrodes generally are placed according to a mapping system that relates surface head anatomy to underlying brain cortical regions. The placement pattern of recording electrodes is called a montage. Use of a standard recording montage permits anatomic localization of signals produced by the brain and allows development of normative EEG patterns and comparison of EEG recordings made at different times. The standard EEG "map" is called the 10-20 system for EEG electrode placement. This system is a symmetric array of scalp electrodes placed systematically based on the distance from the nasion to the inion and from the pretragal bony indentations associated with both tempomandibular joints.

Based on 10% or 20% of these distances, recording electrodes are placed systematically over the frontal (F), parietal (P), temporal (T), and occipital (O) regions at increasing distances from the midline. Left-sided electrodes are given odd number subscripts, and right-sided electrodes are given even number subscripts. Increasing numbers indicate an increasing distance from the midline. Midline electrodes are designated with a "z" subscript. The standard diagnostic EEG uses at least 16 channels of information, but intraoperative recordings have been reported using 1 to 32 discreet channels (Figure 3.1).

Application of 16 channels for the following reasons is more informative than traditional method with fewer channels:

a) The standard 16-channel EEG montage provides more information than can be practically analyzed or displayed by most processed EEG monitors and perhaps more than is needed for routine intraoperative use. Most available processed EEG devices used by anesthesiology personnel use four or fewer channels of information—translating to at most two channels per hemisphere. Processed

EEG devices generally monitor less cerebral territory than a standard 16-channel EEG.

b) Some intraoperative changes are unilateral (e.g., regional ischemia owing to carotid clamping), and some are bilateral (e.g., EEG depression by bolus administration of an anesthetic). An appropriate number of leads over both hemispheres are needed [22].

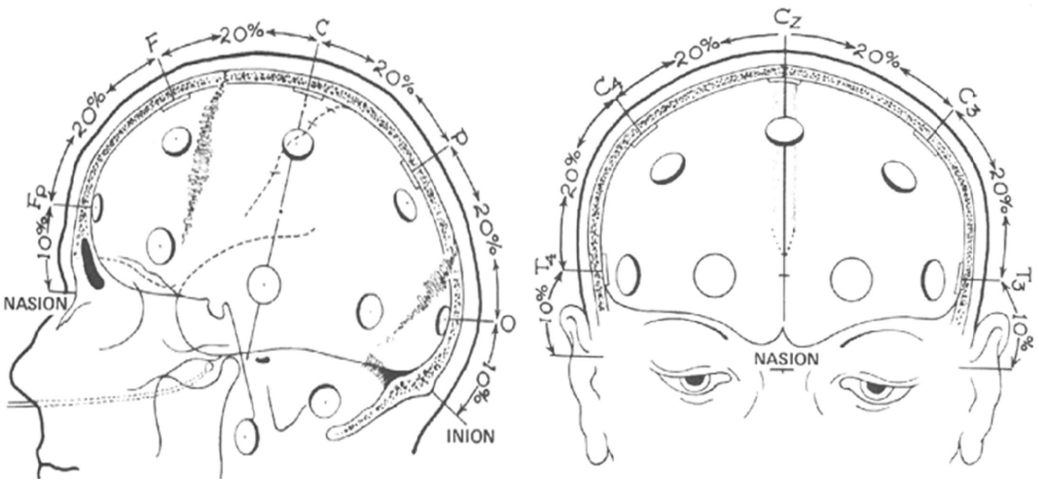

Figure 3.1 Electrode placements in the 10-20 electrode system. (Fp = frontal pole; C = central; P = parietal; O= occipital). *Left*: lateral view showing measurements in the midsagittal plane. C is placed at 50% of the nasion-inion distance; F, P, Fp, and O are placed at 20% intervals. *Right*: frontal view showing measurements in the central coronal plane, with electrodes at 20% intervals of distance between the left and right preauricular points. (Reproduced from EEG Clin Neurophysio 110:372, 1958, with permission of Elsevier Science.)

The EEG electrode montage included 15 channels shown in Figure 3.2 based on 10/20 standard respectively (Fp1, Fp2, F7, F3, Fz, F4, F8, T7, C3, Cz, C4, T8, P3, Pz, P4) and the electrodes referenced to mastoids [21].

Parallel to EEG recordings, the commercially available anesthesia monitor (BIS®, Aspect Medical Systems) was used as a reference, because it is the most used depth of general anesthesia monitoring device. EEG data is sent to BIS device by a specific frontal electrode networks which was provided by BIS Device Company (Figure 3.2). These electrode set should be discarded after a definite duration. On BIS monitor screen beside the every 5 second BIS index updates , the real-time signal quality (SQI:signal Quality index), EMG activity , a specific time duration EEG signal and BIS values are visible.

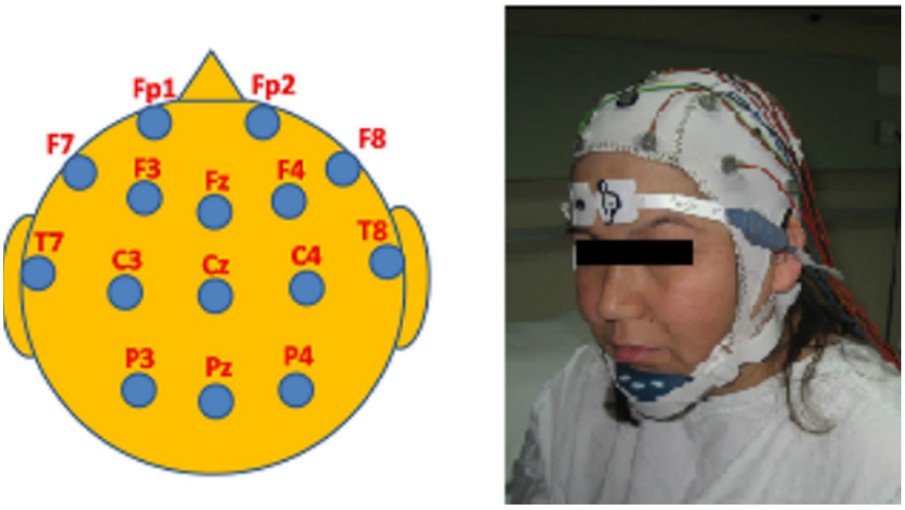

Figure 3.2 EEG electrode montage

3.2 Controlling spontaneous EEG records

During operation, spontaneous EEG segments are controlled by a MATLAB based program. The records were divided into parts as before operation or during operation respectively Pre-op or Op. Then the desirable parts were started by a record operator, and necessary protocol was provided.In addition, digitized 15 channel EEG data during operation by MATLAB software, the operation steps, administered drugs and any changes in patient status were recorded.During recording, the operational data were labeled as comments in Brain vision program.

a. Starting and cessation of drug administration.

b. Entrance to a specific operation steps.

c. Some observed events in patient (movement, emergence)

All recording were stopped when the patient emerged from anesthesia[2] . The data that were saved by Brain vision program in hard disk, include 15 channel EEG signals, the comments was written by operator during surgery and BIS values.From now on, the

[2]As a General rule when BIS values reaches to 90, patient wakes up , but in some instances the patient waked up while BIS value was 70.These discrepancy are from normal physiologic and anatomic variability that induces in some instances abnormal responses to anesthetic agents.

Pre-op and Op data that recorded in hard disk were fulfilled by signal processing steps through improved function in MATLAB field.

3.3 Pre-amplifying and sampling

In this work we used a preamplifier and its software with 32 channel capacity named Brain map device. In addition, Brain vision recorder device (Brain product, Germany) was used to record the sampling frequency of preamplifier and adjust the filter parameters. It can also display real-time EEG data on the screen and save them to a hard disk. By this program we reduced the electrode-skin impedance to lower levels (z<5kΩ) before recordings because high impedances render the signal susceptible to artifacts.The used sampling parameters are shown in Table 3.1.

Table 3.1
Sampling parameters

Amplifier gain (A_ν)	10^6
Sampling frequency (F_s)	1 KHz
Sampling resolution	12 bit
RC filter (DC filter)	0.1 Hz
Highpass filter (anti-aliasing filter):	250 Hz

3.4 Introduced Method

Our aim is to find appropriate channels and approaches to evaluate DOA. The proposed algorithm consists of three main steps: Pre-processing, calculation of modulated signal (MS) between α and δ bands, and determining DOA by measuring Shannon Entropy of MS. These steps are applied to all EEG channels. The above stages are explained in more details at the following subsections.

3.4.1 Pre-processing

Pre-processing aims to simply subsequent processing operations, improving signal quality without losing information. In this step, the recorded signals are processed to clean and de-noise data in order to enhance the relevant information embedded in the signals.

The raw spontaneous EEG data which recorded from 15 channels were cleaned manually of artifacts which are not patient-related (physiological), and corrupted BIS data which identified by BIS monitor were also removed.The recorded brain waves had small amplitude of approximately 100 μV and contained frequency components of up to 300 Hz. To preserve the effective information, the EEG signals were amplified and filtered, to reduce the noise and make the signals proper for process and vision. Highpass filters with a cut-off frequency of less than 0.5 Hz were used to remove the disturbing very low frequency components and high-frequency noise was alleviated by using lowpass filters with a cut-off frequency of approximately 50–70 Hz. Notch filters with a null frequency of 50 Hz were used to guarantee the rejection of 50 Hz power supply noise.Frequency sampling was decimated from 1000 Hz to 100 Hz [55].

3.4.2 Complex continuous wavelet transform

The Fourier transform (FT) is a useful tool to analyze the frequency components of the signal. FT is taken over the whole time axis, hence, cannot provide instant a particular frequency raises. Therefore, *FT is only able to retrieve the global frequency content of a signal, the time information is lost.*However, if the signal is non-stationary, the signal in frequency is actually a function of time and we cannot know when the frequency component changes.

Short-time Fourier transform (STFT) was proposed to overcome this limitation of FT. To achieve information of both time and frequency, STFT uses a sliding window to find spectrogram. The window function is used to extract a portion of x(t)and then

take FT. The output of the STFT has two parameters: one is the time parameter t, which indicating the instant we concern. The other is the frequency parameter f, which has the same role in the FT. However, there is another problem: the width of the window is fixed, which may cause that there is no enough resolution in some interval. *The length of window limits the resolution in frequency which is the major limitation of the STFT.*

$$X_w(a,b) = \frac{1}{\sqrt{b}} \int_{-\infty}^{\infty} x(t)\psi^* \left(\frac{t-a}{b}\right) d\,t \tag{3.1}$$

Wavelet transforms (WT) have become useful tools for time-frequency EEG analysis. A wavelet is a wave-like oscillation that has a limited duration, or mathematically speaking, a function that can be manipulated to transform a signal into another form. These manipulations are achieved through a process of translation (i.e.movement along the time axis), and dilation (i.e. spreading out the wavelet). Wavelet transform seems to be a solution to the window size problem in STFT. The translated-version wavelets locate where we concern. Scaled-version wavelets allow us to analyze the signal in different scale [56, 57]. The mother waveletψ (t) by dilated (parameter b) and translated (parameter α) is designed to balance between the time domain and frequency domain resolution. We can see clearly very low frequency components at large b, which makes the width of the mother wavelet expansive, and very high frequency components at small b, which makes the width of the mother wavelet concentrating. The time-frequency tile allocation of Wavelet transform is:

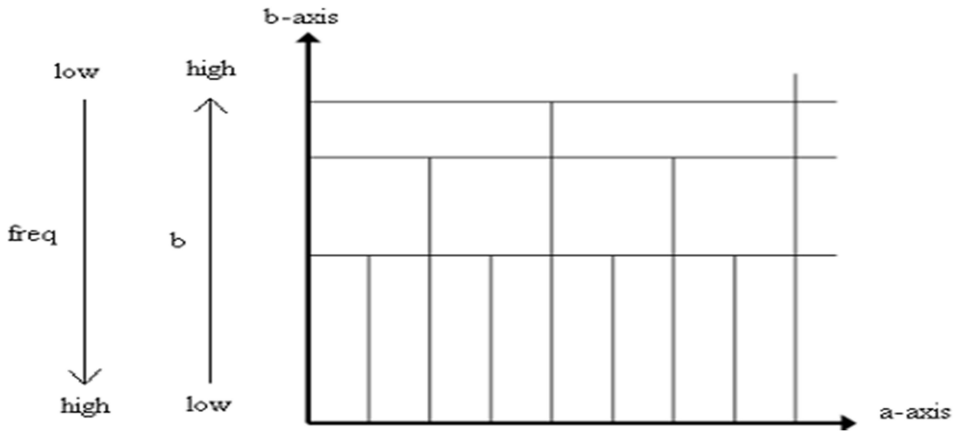

Figure 3.3 Spread of the windowing function defines both temporal and resolution of transform

From Figure 3.3, we can see both the time axisand frequency axis are not divided in fixed interval, and this flexibility is very useful in time-frequency analysis. It is worthy to note that the parameter bis inversely proportional to the frequency and parameter $\alpha$is just like the time. This is another difference between the α-b plot of the Wavelet transform and the t-f plot of the STFT.

The continuous wavelet transform (CWT) provides the scale-dependent structure of a signal as it varies in time. CWT provides a view of the frequency versus time behavior of the signal and therefore has great potential as a preliminary tool for investigating wide band, non-stationary, or other types of signals having time-dependent spectral characteristics.

If $x(t)$ is a square-integrable function i.e., $\int x^2(t)\,dt < \infty$, then the CWT of $x(t)$ relative to a given wavelet$\psi(t)$ is defined as

$$W_\psi(t) = \int_{-\infty}^{\infty} x(t)\psi^*_{a,b}(t)dt \tag{3.2}$$

Where

$$\psi_{a,b}(t) = \frac{1}{\sqrt{a}}\psi\left(\frac{t-a}{b}\right) \tag{3.3}$$

Here, the wavelet $\psi_{a,b}(t)$ is obtained from the mother wavelet ψ(t) by scaling and shifting, where a and b are real positive scaling and shifting factors, respectively.

Standard WT is non-redundant and very powerful tool for many non-stationary signal processing applications, but it suffers from three major limitations; **1**) shift sensitivity, **2**) poor directionality, and **3**) absence of phase information [58]. To reduce these limitations, many researchers developed real-valued extensions to the standard WT such as WP (Wavelet Packet Transform) [59] and SWT (Stationary Wavelet Transform) [60]. These extensions are highly redundant and computationally intensive. Complex Wavelet transform is also an alternate, complex-valued extension to the standard WT [61]. The initial motivation behind the development of complex WT was to avail explicitly both magnitude and phase information to overcome the third

limit. Complex Wavelets transforms use complex-valued filtering (analytic filter) that decomposes the real/complex signals into real and imaginary parts in transform domain. The real and imaginary coefficients are used to compute amplitude and phase information, just the type of information needed to accurately describe the energy localization of oscillating functions (wavelet basis). Morlet wavelet is a complex wavelet that its mother wavelet is defined as

$$\psi(t) = \frac{1}{\sqrt{\pi F_b}} \times \exp\left(j2F_c t\right) \times \exp\left(-\frac{t^2}{F_b}\right) \tag{3.4}$$

whereF_b is the bandwidth parameter and F_c is the center frequency. In this paper, all wavelets have the same bandwidth i.e., 1 Hz, and the only difference is in the frequency center of them. Therefore, all of them have the same F_b and F_c varies from one wavelet to other. In Figure 3.4, the characteristic of Complex Morlet filter including real and imaginary parts, absolute and phase of frequency spectrum, with $F_b = 1$ and $F_c = 0.5$ are shown.

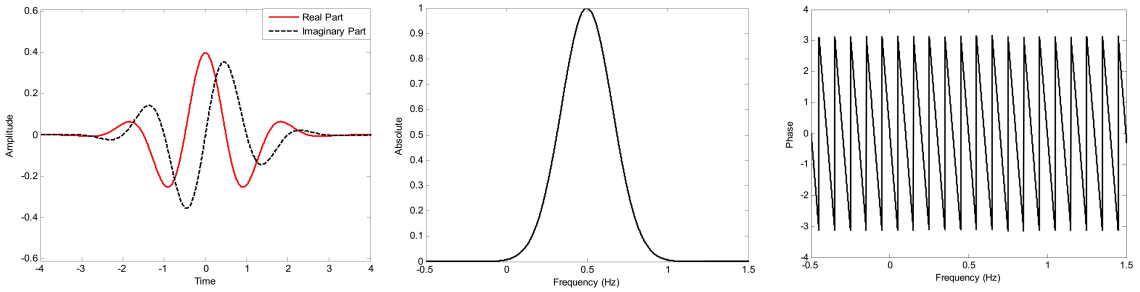

(a) **(b)** **(c)**

Figure 3.4 Characteristics of Complex Morlet filter with $F_b = 1.5$ and $F_c = 0.5$; (a) real and imaginary parts, (b) absolute of Fourier transform, (c) phase of Fourier transform.

3.4.3 Shannon Entropy

From the statistical mechanics perspective of Shannon, entropy is a measure of uncertainty associated with a random variable.*Entropy describes the irregularity, complexity, or unpredictability characteristics of a signal.*If $p(x)$ is the probability that the outcome is x, then $\log(1/p(x))$ is how surprised we would be if the outcome were x. Since $p(x)$ ranges from 0 to 1, the surprise ranges from infinity to zero. *Entropy is the weighted average of the surprise across all outcomes.* Shannon's entropy uses

$h(p(x))$=log$(1/p(x))$ and is the average surprise on discovering the outcome of a random experiment as

$$H(X) = E[h(X)] = E[-\log(p(X))] = -\sum_{x \in \chi} p(x) \log(p(x)) \tag{3.5}$$

Entropy maximizes when p(x) is the same for all x. In the other words, if the histogram or probability density function of x becomes uniform, the entropy of x maximizes [62]. EEG changes from irregular to more regular patterns when anesthesia deepens. Entropy of the signal has been shown to drop when a patient falls asleep and increase again when the patient wakes up [63].

3.4.4 Alpha and Delta Band Partitioning

The behavior of EEG in the whole of α and δ bands is not same. Therefore, these bands should be partitioned into smaller sub-bands.In order to calculate modulation effect, α and δ bands should be partitioned into smaller sub-bands. We consider three different scenarios. *In the first scenario*, partitioning is the same as approach that was used by B. Molaee Ardekan *et al* [53]. They partitioned delta band into three sub-bands; very slow delta (VSD), slow delta (SD), and fast delta (FD) with frequency covering in the range (0.1-0.5) Hz, (0.7-1.7) Hz, and (2-4) Hz, respectively. Whole of the alpha band is considered as one band in the range (8-13) Hz. *The second and third scenarios* are proposed in this thesis. In these scenarios, delta and alpha bands are partitioned into five sub-bands with 1 Hz bandwidth. In both scenarios, the edge frequencies of delta sub-bands are located at integer frequencies. In this manner, different δ sub-bands are (0-1) Hz, (1-2) Hz, (2-3) Hz, (3-4) Hz, and (4- 5) Hz. Difference between second and third scenarios is in the edge frequencies of sub-bands of alpha band. *In the second scenario*, edge frequencies of alpha sub-bands are located at integer frequencies. Therefore, in second scenario, alpha sub-bands are (8-9) Hz, (9-10) Hz, (10-11) Hz, (11-12) Hz, and (12-13) Hz. *In the third scenario*, the center frequencies of alpha sub-bands are located at integer frequencies. So, edge frequencies are the middle of two consecutive integers. Therefore, alpha sub-bands are (7.5-8.5) Hz, (8.5-9.5) Hz,

(9.5-10.5) Hz, (10.5-11.5) Hz, (11.5-12.5) Hz.

The bandwidth parameter of Morlet filter i.e., F_b, is chosen in the way that the absolute of the frequency response is below 0.05 at the edge of each considered frequency band. The obtained values for F_b in first scenario for the very slow delta (VSD), slow delta (SD), fast delta (FD) and alpha band are 10, 1.5, 0.5, and 0.08, respectively. The frequency response of wavelets of different frequency bands are shown in the Figure 3.5. Also, since all sub-bands in the second and third scenarios have the same bandwidth, the value of F_b is equal to 2 for all of them. These sub-bands are shown in Figure 3.6 for second and third scenarios.

3.4.5 Calculation of Signal Modulation

Details of modulation signal calculation between different alpha and delta sub-bands will be discussed in this section. To find the modulation between different delta and alpha sub-bands, we have used the instruction described in the Algorithm 1.

Algorithm 1: Pseudo code of signal modulation calculating algorithm
1 **For** each channel
2 Extract the EEG signal of corresponding channel
3 Segment the EEG signal into different epochs
4 **For** each epoch
5 Remove mean
6 Apply wavelet of alpha band on selected epoch
7 Calculate absolute of signal obtained at line (**6**)
8 Apply wavelet of corresponding delta band on the signal obtained at line (**7**)
9 Calculate absolute of signal obtained at line (**8**)
10 Apply wavelet of corresponding delta band
11 Calculate phase of signal obtained at line (**10**)
12 Calculate the modulation between the signals obtained in the lines **9** and **11** to obtain MS

13 Calculate histogram of MS

14 Calculate Shannon entropy of the MS

15 **End for**

16 **End for**

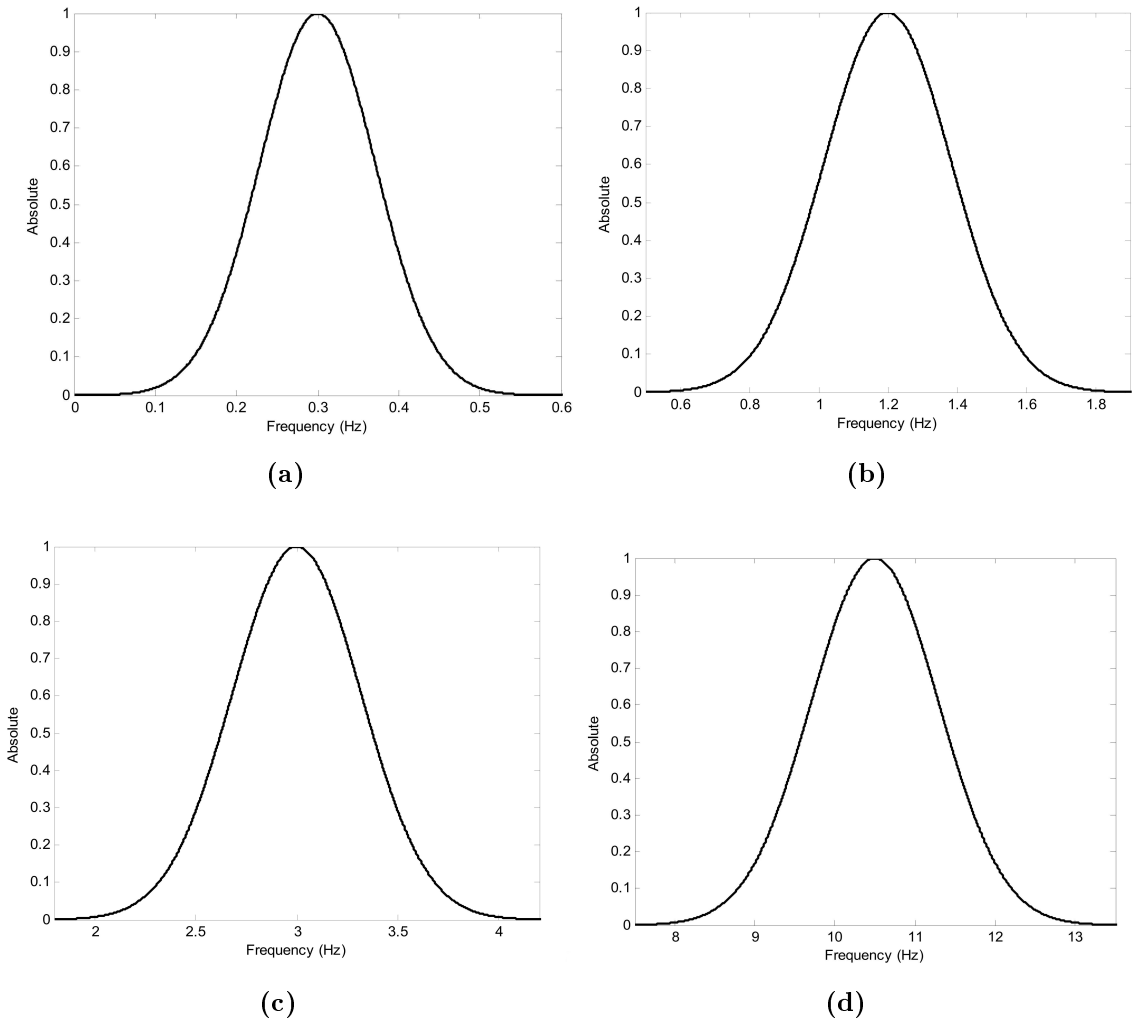

Figure 3.5 Absolute of different Morlet wavelets that used in first scenario; (a) very slow delta sub-band, (b) slow delta sub-band, (a) fast delta sub-band, (d) alpha band.

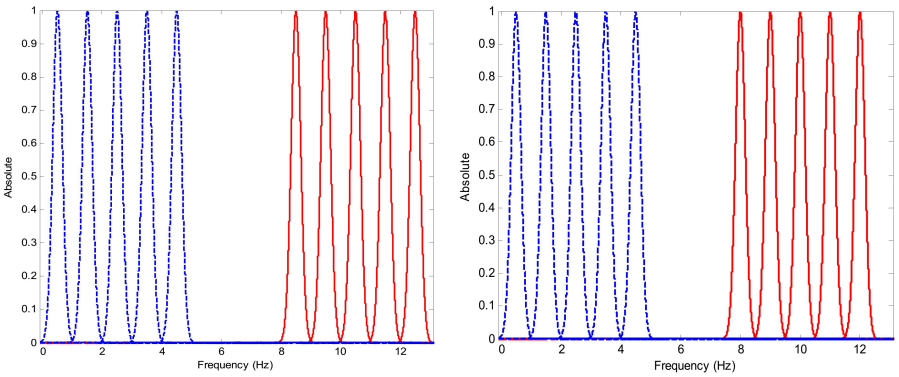

Figure 3.6 Absolute of different Morlet wavelets that used in second and third scenarios; (a) second scenario, (b) third scenario. Blue dashed curves and red solid curves are delta and alpha sub-bands, respectively.

At first, sampling frequency was decimated from 1000 Hz to 100 Hz. EEG signal of each channel was extracted and segmented to 30 epochs of duration 30 seconds with 50% overlapping with each other and then mean of each epoch is removed as in Figure 3.7.

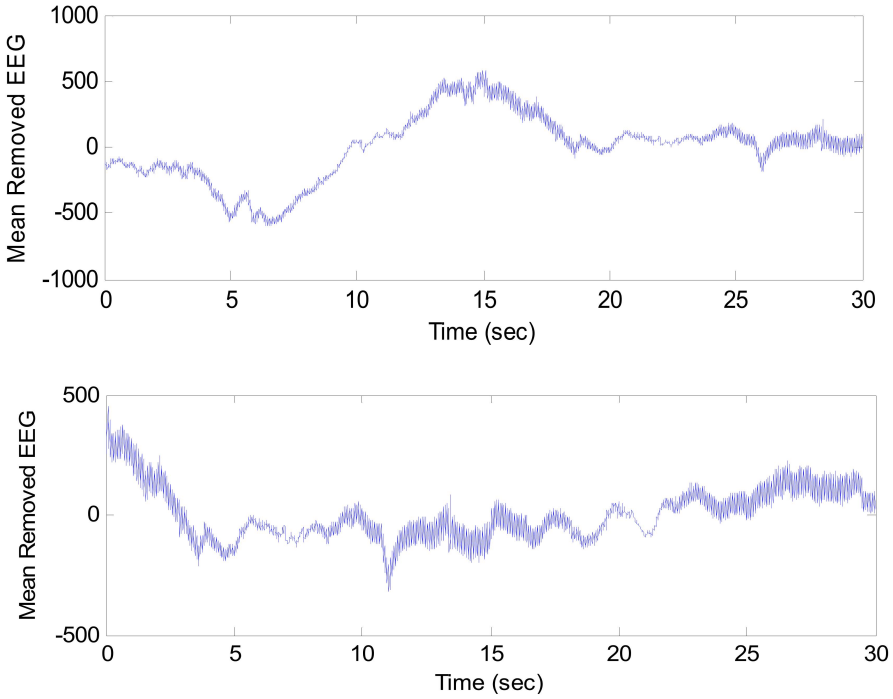

Figure 3.7 Two successive EEG epochs which their means of them are removed.

The ith sub-band of alpha band and jth sub-band of delta band are denoted by α_i and δ_j, respectively. The wavelet of the ith sub-band of α and the jth sub-band of δ are shown by $\psi_{\alpha_i}$and ψ_{δ_j}, respectively. In the first part, the kth preprocessed epoch

$(x_k(t))$ is decomposed by wavelet of the ith sub-band of α as:

$$W_{\alpha_i}^k(t) = \int_{-\infty}^{\infty} x_k(t)\, \psi_{\alpha_i}^*(t)\, dt \tag{3.6}$$

Then, the absolute of $W_{\alpha_i}^k(t)$ is calculated as

$$\left|W_{\alpha_i}^k(t)\right| = \sqrt{\left(\Re\left\{W_{\alpha_i}^k(t)\right\}\right)^2 + \left(\Im\left\{W_{\alpha_i}^k(t)\right\}\right)^2} \tag{3.7}$$

where$\Re\{.\}$ and $\Im\{.\}$ denote the real and imaginary parts of the signal, respectively. Then, $\left|W_{\alpha_i}^k\right|$ is decomposed by wavelet of the jth sub-band of δ band as

$$W_{\alpha_i,\delta_j}^k(t) = \int_{-\infty}^{\infty} \left|W_{\alpha_i}^k(t)\right| \psi_{\delta_j}^*(t)\, dt \tag{3.8}$$

In order to compare the envelope of the alpha band and phase of delta band together, they must have the same frequency range. Therefore, at first envelope of the signal in the alpha band is obtained by applying the wavelet of corresponding alpha sub-band and then its absolute is calculated. Then, the obtained envelope in the alpha band is passed through wavelet of the corresponding delta band to obtain the activity of the alpha envelope in the corresponding delta sub-band. This envelope in the delta band is compared by the phase of the signal obtained by applying the wavelet of delta band to calculate the modulation signal. This approach is similar to the approach used in amplitude-modulated radios.

At the end of the first part, the absolute value of $W_{\alpha_i,\delta_j}^k$is calculated and denoted by $(\left|W_{\alpha_i,\delta_j}^k(t)\right|)$.

In the second part, at first, $x_k(t)$ is decomposed by the decomposition wavelet of $j$thsub-band of δ as:

$$W_{\delta_j}^k(t) = \int_{-\infty}^{\infty} x_k(t)\, \psi_{\delta_i}^*(t)\, dt \tag{3.9}$$

At the end of the second part, phase of $W_{\delta_j}^k(t)$ is calculated as:

$$\angle W_{\delta_j}^k(t) = \tan^{-1}\left(\frac{\Re\left\{W_{\delta_j}^k(t)\right\}}{\Im\left\{W_{\delta_j}^k(t)\right\}}\right) \tag{3.10}$$

To calculate the MS between α_i and δ_j ($\mathrm{MS}(\alpha_i, \delta_j)$), Molaee Ardekan's [53], approach is used. The range [-π π) is divided into 62 non-overlapping bins (about 0.1 rad for each bin). Then, the samples of $\angle W_{\delta_j}^k(t)$ that have the same bin are identified. Finally, each sample of MS is the mean of $\left|W_{\alpha_i,\delta_j}^k\right|$ that has the same$\angle W_{\delta_j}^k(t)$. At the last step, the Shannon entropy of MS is calculated [64]. To calculate the entropy, 62 bin histograms of the MS are computed and then the entropy is calculated as:

$$H = -\sum_{n=1}^{62} P_n \log_2(P_n) \tag{3.11}$$

where P_n is the probability of each bin in the histogram which is calculated as

$$P_n = \frac{N_n}{62} \tag{3.12}$$

3.5 Mann-Whitney U Test

This is a non-parametric test that can be used in place of an unpaired t-test. It is used to test the null hypothesis that two samples come from the same population (i.e. have the same median) or, alternatively, whether observations in one sample tend to be larger than observations in the other. Although it is a non-parametric test, it does assume that the two distributions are similar in shape [64]. In this thesis, Mann-Whitney U test was used to analysis the difference between probability density function (PDF) of the entropies related to different BIS intervals.

Assume there are sample of n_x observations {x_1, x_2, ...,x_n} in one group (i.e. from one population) and a sample of n_y observations {y_1, y_2, ..., y_n} in another group (i.e. from another population). The Mann-Whitney test is based on a comparison of

every observation x_i in the first sample with every observation y_j in the other sample. The total number of pairwise comparisons that can be made is $n_x \times n_y$. If the samples have the same median, then each x_i has an equal chance (i.e. probability 0.5) of being greater or smaller than each y_j.

Therefore, null hypothesis can be expressed as:

$$H_0 = P\left(x_i > y_j\right) = 0.5 \tag{3.13}$$

And alternative hypothesis can be expressed as:

$$H_1 = P\left(x_i > y_j\right) \neq 0.5 \tag{3.14}$$

The number of times one x_i from sample 1 is greater than an y_j from sample 2 is counted. This number is denoted by U_x. Similarly, the number of times ax_i from sample 1 is smaller than an y_j from sample 2 is denoted by Uy. Under the null hypothesis, it should be expected that U_x and U_y to be approximately equal. Procedure for carrying out the test is as follows:

a. Arrange all the observations in order of magnitude.

b. Under each observation, write down X or Y (or some other relevant symbol) to indicate which sample they are from.

c. Under each x write down the number of ys which are to the left of it (i.e. smaller than it); this indicates $x_i > y_j$. Under each y write down the number of xs which are to the left of it (i.e. smaller than it); this indicates $y_j > x_i$.

d. Add up the total number of times $x_i > y_j$, and denote by U_x. Also, add up the total number of times $y_j > x_i$, and denote by U_y. Check that $U_x + U_y = n_x \times n_y$

e. Calculate $U = \min\{U_x, U_y\}$

Use statistical tables for the Mann-Whitney U test to find the probability of observing a value of U or lower. If the test is one-sided, this is your p-value; if the test is a

two-sided test, double this probability to obtain the p-value.

4. RESULTS

4.1 Results of First Scenario

In first scenario, we have three delta sub-bands i.e., very slow delta (δ_1), slow delta (δ_2), and fast delta (δ_3)) and one alpha sub-band (α_1). In the Figure 4.1, the different signals obtained during the modulation calculation for one epoch are shown.

The BIS values were partitioned to four ranges as 20-40, 40-60, 60-80, and 80-100, in order to compare the calculated entropy of modulation signal with corresponding recorded BIS values.From the anesthesiologist point of view BIS values lower than 20 has vital risks to patients. So we choose 20 as a beginning point to segmentation of the BIS index. Then the BIS value of each epoch is averaged.The entropies of epochs that their BIS are in the before mentioned ranges are averaged for every patient. The obtained results are shown for them as following.

In figures from 4.2 to 4.7, the mean entropy of epochs that their BIS belongs to predefined ranges i.e., 20-40, 40-60, 60-80, and 80-100, are plotted for different patients. As seen the modulation between alpha and three delta sub-bands (very slow, slow and fast) is considerable.

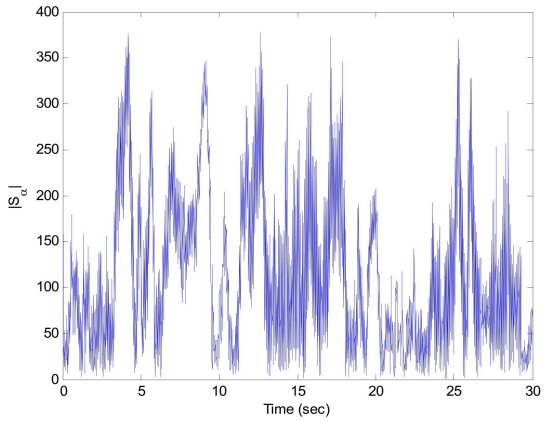
|S_α|
Time (sec)

(a)

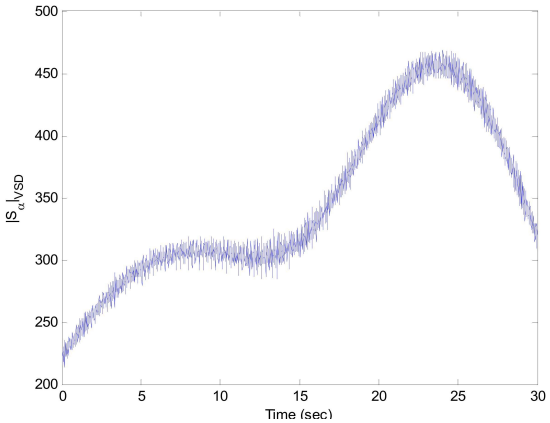
|S_α|_VSD
Time (sec)

(b)

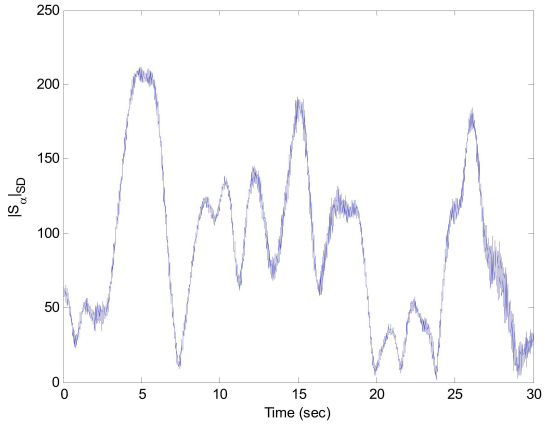
|S_α|_SD
Time (sec)

(c)

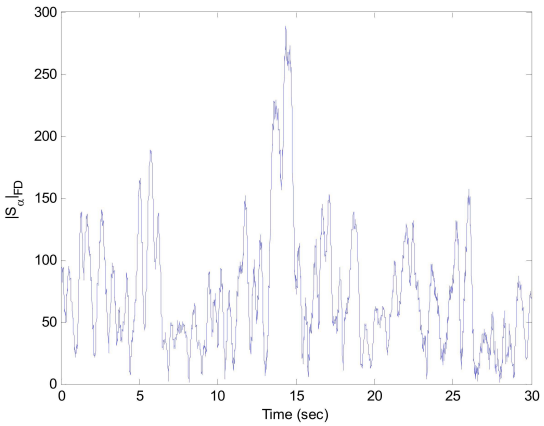
|S_α|_FD
Time (sec)

(d)

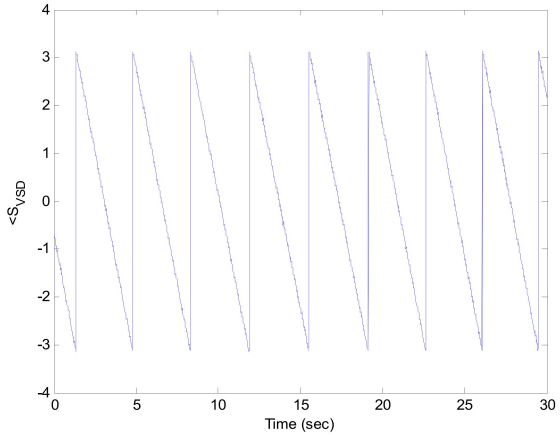
<S_VSD
Time (sec)

(e)

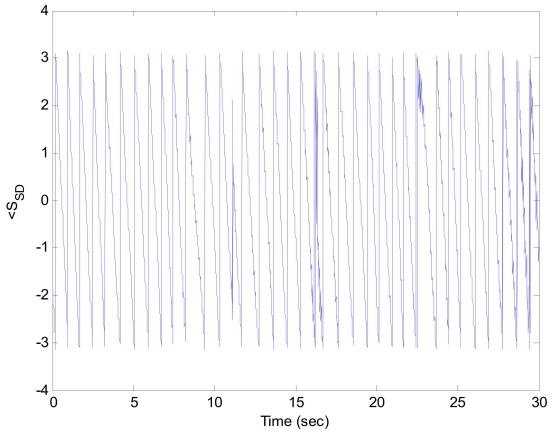
<S_SD
Time (sec)

(f)

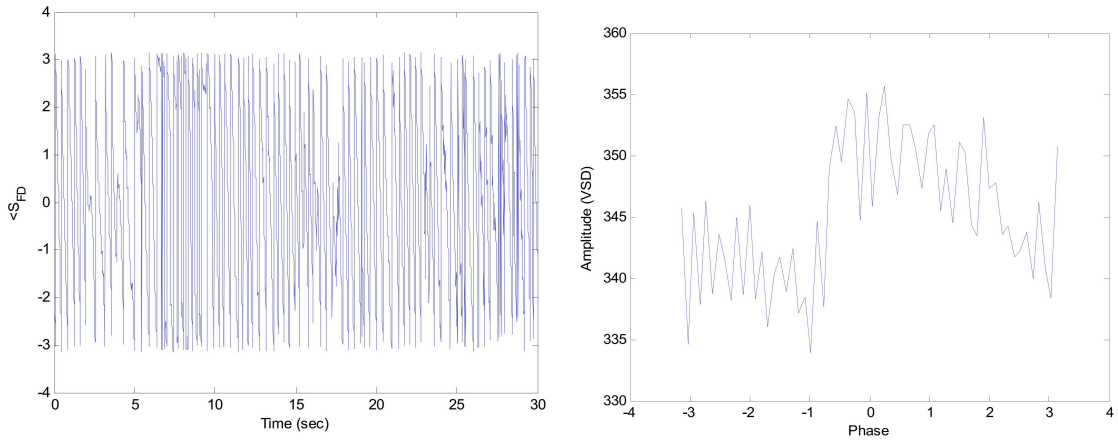

(g) **(h)**

Figure 4.1 The signals obtained during algorithm 1 for the first scenario. (a) $\left|W^k_{\alpha_1}(t)\right|$, (b) $\left|W^k_{\alpha_1,\delta_1}(t)\right|$, (c) $\left|W^k_{\alpha_1,\delta_2}(t)\right|$, (d) $\left|W^k_{\alpha_1,\delta_3}(t)\right|$, (e) $\angle W^k_{\delta_1}(t)$, (f) $\angle W^k_{\delta_2}(t)$, (g) $\angle W^k_{\delta_3}(t)$, (h) $\mathrm{MS}(\alpha_1,\delta_1)$, (i) $\mathrm{MS}(\alpha_1,\delta_2)$, (j) $\mathrm{MS}(\alpha_1,\delta_3)$

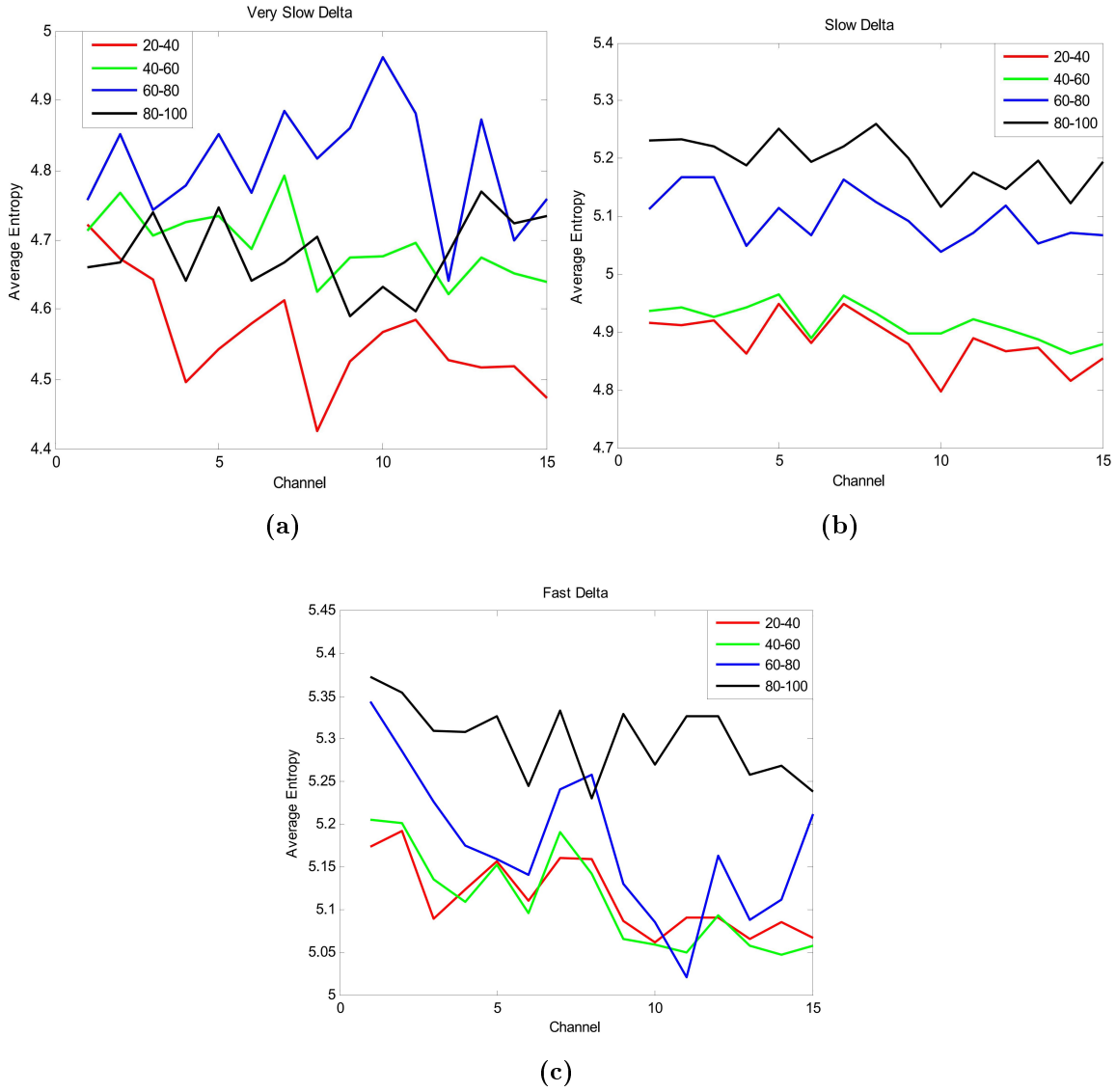

Figure 4.2 Mean entropy of epochs that their BIS belongs to predefined ranges i.e., 20-40, 40-60, 60-80, and 80-100 for **patient 12**; (a) Very slow delta, (b) Slow delta, (c) Fast delta

In the Table 4.1, the channels that have modulation among their alpha and delta sub-bands are presented. As seen, the modulation effect between alpha and slow delta sub-band is exist in most channels of all patients except patient 23.

As seen, there is no common channel in all patients for very slow and fast delta sub-bands. For slow sub-band, the modulation effect is seen in channels 8, 9, 10, 11, 13, 14, and 15 in all patients, except patient 23(During Op period despite the presence of BIS value at 23,signs of awareness were seen in this patient). We conclude that for the modulation effect between alpha and slow delta sub-band, in channels 8, 9, 10, 11,

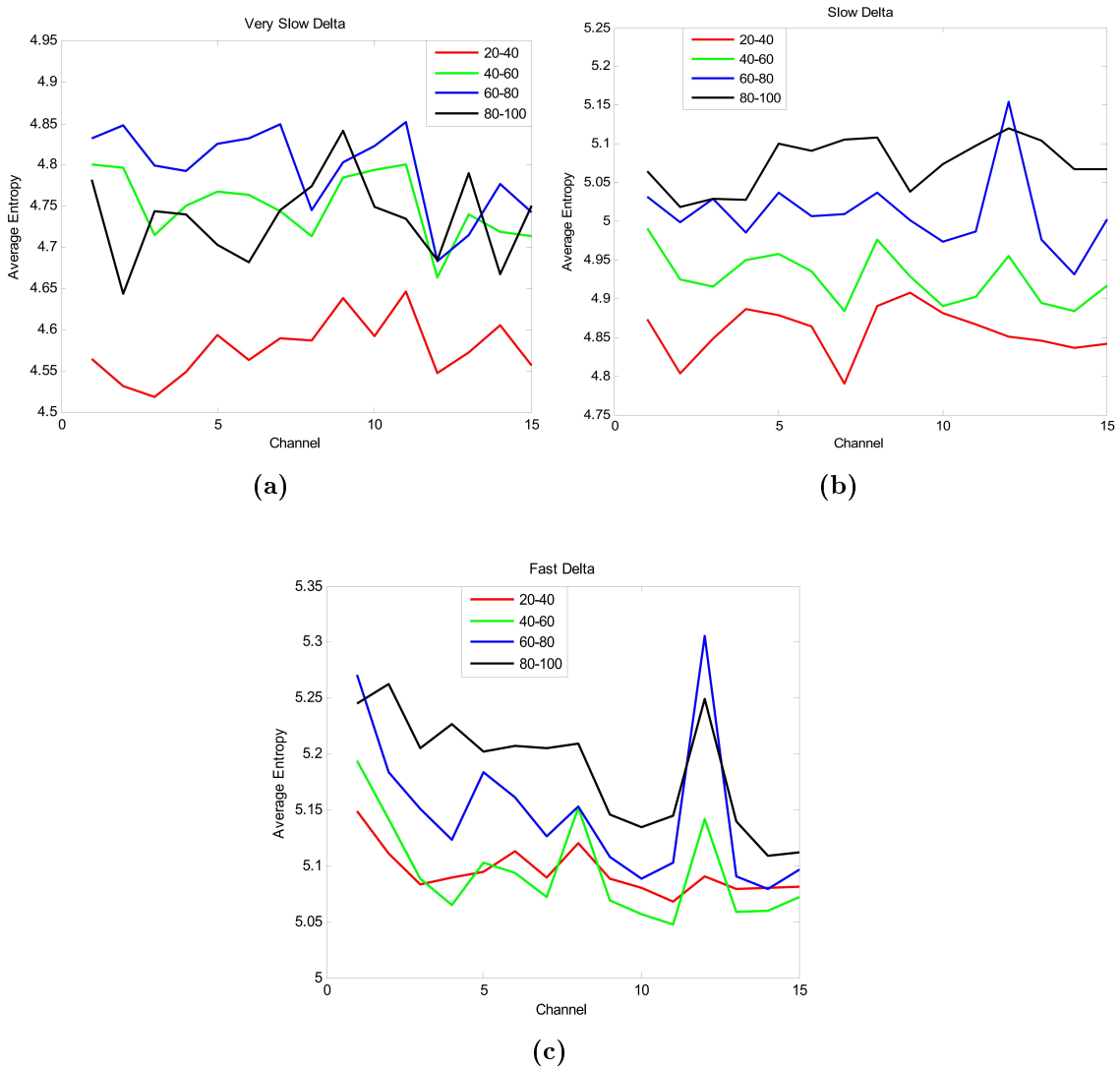

Figure 4.3 Mean entropy of epochs that their BIS belongs to predefined ranges i.e., 20-40, 40-60, 60-80, and 80-100 for **patient 13**; (a) Very slow delta, (b) Slow delta, (c) Fast delta

Table 4.1
Channels that have modulation effect in first scenario

Patient	Alpha	Delta		
		Very Slow Delta	***Slow Delta***	***Fast Delta***
12	***Alpha***	12	**All**	1, 2, 7
13	***Alpha***	9	**All** (E. 3, 12)	2, 8, 12
14	***Alpha***	9, 11, 12, 13, 14, 15	**All**	6, 11, 13, 14, 15
17	***Alpha***	10, 13	**All**	5, 6
23	***Alpha***	—	Partly 9	—
24	***Alpha***	6, 8, 12	9, 13, 14	3, 4, 5, 6, 8, 9, 10

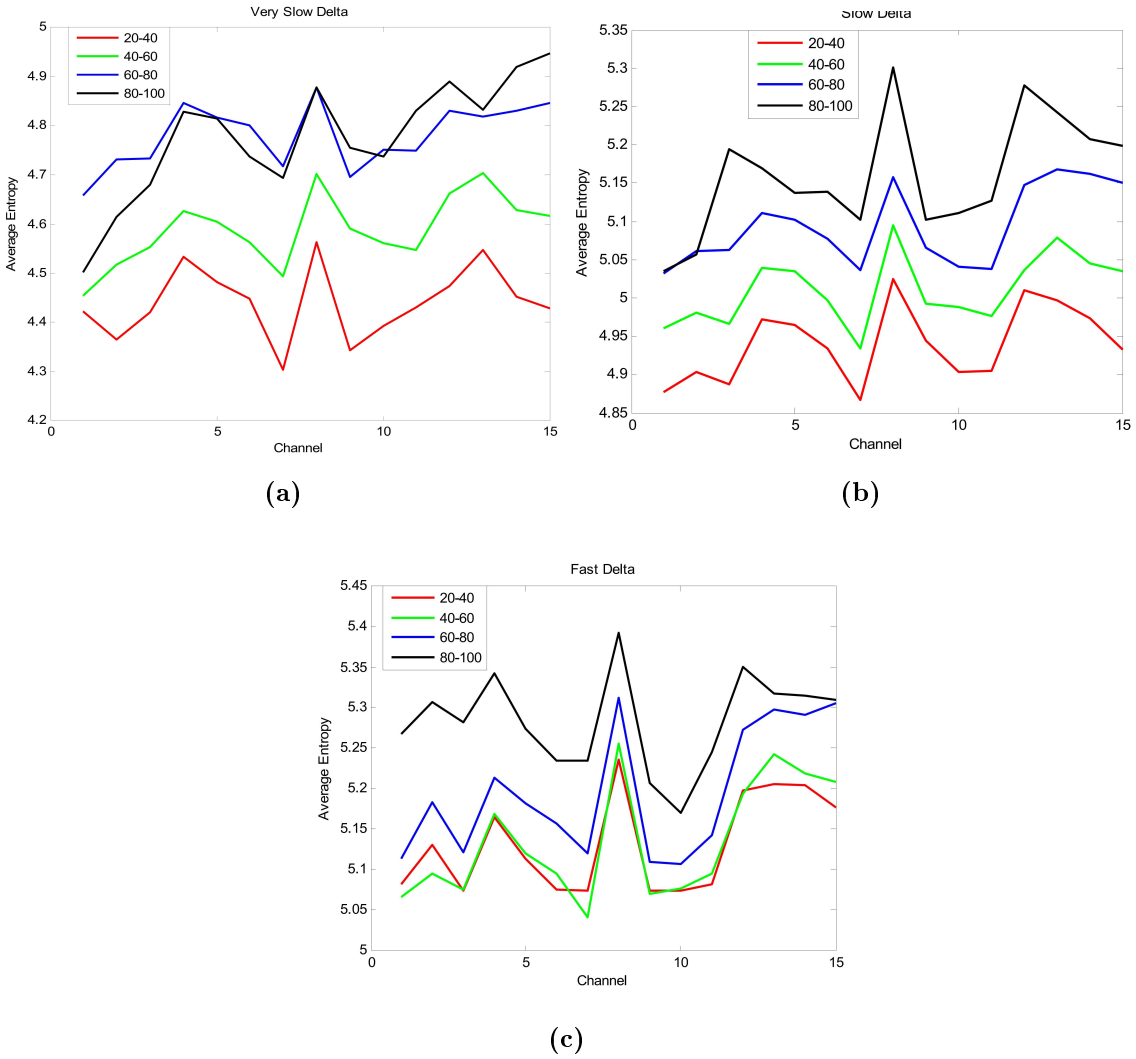

Figure 4.4 Mean entropy of epochs that their BIS belongs to predefined ranges i.e., 20-40, 40-60, 60-80, and 80-100 for **patient 14**; (a) Very slow delta, (b) Slow delta, (c) Fast delta

13, 14, and 15 can be used to determine depth of anesthesia. So the channel **9** ($\mathbf{C_3}$) which is common in all patients is selected to do the rest of processing on it. We plot the mean and standard deviation of the entropy of the channel 9 for slow delta-band in Figure 4.8, which is common in all patients.

The histogram of modulation signal between alpha and slow delta sub- band for various BIS intervals are shown at channel 9 in Figure 4.9 for all patients.

The entropy of modulation between alpha and slow delta band for the different patients in channel 9 is presentedin Figure 4.10 and the BISs are also shown for

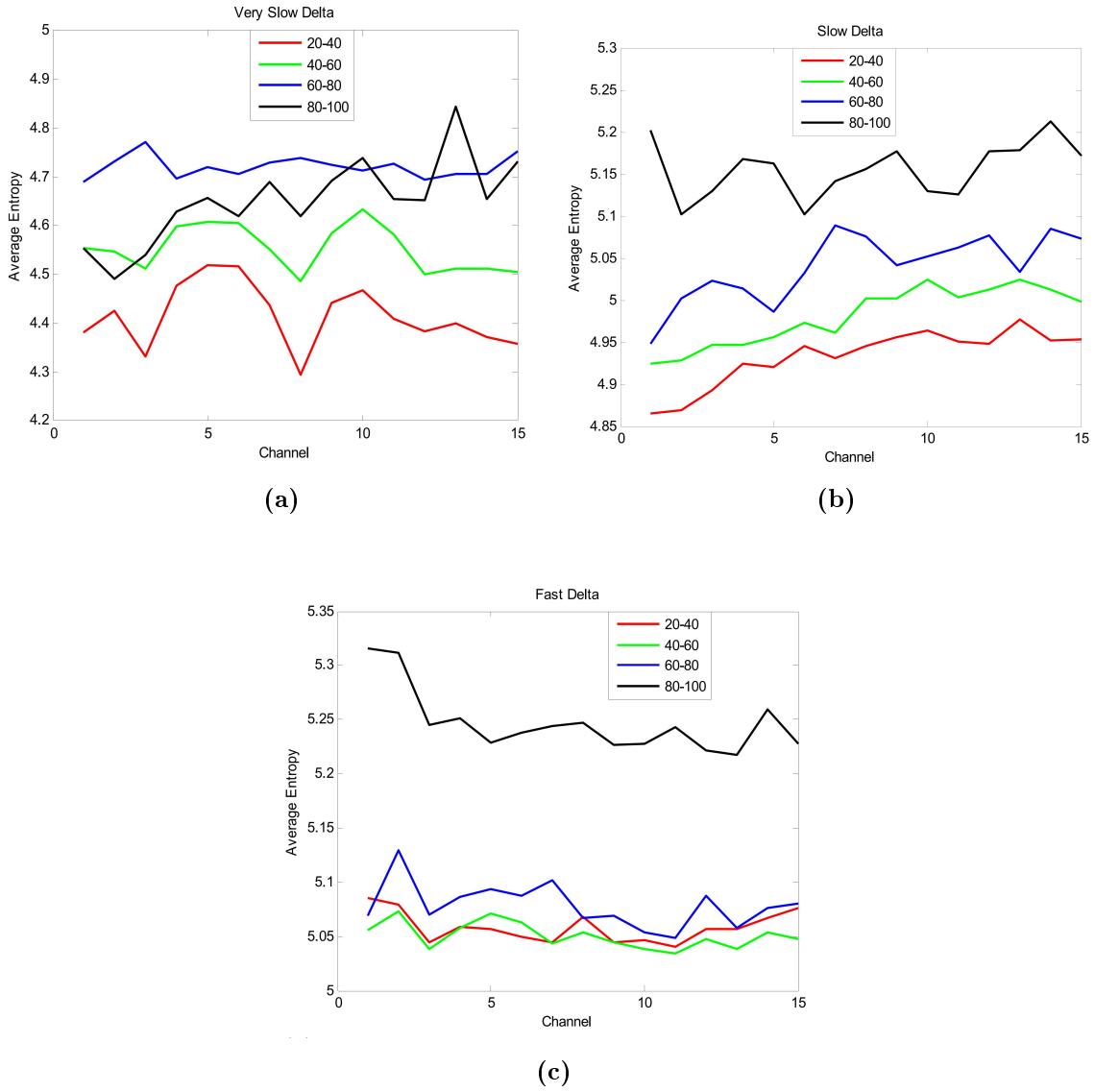

Figure 4.5 MMean entropy of epochs that their BIS belongs to predefined ranges i.e., 20-40, 40-60, 60-80, and 80-100 for **patient 17**; (a) Very slow delta, (b) Slow delta, (c) Fast delta

comparison. It is observed that the variation in BIS is captured by entropy.

We divided the BIS ranges from 0 to 100 into four intervals, 20-40 (R_a), 40-60 (R_b), 60-80 (R_c) and 80-100 (R_d)in order to compare the statistics of entropies correspond to different BIS intervals. For each patient, Mann-Whitney test is performed for all possible pairs of entropies related to R_a, R_b, R_c and R_d, where significance level is set to 0.05. Obtained results are presented in the Table 2.1, where p and h denote the p-value and test decision, respectively. If p-value is smaller than the significance level, null hypothesis is rejected i.e., $h = 1$(x and y comes from different continuous

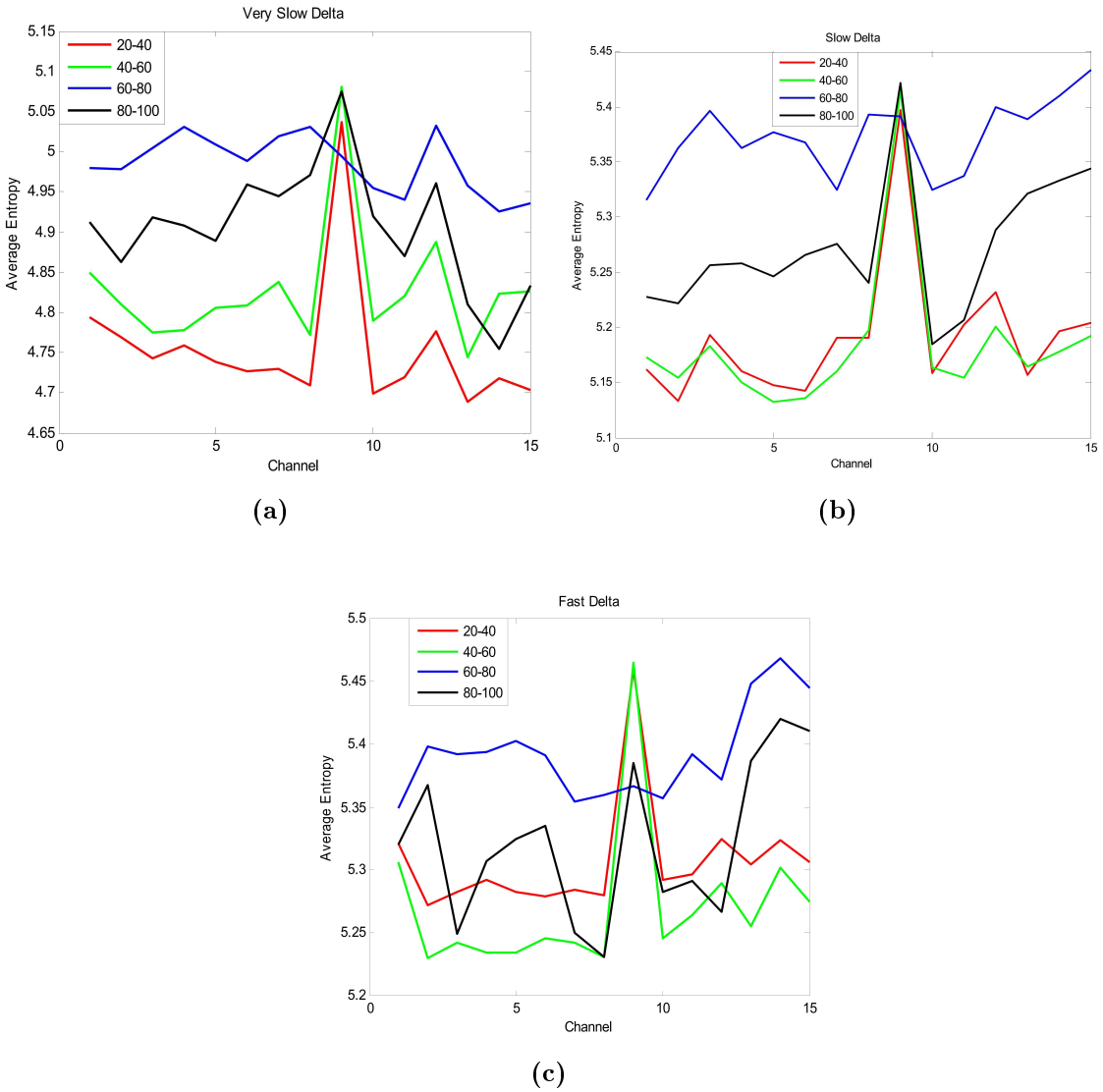

Figure 4.6 Mean entropy of epochs that their BIS belongs to predefined ranges i.e., 20-40, 40-60, 60-80, and 80-100 for **patient 23**; (a) Very slow delta, (b) Slow delta, (c) Fast delta

distribution), otherwise test is accepted i.e., $h = 0$. As seen, in most cases, the null hypothesis is rejected. Also, obtained p-values in the case of test rejection are much smaller than the 0.05 which indicates that the test rejects the null hypothesis strongly and related entropies of different BIS intervals (i.e., R_a, R_b, R_c and R_d) have different continuous distributions. We also, merge the entropies of all patients together and then perform statistical test. Obtained results are presented in last column of Table 4.2. In this case also results indicate that null hypothesis strongly is rejected. Most results in this Table indicate that entropies of the different BIS intervals come from different distributions which indicate that proposed method can be used to measure DOA.

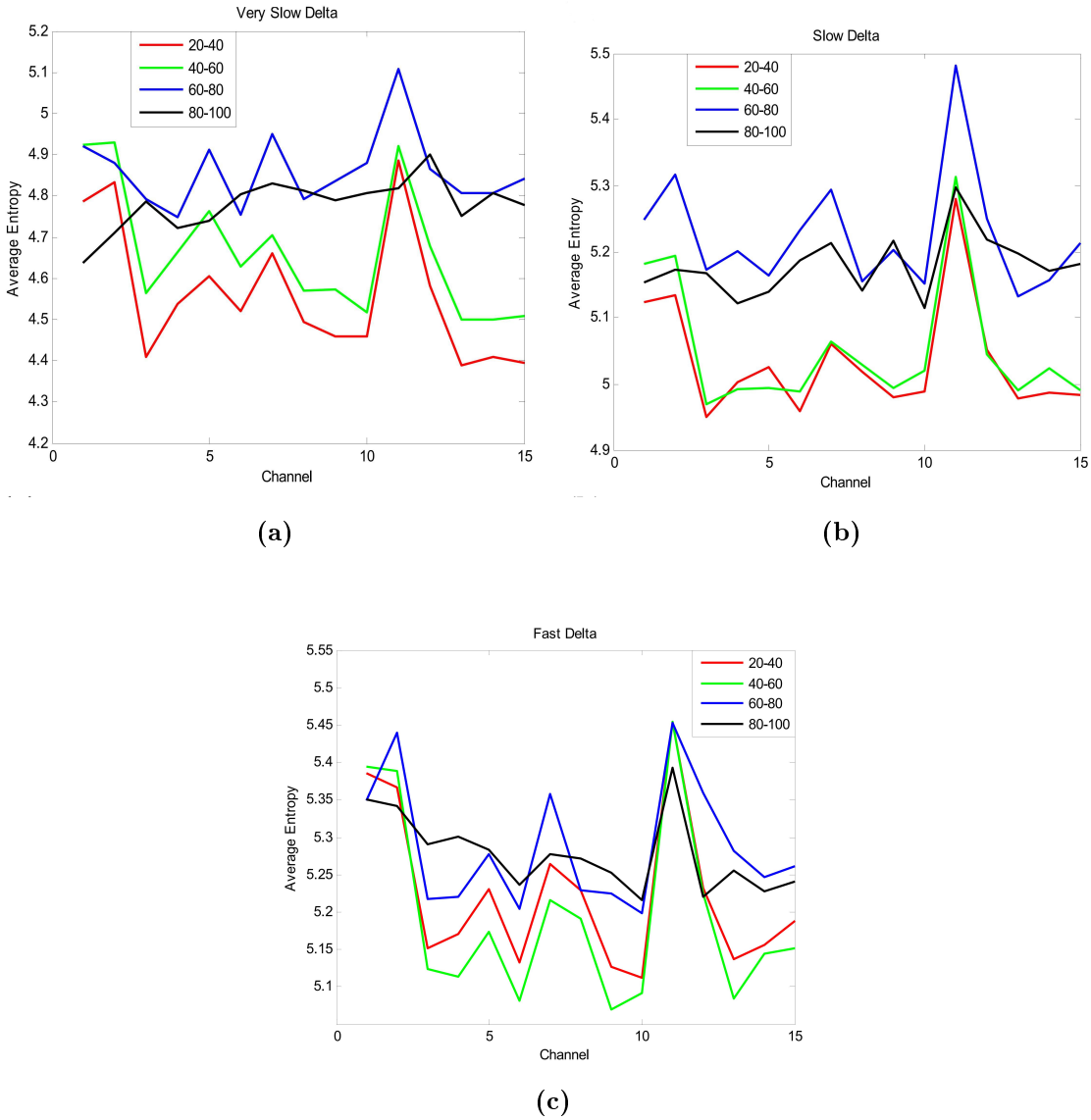

Figure 4.7 Mean entropy of epochs that their BIS belongs to predefined ranges i.e., 20-40, 40-60, 60-80, and 80-100 for **patient 24**; (a) Very slow delta, (b) Slow delta, (c) Fast delta

Table 4.2
Results of Mann-Whitney Test for first scenario, $h = 1$ denotes BIS ranges have different distributions, While $h = 0$ indicates, they have same distributions

BIS ranges	Test Result	Patient						
		12	13	14	17	23	24	Overall
R_a, R_b	h (p)	0 (0.51)	0 (0.33)	1 (0.011)	1 (0.0025)	0 (0.081)	0 (0.36)	1 (2.9e-14)
R_a, R_c	h (p)	1 (0.0011)	1 (0.00011)	1 (5.1e-08)	1 (7.1e-06)	0 (0.78)	1 (9.3e-10)	0 (0.33)
R_a, R_d	h (p)	1 (6.9e-07)	1 (7.5e-05)	1 (7.7e-07)	1 (1.2e-10)	0 (0.16)	1 (4.5e-12)	1 (4.6e-09)
R_b, R_c	h (p)	1 (0.00023)	1 (0.00023)	1 (1.31e-05)	1 (0.027)	0 (0.39)	1 (1.5e-08)	1 (5.4e-16)
R_b, R_d	h (p)	1 (8.6e-09)	1 (0.00022)	1 (5.2e-05)	1 (1.1e-07)	0 (0.61)	1 (9.9e-11)	1 (3.3e-29)
R_c, R_d	h (p)	0 (0.058)	0 (0.22)	0 (0.099)	1 (3.3e-05)	0 (0.36)	0 (0.56)	1 (4.5e-09)

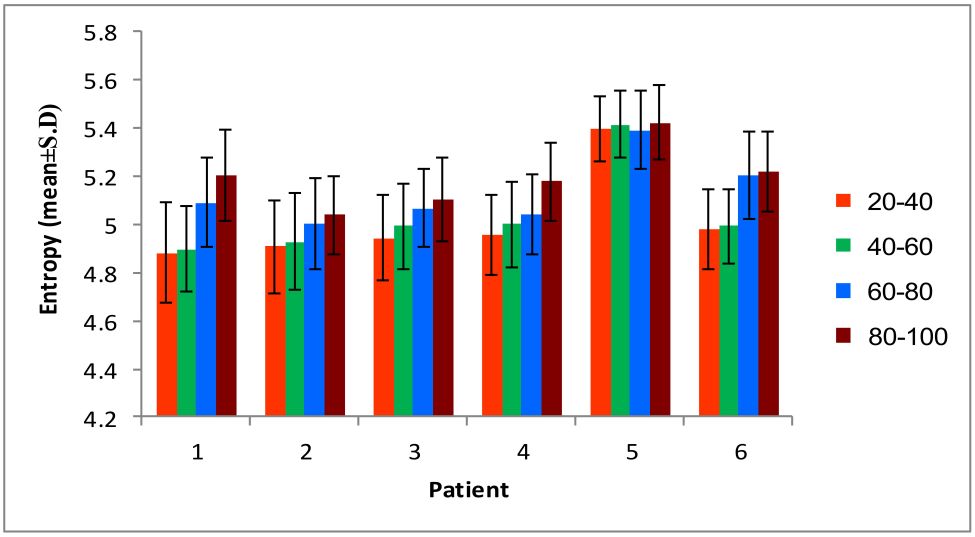

Figure 4.8 Mean and standard deviation of entropy of modulation signal at slow delta sub-band in channel 9 for different BIS intervals in first scenario

4.2 Results of Second Scenario

The procedure is similar to one that introduced in the previous section. The obtained results are as following. The average entropies of BISs related to different alpha and delta bands are shown in Figures from 4.11 to 4.16. By analyzing these Figures, the channels which have modulation effect between alpha and delta sub-bands in all patients, is presented in Table 4.3. In some cells, "All (E. x)" was written, it means that all channels have modulation effect except channel/channels x.

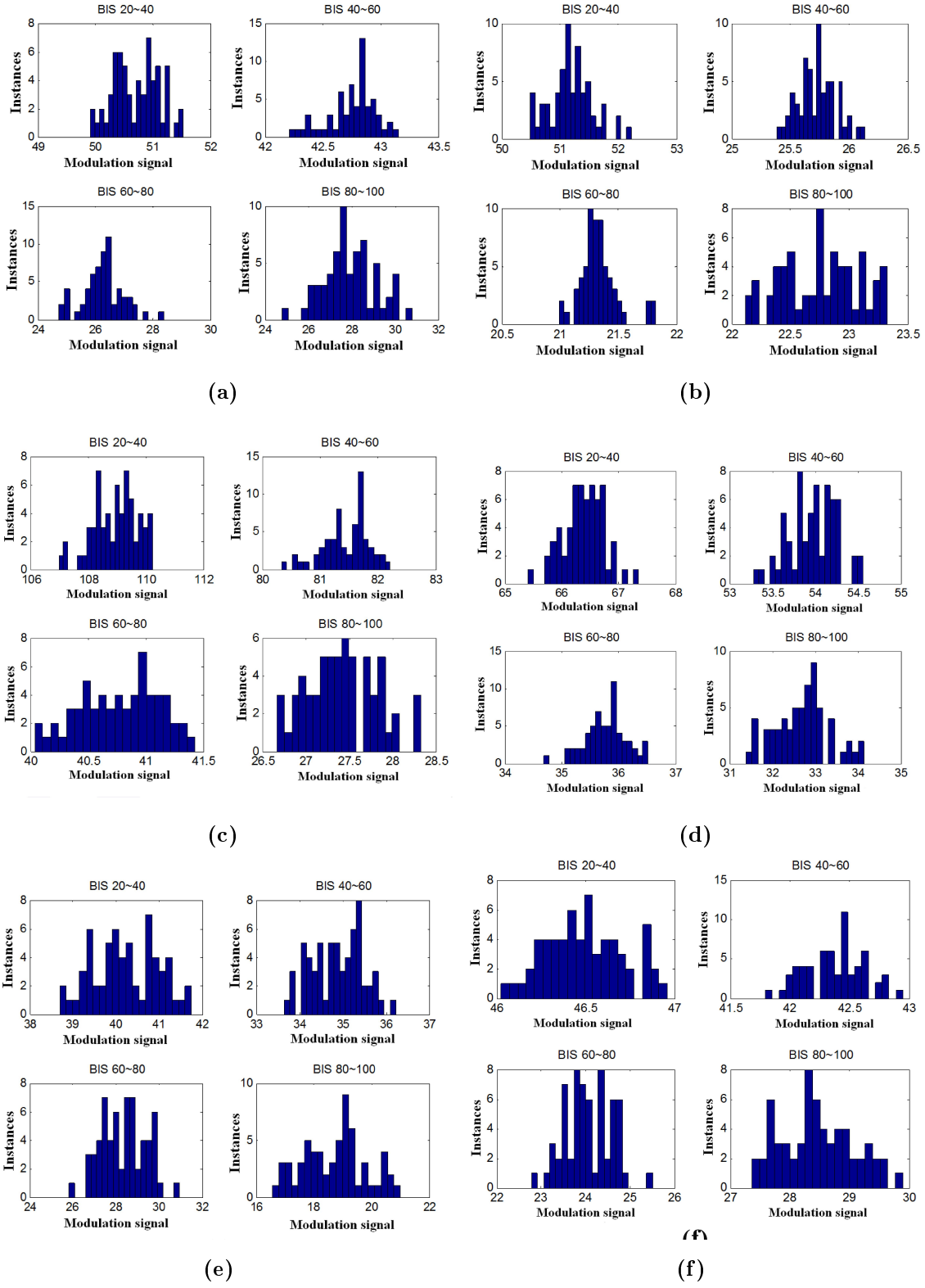

Figure 4.9 Histogram of modulated signal for different BIS ranges in first scenario; (a) Patient 12, (b) Patient 13, (c) Patient 14, (d) Patient 17, (e) Patient 23, (f) Patient 24,

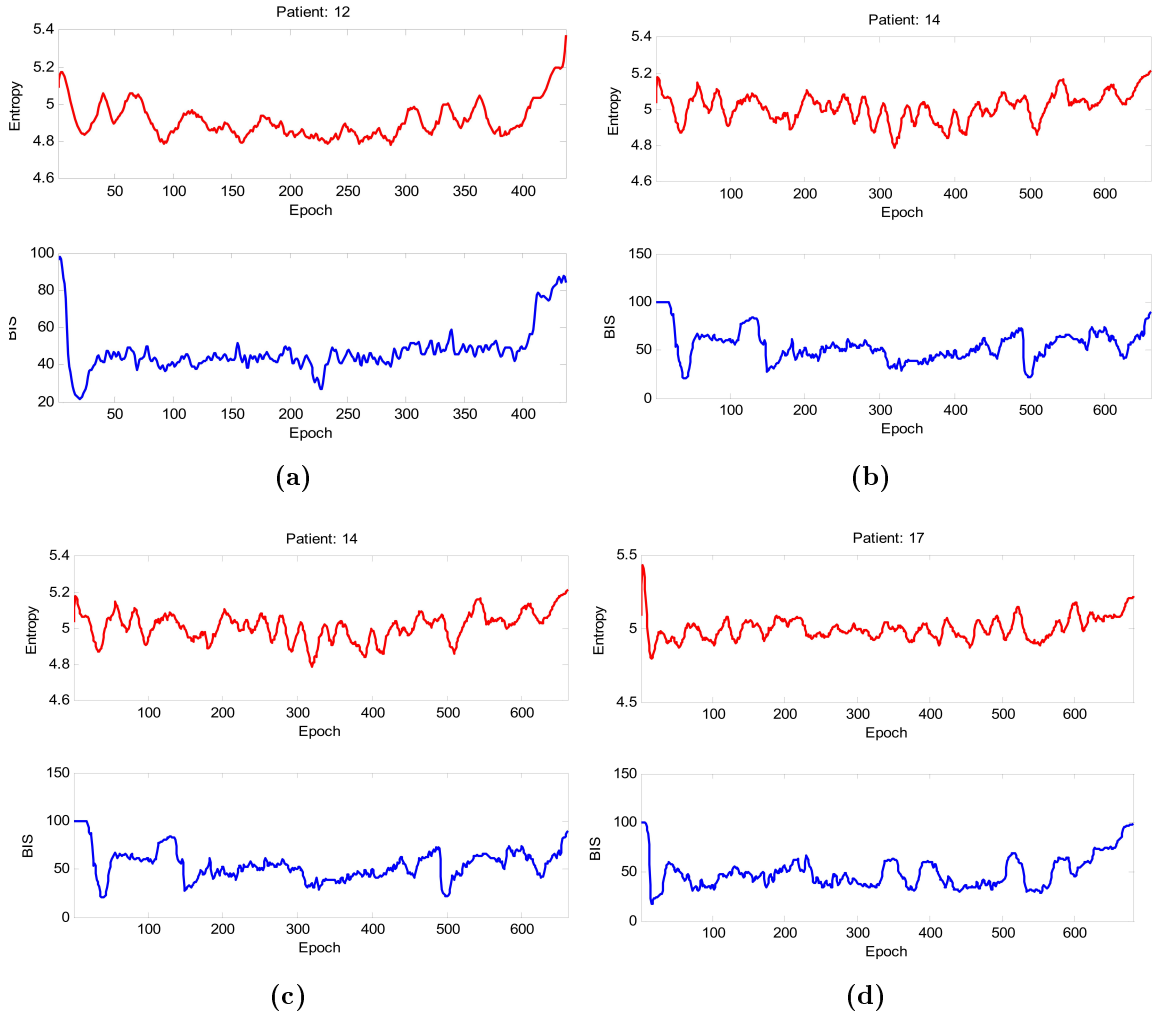

Figure 4.10 The variation of entropy and BIS during time in first scenario; (a) Patient 12, (b) Patient 13, (c) Patient 14, (d) Patient 17, (e) Patient 23, (f) Patient 24

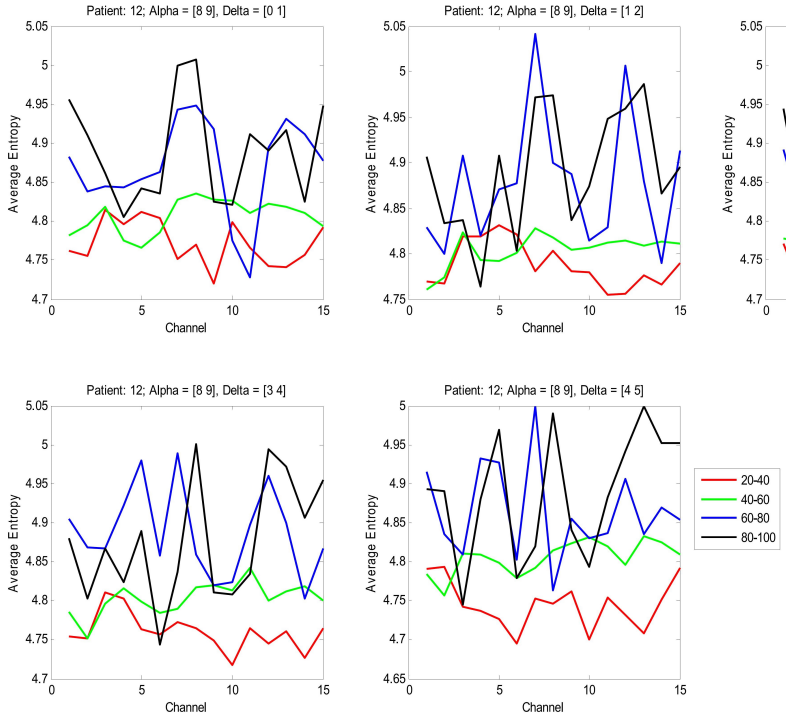
Patient: 12; Alpha = [8 9], Delta = [0 1]
Patient: 12; Alpha = [8 9], Delta = [1 2]
Patient: 12; Alpha = [8 9], Delta = [2 3]
Patient: 12; Alpha = [8 9], Delta = [3 4]
Patient: 12; Alpha = [8 9], Delta = [4 5]
Average Entropy
Channel
20-40
40-60
60-80
80-100

(a)

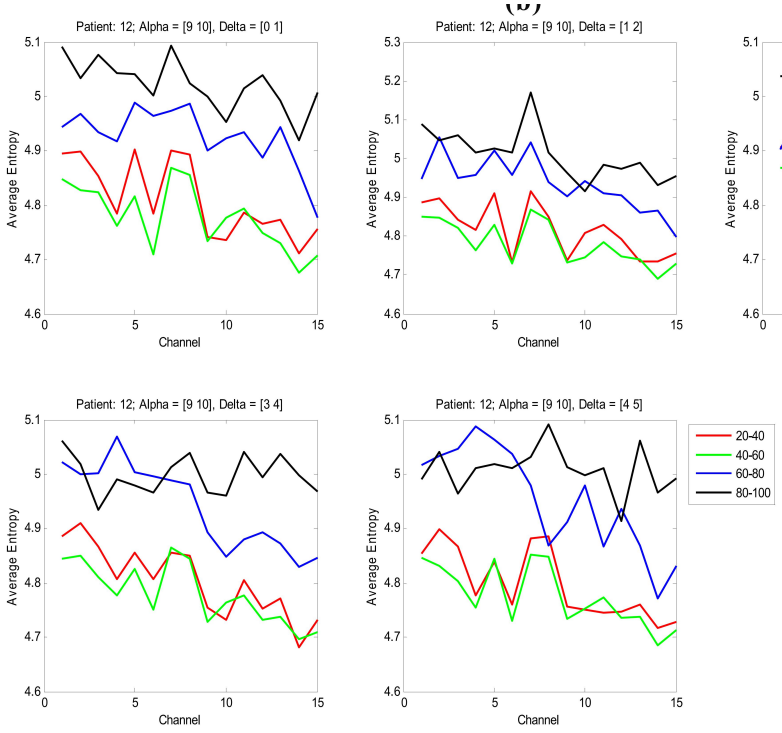
Patient: 12; Alpha = [9 10], Delta = [0 1]
Patient: 12; Alpha = [9 10], Delta = [1 2]
Patient: 12; Alpha = [9 10], Delta = [2 3]
Patient: 12; Alpha = [9 10], Delta = [3 4]
Patient: 12; Alpha = [9 10], Delta = [4 5]
Average Entropy
Channel
20-40
40-60
60-80
80-100

(b)

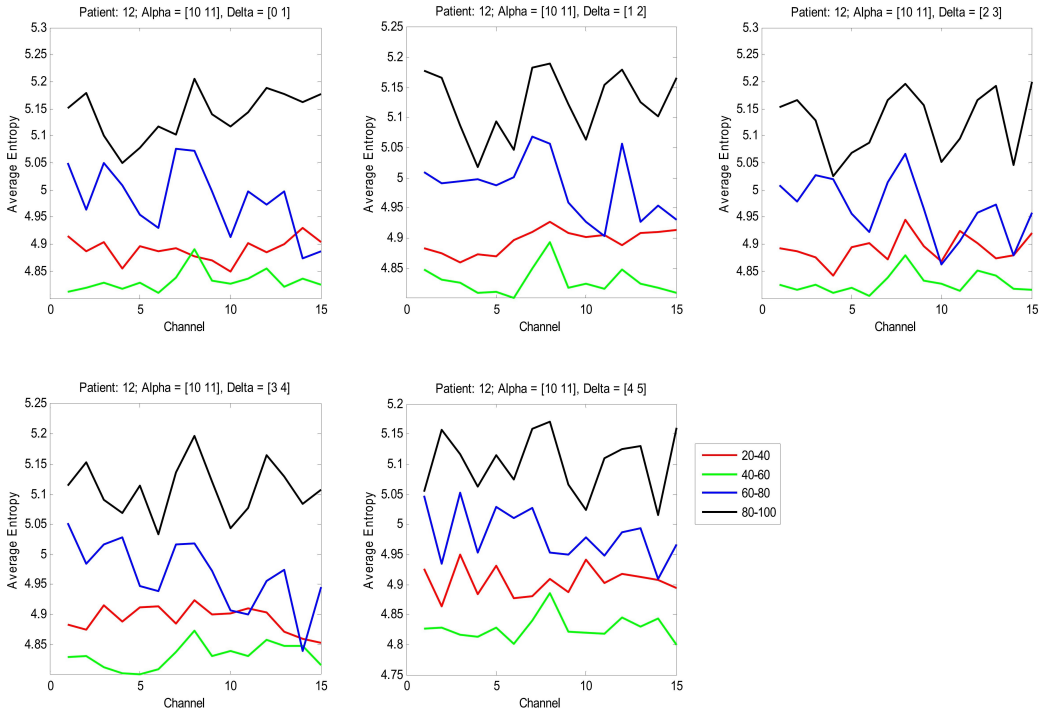
Patient: 12; Alpha = [10 11], Delta = [0 1]
Patient: 12; Alpha = [10 11], Delta = [1 2]
Patient: 12; Alpha = [10 11], Delta = [2 3]
Patient: 12; Alpha = [10 11], Delta = [3 4]
Patient: 12; Alpha = [10 11], Delta = [4 5]
Average Entropy
Channel
20-40
40-60
60-80
80-100

(c)

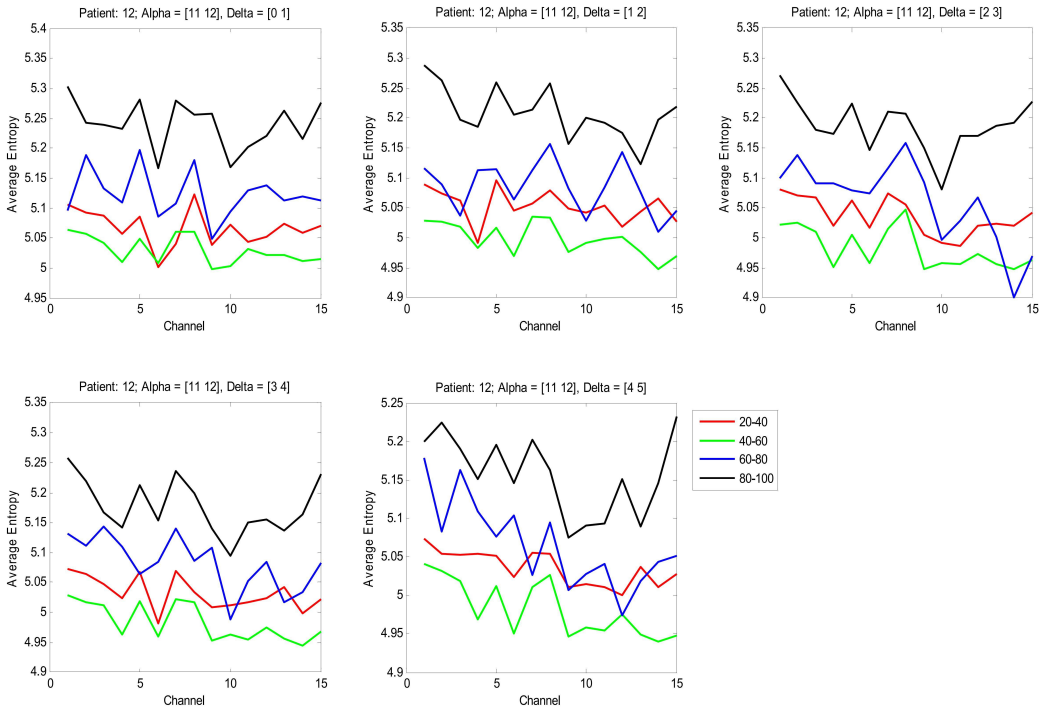
Patient: 12; Alpha = [11 12], Delta = [0 1]
Patient: 12; Alpha = [11 12], Delta = [1 2]
Patient: 12; Alpha = [11 12], Delta = [2 3]
Patient: 12; Alpha = [11 12], Delta = [3 4]
Patient: 12; Alpha = [11 12], Delta = [4 5]
Average Entropy
Channel
20-40
40-60
60-80
80-100

(d)

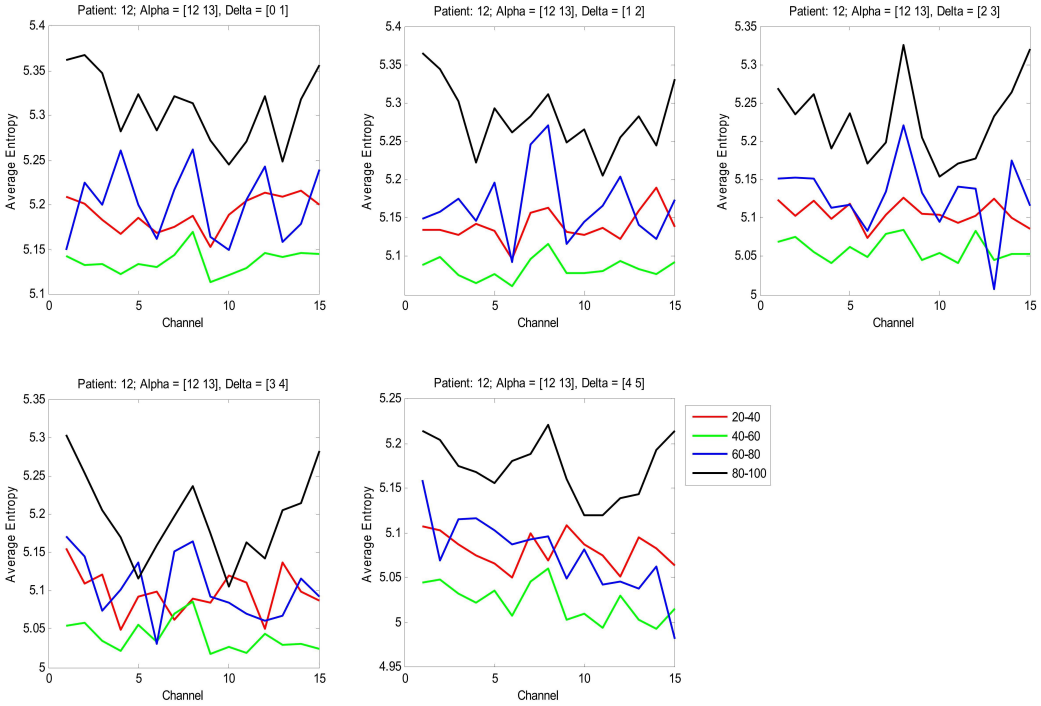

(e)

Figure 4.11 Average entropies of different BIS ranges for **patient 12**. In each sub-figure, for specific alpha sub-bands, results are shown for all delta sub-bands. (a) α = [8-9],(b) α = [9-10], (c) α = [10-11], (d) α = [11-12], (e) α = [12-13]

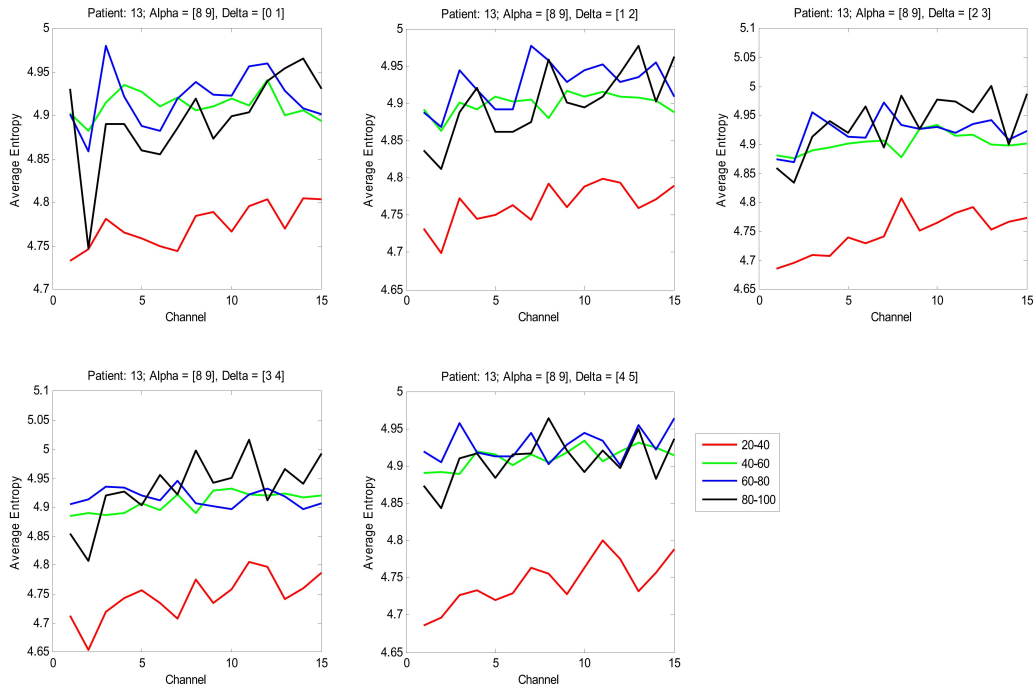
Patient: 13; Alpha = [8 9], Delta = [0 1]
Patient: 13; Alpha = [8 9], Delta = [1 2]
Patient: 13; Alpha = [8 9], Delta = [2 3]
Patient: 13; Alpha = [8 9], Delta = [3 4]
Patient: 13; Alpha = [8 9], Delta = [4 5]
Average Entropy
Channel
20-40
40-60
60-80
80-100

(a)

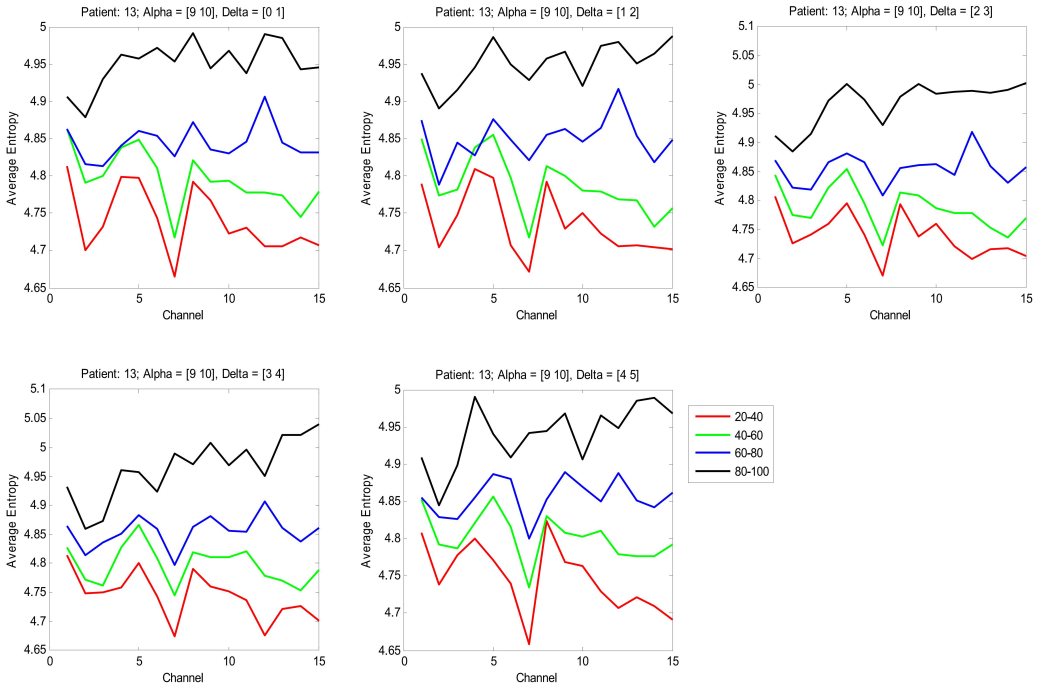
Patient: 13; Alpha = [9 10], Delta = [0 1]
Patient: 13; Alpha = [9 10], Delta = [1 2]
Patient: 13; Alpha = [9 10], Delta = [2 3]
Patient: 13; Alpha = [9 10], Delta = [3 4]
Patient: 13; Alpha = [9 10], Delta = [4 5]
Average Entropy
Channel
20-40
40-60
60-80
80-100

(b)

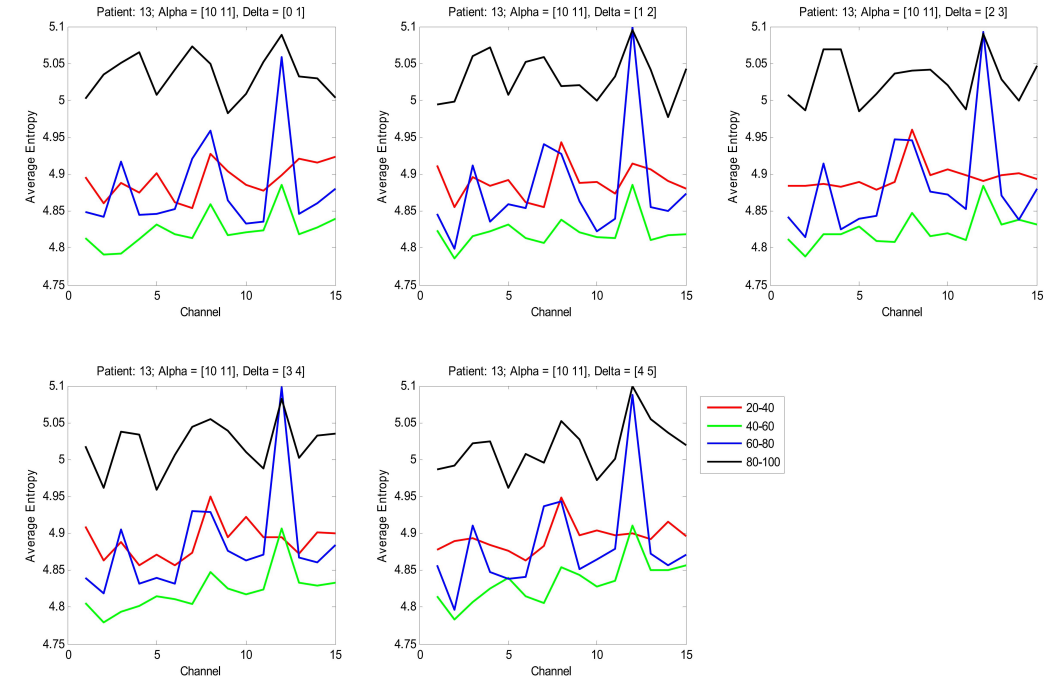
Patient: 13; Alpha = [10 11], Delta = [0 1]
Patient: 13; Alpha = [10 11], Delta = [1 2]
Patient: 13; Alpha = [10 11], Delta = [2 3]
Patient: 13; Alpha = [10 11], Delta = [3 4]
Patient: 13; Alpha = [10 11], Delta = [4 5]
Average Entropy
Channel
20-40
40-60
60-80
80-100

(c)

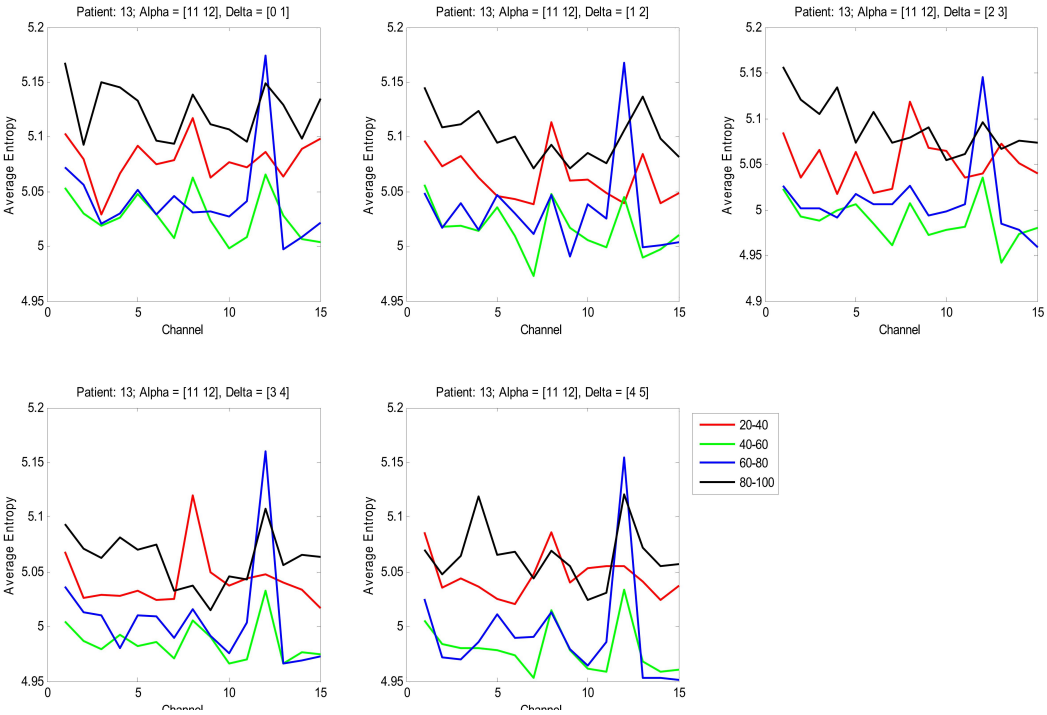
Patient: 13; Alpha = [11 12], Delta = [0 1]
Patient: 13; Alpha = [11 12], Delta = [1 2]
Patient: 13; Alpha = [11 12], Delta = [2 3]
Patient: 13; Alpha = [11 12], Delta = [3 4]
Patient: 13; Alpha = [11 12], Delta = [4 5]
Average Entropy
Channel
20-40
40-60
60-80
80-100

(d)

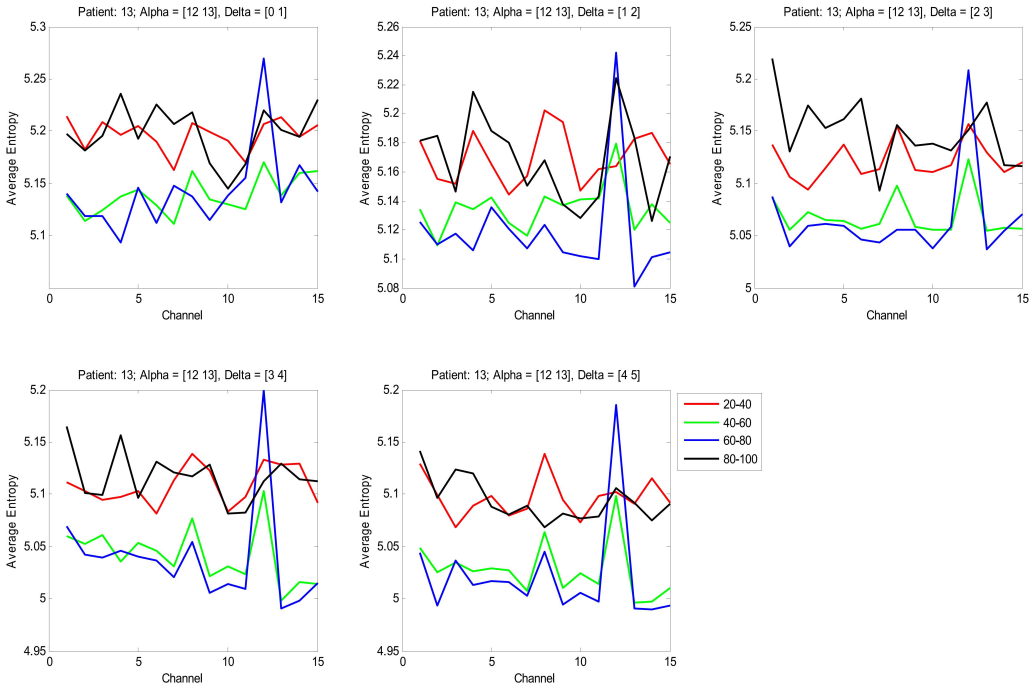

(e)

Figure 4.12 Average entropies of different BIS ranges for **patient 13**. In each sub-figure, for specific alpha sub-bands, results are shown for all delta sub-bands. (a) α = [8-9], (b) α = [9-10], (c) α = [10-11], (d) α = [11-12], (e) α = [12-13]

Now, we provide the channels that in all patients had modulation effect in certain frequency ranges. The term "8 (E. 13)" means that in all patients except in patient 13, the channel 8 has modulation effect at ranges (8-9) Hz and (1-2) Hz.

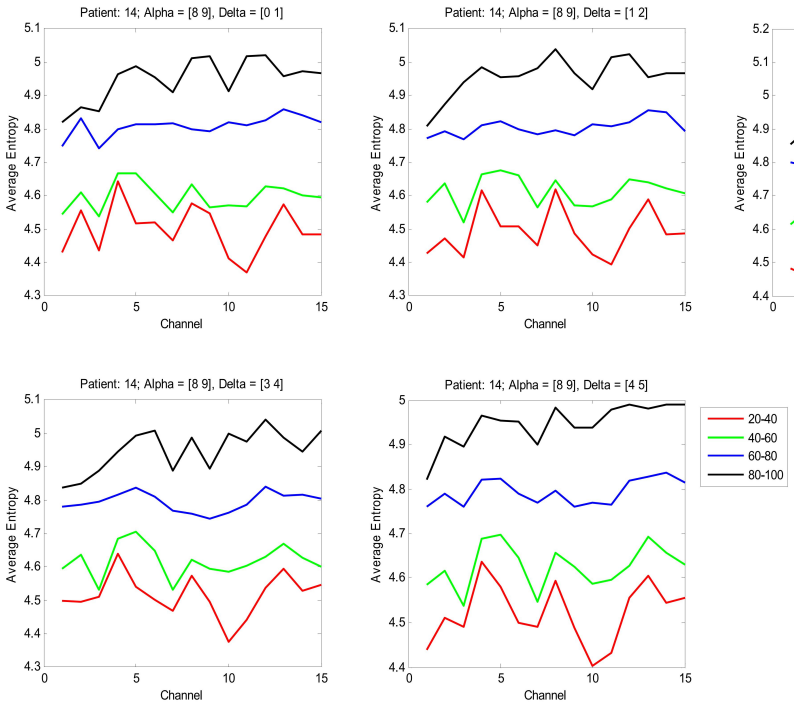
Patient: 14; Alpha = [8 9], Delta = [0 1]
Patient: 14; Alpha = [8 9], Delta = [1 2]
Patient: 14; Alpha = [8 9], Delta = [2 3]
Patient: 14; Alpha = [8 9], Delta = [3 4]
Patient: 14; Alpha = [8 9], Delta = [4 5]
Average Entropy
Channel
20-40
40-60
60-80
80-100

(a)

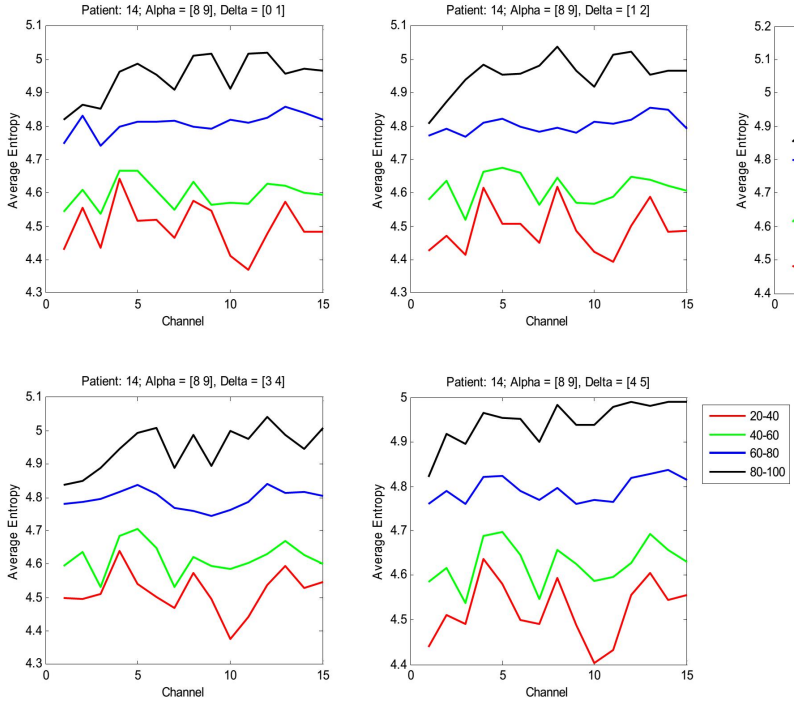
Patient: 14; Alpha = [8 9], Delta = [0 1]
Patient: 14; Alpha = [8 9], Delta = [1 2]
Patient: 14; Alpha = [8 9], Delta = [2 3]
Patient: 14; Alpha = [8 9], Delta = [3 4]
Patient: 14; Alpha = [8 9], Delta = [4 5]
Average Entropy
Channel
20-40
40-60
60-80
80-100

(b)

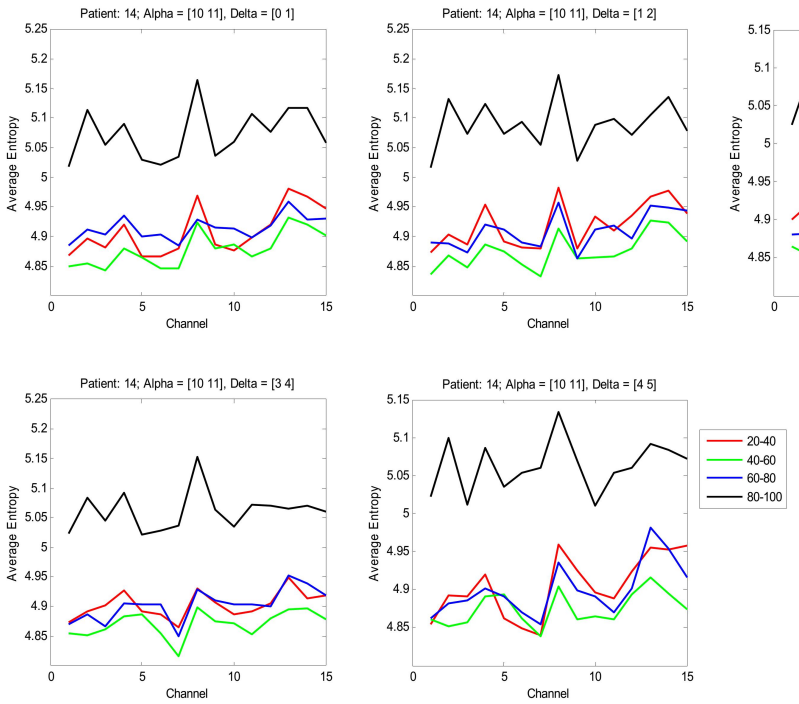
Patient: 14; Alpha = [10 11], Delta = [0 1]
Patient: 14; Alpha = [10 11], Delta = [1 2]
Patient: 14; Alpha = [10 11], Delta = [2 3]
Patient: 14; Alpha = [10 11], Delta = [3 4]
Patient: 14; Alpha = [10 11], Delta = [4 5]
Average Entropy
Channel
20-40
40-60
60-80
80-100

(c)

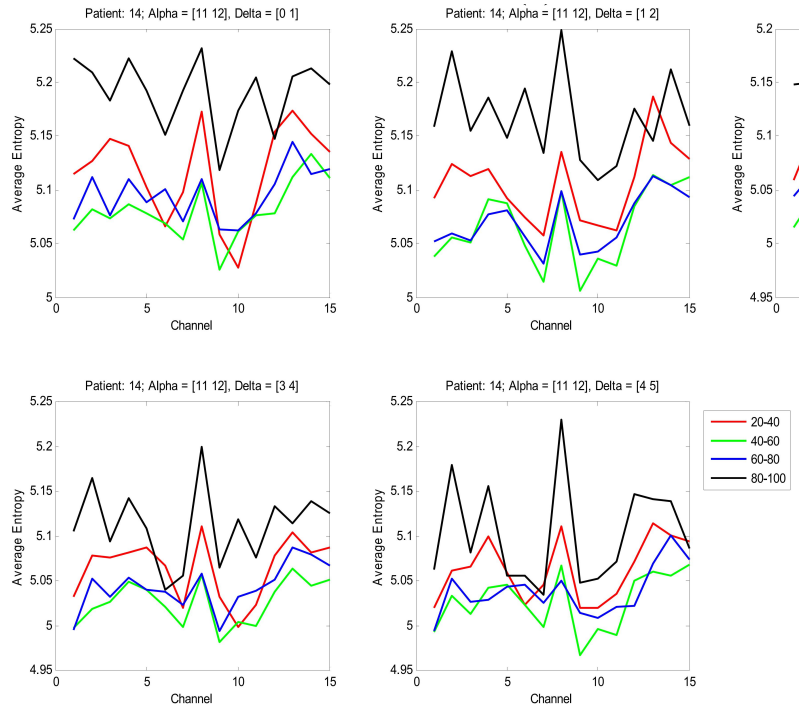
Patient: 14; Alpha = [11 12], Delta = [0 1]
Patient: 14; Alpha = [11 12], Delta = [1 2]
Patient: 14; Alpha = [11 12], Delta = [2 3]
Patient: 14; Alpha = [11 12], Delta = [3 4]
Patient: 14; Alpha = [11 12], Delta = [4 5]
Average Entropy
Channel
20-40
40-60
60-80
80-100

(d)

Table 4.3
Channels that have modulation effect in different patients in second scenario

Patient	Alpha	Delta				
		0 - 1	**1 - 2**	**2 - 3**	**3 – 4**	**4 - 5**
12	**8 – 9**	1, 2, 3, 7, 8	8	1, 2	8, 12, 15	5, 11, 12, 13, 14, 15
	9 - 10	10	10	10	10, 14	10, 11
	10 - 11	8	—	—	—	—
	11 - 12	6	—	—	—	—
	12 - 13	7	—	—	—	—
13	**8 - 9**	13, 14, 15	12, 13, 15	6, 8, 12, 13, 15	6, 8	—
	9 - 10	All	All (E. 4)	All	All	All
	10 - 11	—	—	—	—	12
	11 - 12	—	—	—	—	—
	12 - 13	—	—	—	—	—
	8 - 9	All	All	All	All	All
14	**9 - 10**	6, 9, 10, 13	2, 10, 12	1	1, 6	1, 2
	10 - 11	10	—	—	—	—
	11 - 12	—	—	—	10	—
	12 - 13	—	12	—	—	—
17	**8 - 9**	All (E. 5)	All (E. 3, 5)	All (E. 3)	All	All (E. 5)
	9 - 10	All	1, 8, 9, 10, 11, 14, 15	1, 2, 4, 11, 13, 14, 15	1, 3, 10, 11, 12, 13, 14, 15	1, 3, 5, 6, 11, 13, 15
	10 - 11	All (E. 13, 15)	All (E. 14)	All (E. 14)	All (E. 13, 14, 15)	All (E. 14, 15)
	11 - 12	1, 2, 4, 5, 6, 7, 9, 12	1, 2, 3, 5, 6, 7, 9, 10, 12	2, 3, 6, 8, 10, 13	1, 3, 4, 6, 7, 8, 9, 11, 12	3, 4, 6, 7, 12
	12 - 13	7, 11	7, 9	—	8	2, 3, 7
23	**8 - 9**	All (E. 8)	1, 2, 4, 5, 6, 7, 8	All (E. 8, 12)	All	1, 2, 5, 6, 7
	9 - 10	—	—	—	—	—
	10 - 11	—	—	—	—	—
	11 - 12	—	—	—	—	—
	12 - 13	—	—	—	—	—
24	**8 - 9**	8, 12	8, 9, 10, 12, 13, 14, 15	8, 14	8, 9, 14	8, 14
	9 - 10	—	—	—	—	—
	10 – 11	—	—	—	—	—
	11 – 12	—	—	—	—	—
	12 – 13	—	—	—	—	—

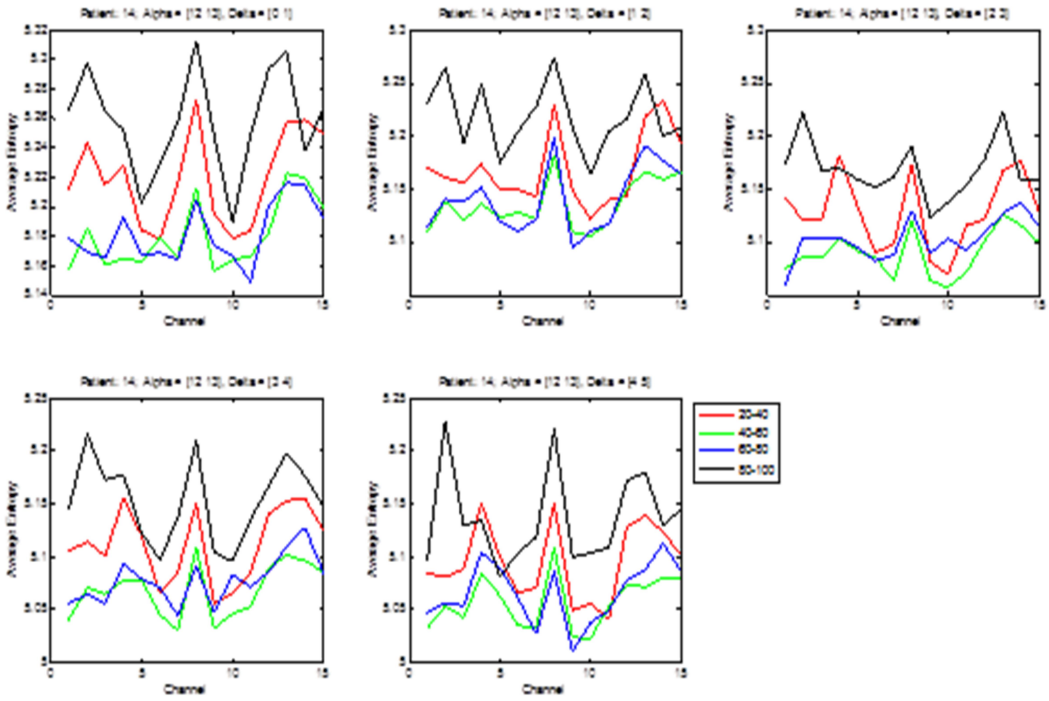

(e)

Figure 4.13 Average entropies of different BIS ranges for **patient 14**. In each sub-figure, for specific alpha sub-bands, results are shown for all delta sub-bands. (a) α = [8-9], (b) α = [9-10], (c) α = [10-11], (d) α = [11-12], (e) α = [12-13]

Table 4.4
Channels that have modulation effect in all patients in second scenario

		Delta				
		0 - 1	**1 – 2**	**2 – 3**	**3 - 4**	**4 - 5**
Alpha	**8 – 9**	—	8 (E. 13), 13 (E. 12), 15 (E. 12)	—	8	—
	9 – 10	—	—	—	—	—
	10 – 11	—	—	—	—	—
	11 – 12	—	—	—	—	—
	12 – 13	—	—	—	—	—

As seen in Table 4.4, there is modulation among alpha and delta sub-bands in the range (8-9) Hz and (3-4) Hz, respectively, in channel 8 (T_7) in all patients. In the Figure 4.17, we present the average entropy and standard deviation of entropy for different anesthesia depths in channel 8 for all patients. As seen, in all patients the average entropy increases as BIS increases.

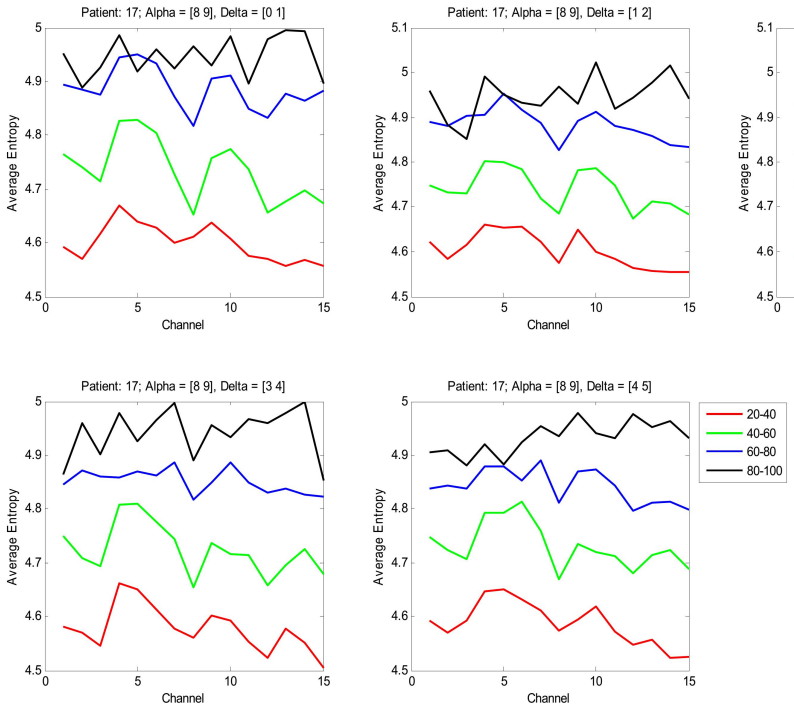
Patient: 17; Alpha = [8 9], Delta = [0 1]
Patient: 17; Alpha = [8 9], Delta = [1 2]
Patient: 17; Alpha = [8 9], Delta = [2 3]
Patient: 17; Alpha = [8 9], Delta = [3 4]
Patient: 17; Alpha = [8 9], Delta = [4 5]
Average Entropy
Channel
20-40
40-60
60-80
80-100

(a)

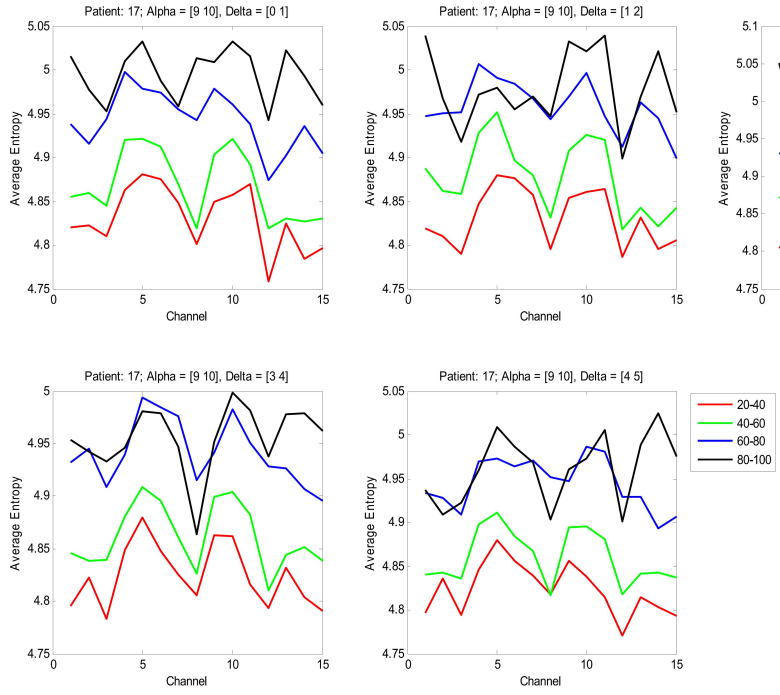
Patient: 17; Alpha = [9 10], Delta = [0 1]
Patient: 17; Alpha = [9 10], Delta = [1 2]
Patient: 17; Alpha = [9 10], Delta = [2 3]
Patient: 17; Alpha = [9 10], Delta = [3 4]
Patient: 17; Alpha = [9 10], Delta = [4 5]
Average Entropy
Channel
20-40
40-60
60-80
80-100

(b)

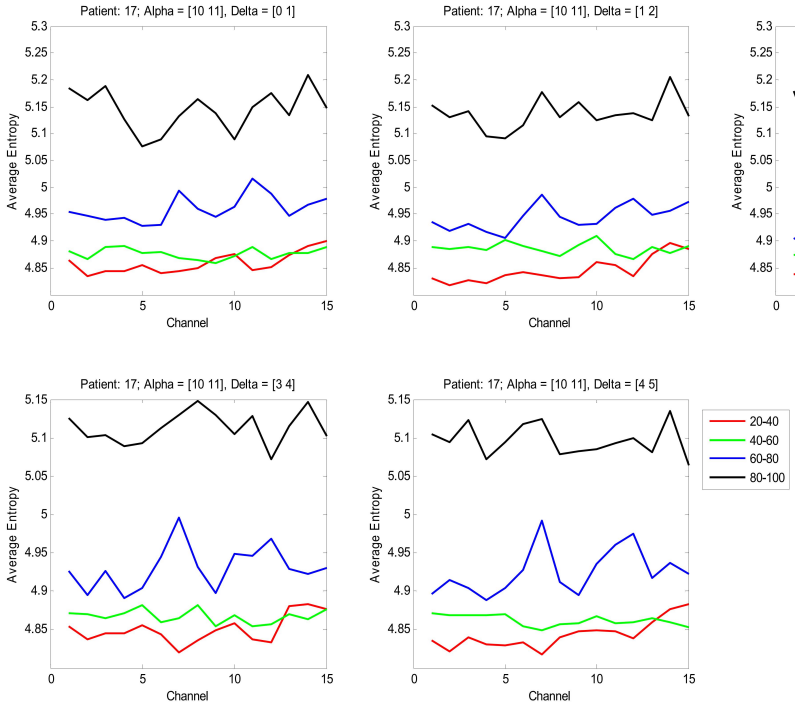
Patient: 17; Alpha = [10 11], Delta = [0 1]
Patient: 17; Alpha = [10 11], Delta = [1 2]
Patient: 17; Alpha = [10 11], Delta = [2 3]
Patient: 17; Alpha = [10 11], Delta = [3 4]
Patient: 17; Alpha = [10 11], Delta = [4 5]
Average Entropy
Channel
20-40
40-60
60-80
80-100

(c)

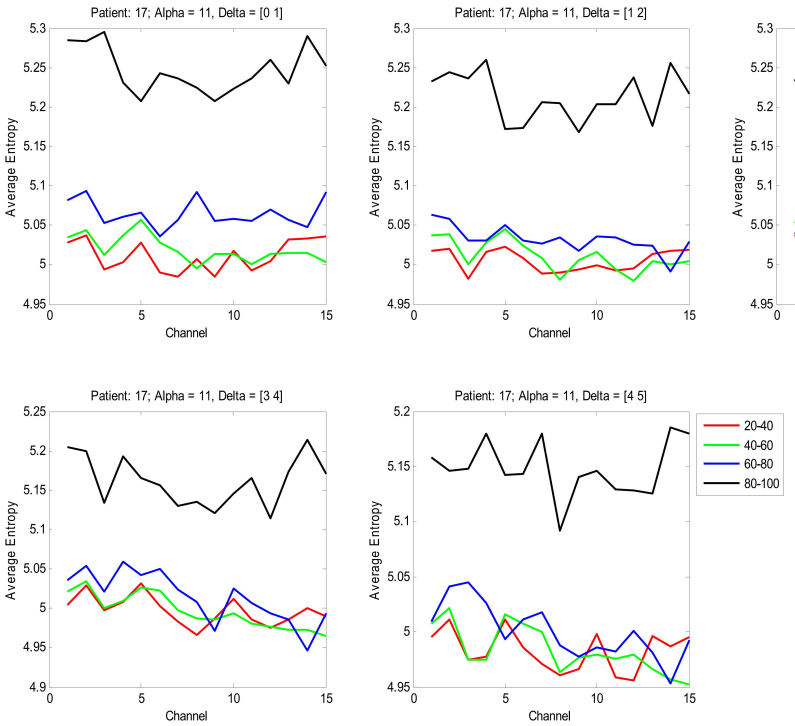
Patient: 17; Alpha = 11, Delta = [0 1]
Patient: 17; Alpha = 11, Delta = [1 2]
Patient: 17; Alpha = 11, Delta = [2 3]
Patient: 17; Alpha = 11, Delta = [3 4]
Patient: 17; Alpha = 11, Delta = [4 5]
Average Entropy
Channel
20-40
40-60
60-80
80-100

(d)

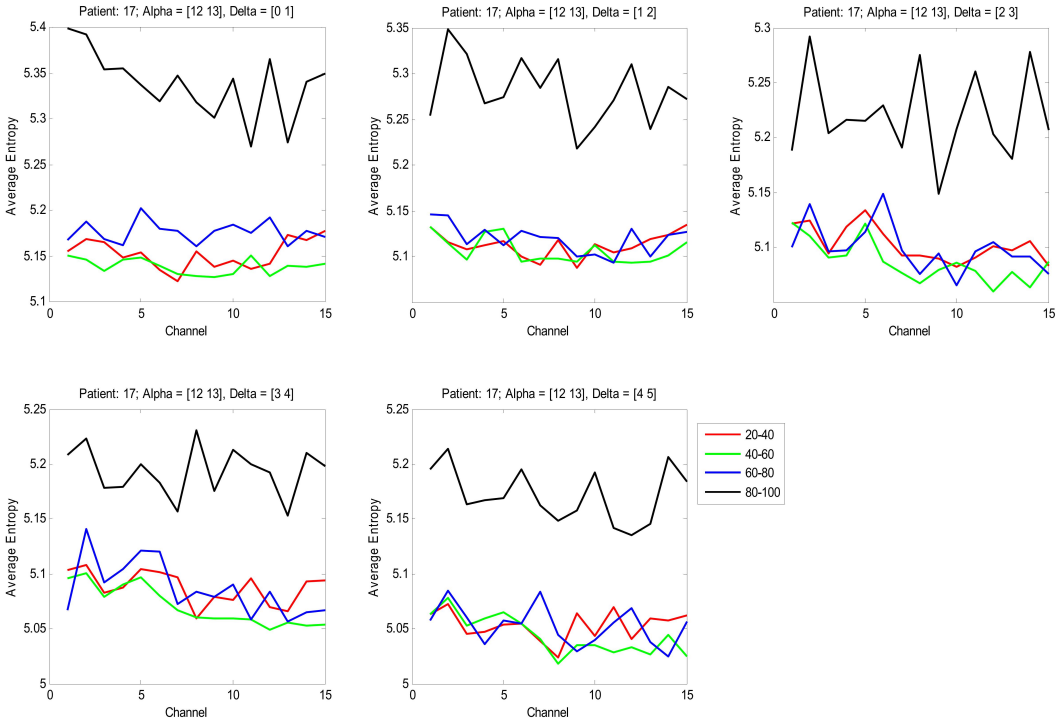

(e)

Figure 4.14 Average entropies of different BIS ranges for **patient 17**. In each sub-figure, for specific alpha sub-bands, results are shown for all delta sub-bands. (a) α= [8-9], (b) α = [9-10], (c) α = [10-11], (d) α = [11-12], (e) α = [12-13]

In the following, Figure 4.18, the histogram of mean modulated signals for different BIS intervals between the (8-9) Hz in alpha band and (3-4) Hz in delta band in channel 8 are shown.

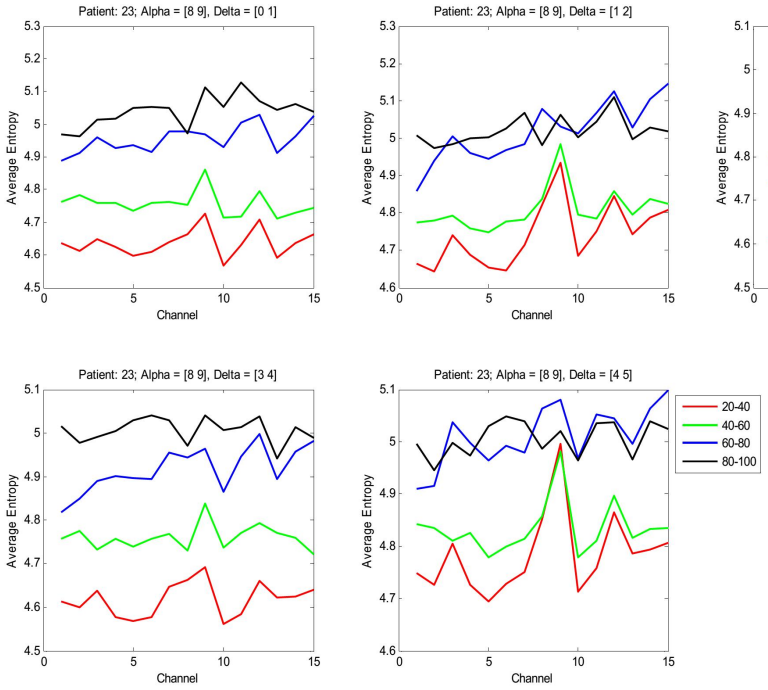
Patient: 23; Alpha = [8 9], Delta = [0 1]
Patient: 23; Alpha = [8 9], Delta = [1 2]
Patient: 23; Alpha = [8 9], Delta = [2 3]
Patient: 23; Alpha = [8 9], Delta = [3 4]
Patient: 23; Alpha = [8 9], Delta = [4 5]
Average Entropy
Channel
20-40
40-60
60-80
80-100

(a)

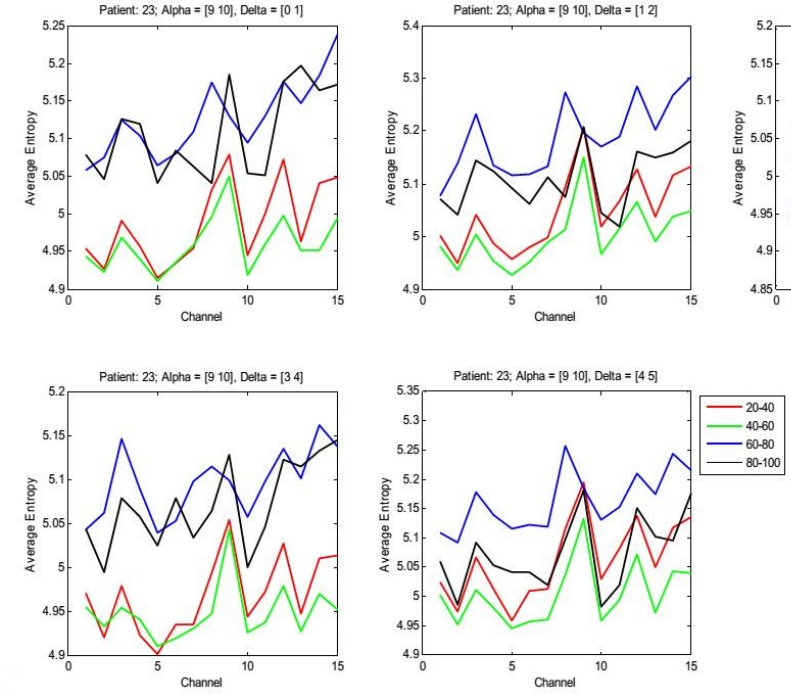
Patient: 23; Alpha = [9 10], Delta = [0 1]
Patient: 23; Alpha = [9 10], Delta = [1 2]
Patient: 23; Alpha = [9 10], Delta = [2 3]
Patient: 23; Alpha = [9 10], Delta = [3 4]
Patient: 23; Alpha = [9 10], Delta = [4 5]
Average Entropy
Channel
20-40
40-60
60-80
80-100

(b)

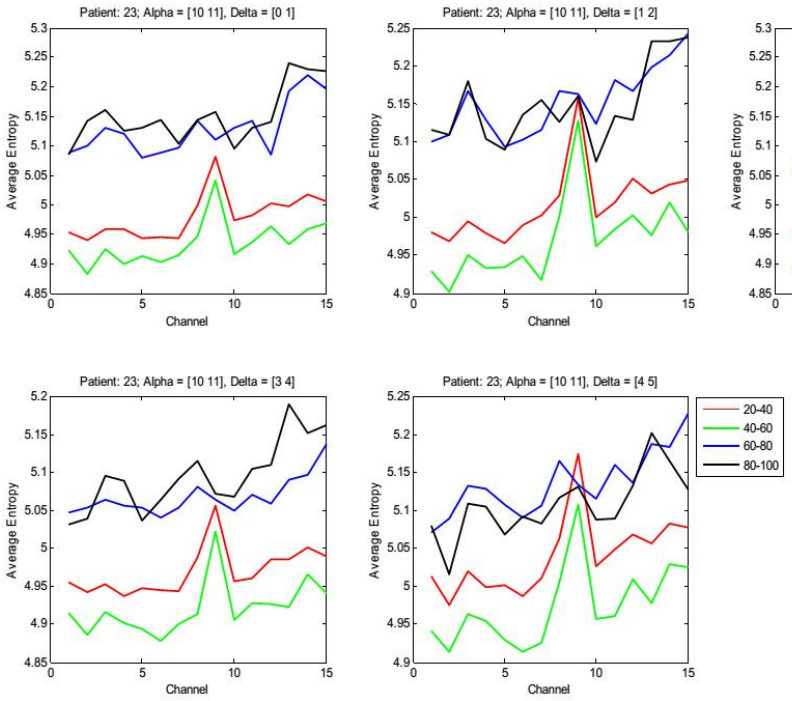
Patient: 23; Alpha = [10 11], Delta = [0 1]
Patient: 23; Alpha = [10 11], Delta = [1 2]
Patient: 23; Alpha = [10 11], Delta = [2 3]
Patient: 23; Alpha = [10 11], Delta = [3 4]
Patient: 23; Alpha = [10 11], Delta = [4 5]
Average Entropy
Channel
20-40
40-60
60-80
80-100

(c)

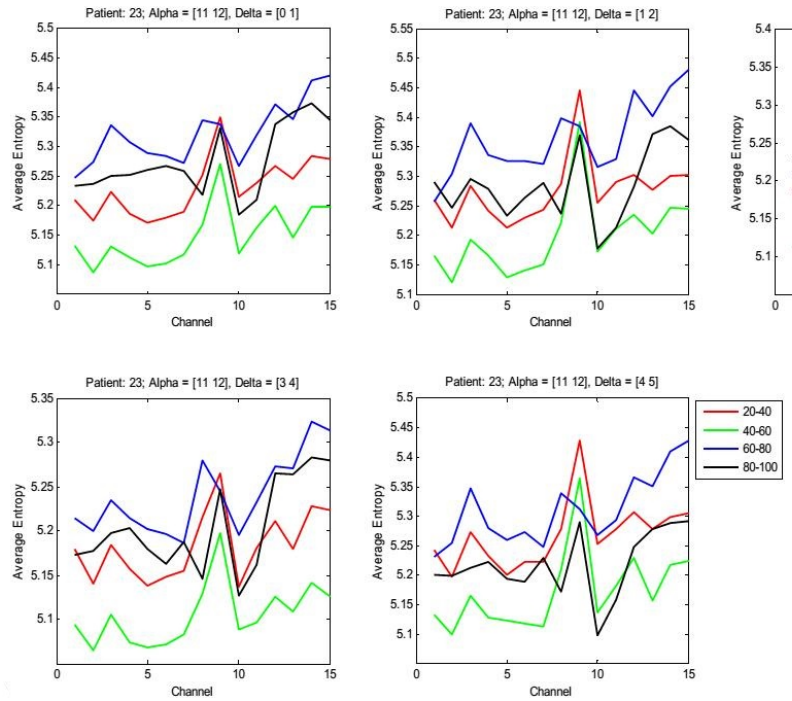
Patient: 23; Alpha = [11 12], Delta = [0 1]
Patient: 23; Alpha = [11 12], Delta = [1 2]
Patient: 23; Alpha = [11 12], Delta = [2 3]
Patient: 23; Alpha = [11 12], Delta = [3 4]
Patient: 23; Alpha = [11 12], Delta = [4 5]
Average Entropy
Channel
20-40
40-60
60-80
80-100

(d)

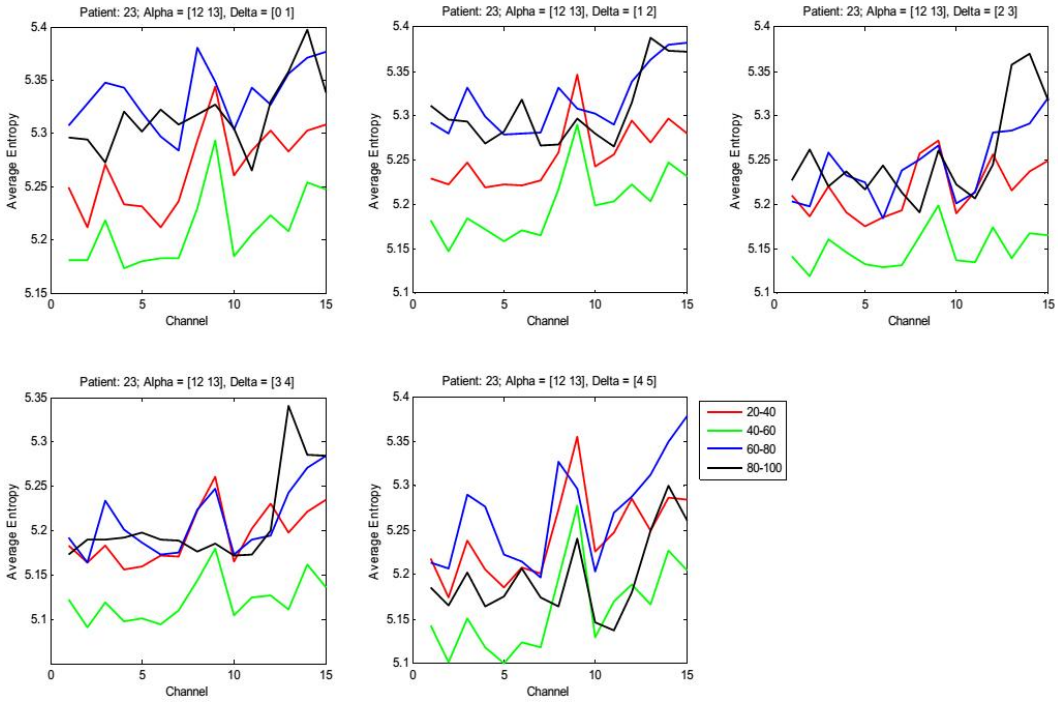

(e)

Figure 4.15 Average entropies of different BIS ranges for **patient 23**. In each sub-figure, for specific alpha sub-bands, results are shown for all delta sub-bands.(a) α= [8-9],(b) α = [9-10], (c) α = [10-11], (d) α = [11-12], (e) α = [12-13]

At Figure 4.19 variation of entropy of modulation in (8-9) Hz and delta (3-4) Hz at channel 8 for different epochs are seen. As seen, the variations in entropy follow the variations in BIS, and when entropy increases, also BIS increases, and vice versa.

In Table 4.5, the results of Mann-Whitney U test for second scenario in different BIS intervals are shown.

Table 4.5
Results of Mann-Whitney Test for second scenario, $h = 1$ denotes BIS ranges have different distributions, while $h = 0$ indicates they have same distributions

BIS ranges	**Test Result**	**Patient**						
		12	**13**	**14**	**17**	**23**	**24**	**Overall**
R_a, R_b	h (p)	0(0.075)	1 (0.0022)	0 (0.078)	1 (3.3e-05)	0 (0.052)	1 (0.048)	1 (4.1e-18)
R_a, R_c	h (p)	0 (0.13)	1 (0.0011)	1 (8.1e-07)	1 (4.1e-14)	1 (7.4e-14)	1 (1.4e-10)	1 (1.1e-45)
R_a, R_d	h (p)	1 (0.0055)	1 (1.1e-05)	1 (1.3e-12)	1 (4.9e-10)	1 (7.1e-14)	1 (4.6e-15)	1 (7.4e-58)
R_b, R_c	h (p)	0 (0.38)	0 (0.49)	1 (2.5e-07)	1 (7.2e-08)	1 (5.7e-09)	1 (3.7e-08)	1 (7.7e-19)
R_b, R_d	h (p)	1 (0.0065)	1 (0.00076)	1 (1.1e-16)	1 (2.9e-06)	1 (1.6e-09)	1 (5.1e-12)	1 (9.8e-40)
R_c, R_d	h (p)	0 (0.11)	1 (0.0036)	1 (3.5e-09)	0 (0.37)	0 (0.52)	0 (0.31)	1 (1.6e-11)

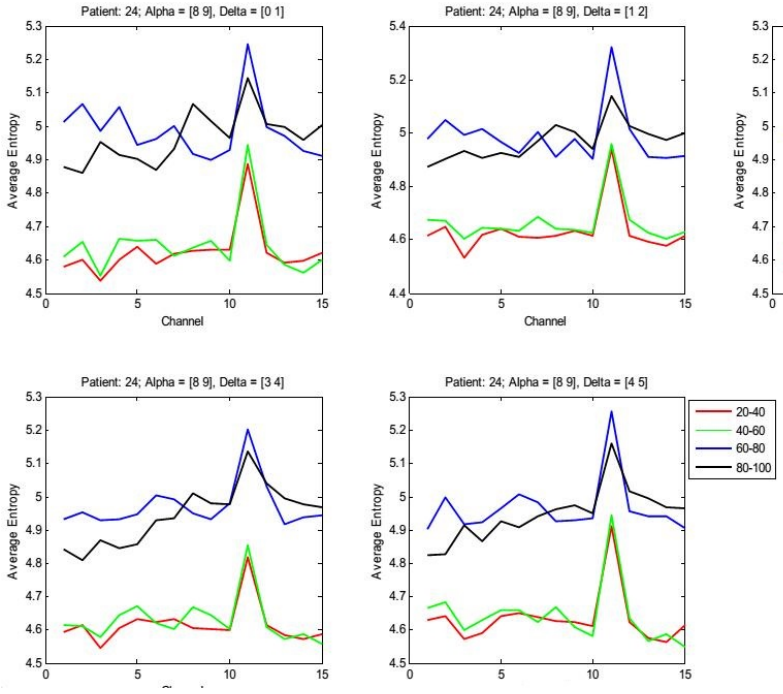
Patient: 24; Alpha = [8 9], Delta = [0 1]
Patient: 24; Alpha = [8 9], Delta = [1 2]
Patient: 24; Alpha = [8 9], Delta = [2 3]
Patient: 24; Alpha = [8 9], Delta = [3 4]
Patient: 24; Alpha = [8 9], Delta = [4 5]
Average Entropy
Channel
20-40
40-60
60-80
80-100

(a)

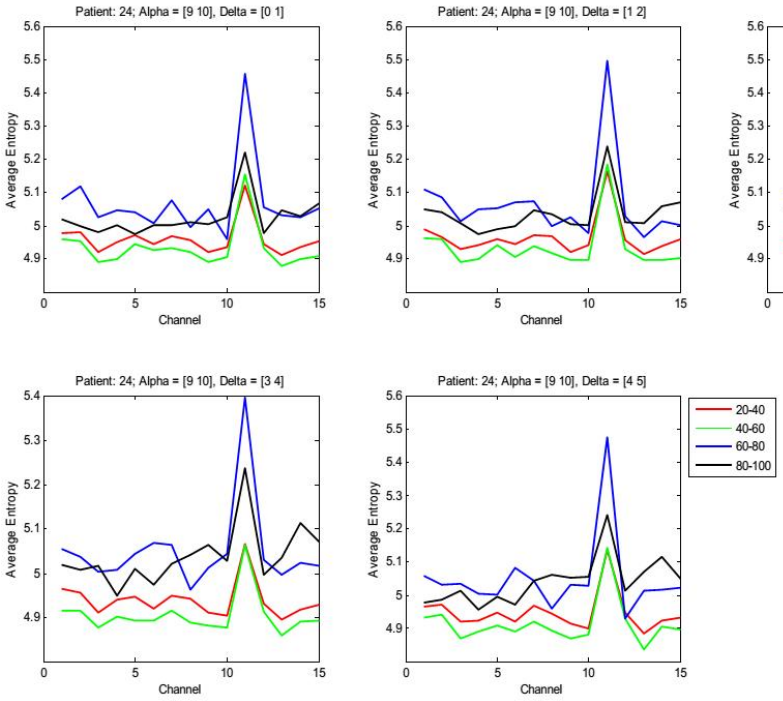
Patient: 24; Alpha = [9 10], Delta = [0 1]
Patient: 24; Alpha = [9 10], Delta = [1 2]
Patient: 24; Alpha = [9 10], Delta = [2 3]
Patient: 24; Alpha = [9 10], Delta = [3 4]
Patient: 24; Alpha = [9 10], Delta = [4 5]
Average Entropy
Channel
20-40
40-60
60-80
80-100

(b)

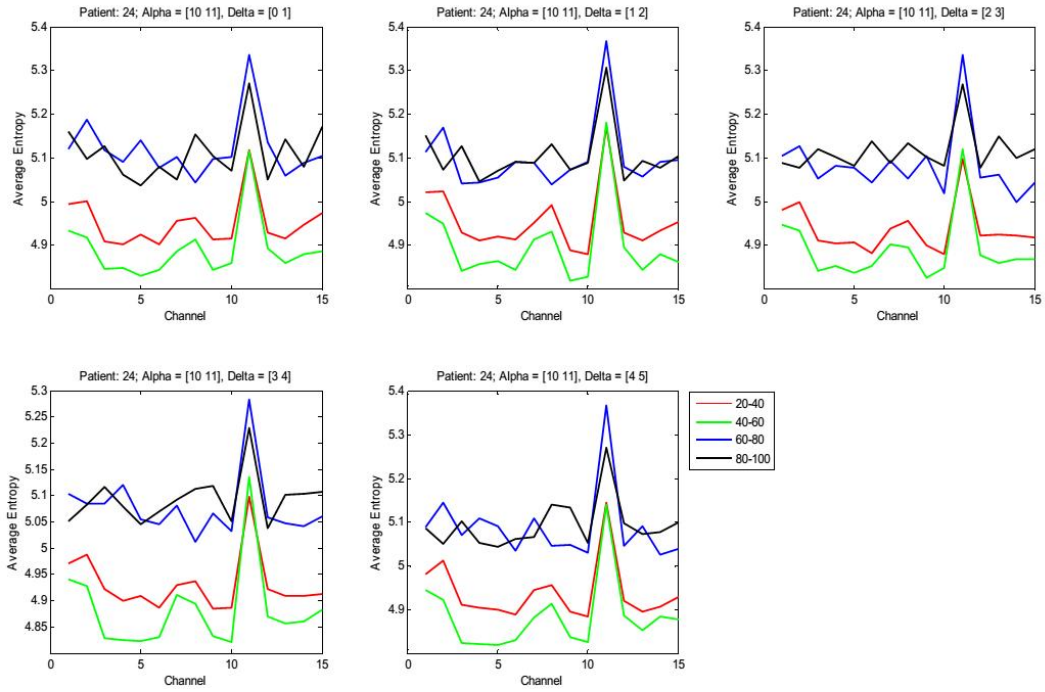

(c)

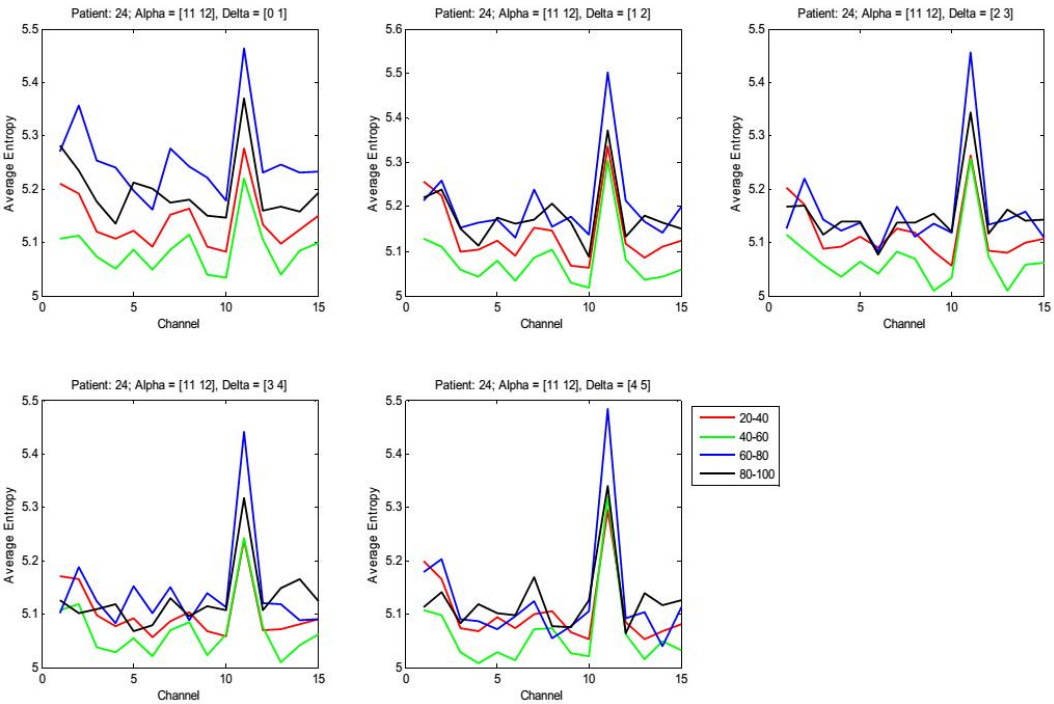

(d)

Figure 4.16 Average entropies of different BIS ranges for **patient 24**. In each sub-figure, for specific alpha sub-bands, results are shown for all delta sub-bands. (a) α= [8-9], (b) α = [9-10], (c) α = [10-11], (d) α = [11-12], (e) α = [12 13]

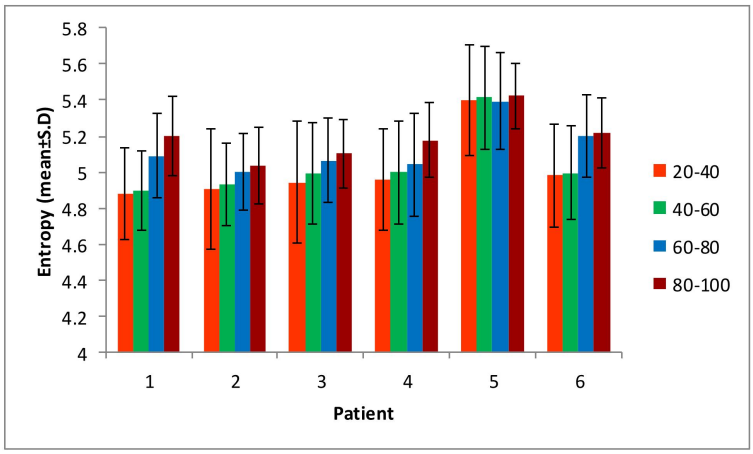

Figure 4.17 Mean and standard deviation of entropy of modulation signal between delta sub-band [3-4] Hz and alpha sub-band [8-9] obtained in channel 8 (T_7) for different BIS intervals in second scenario

4.3 Results of Third Scenario

The procedure is similar to the procedure which introduced in second scenario. The obtained results are as following. The average entropies of BISs related to different alpha and delta bands are shown in Figurer from 4.20 to 4.25. By analyzing these Figures, the channels which have modulation effect among alpha and delta sub-bands for all patients, was presented in Table 4.3. In some cells, "All (E. x)" was written, it means that all channels have modulation effect except channel/channels x.

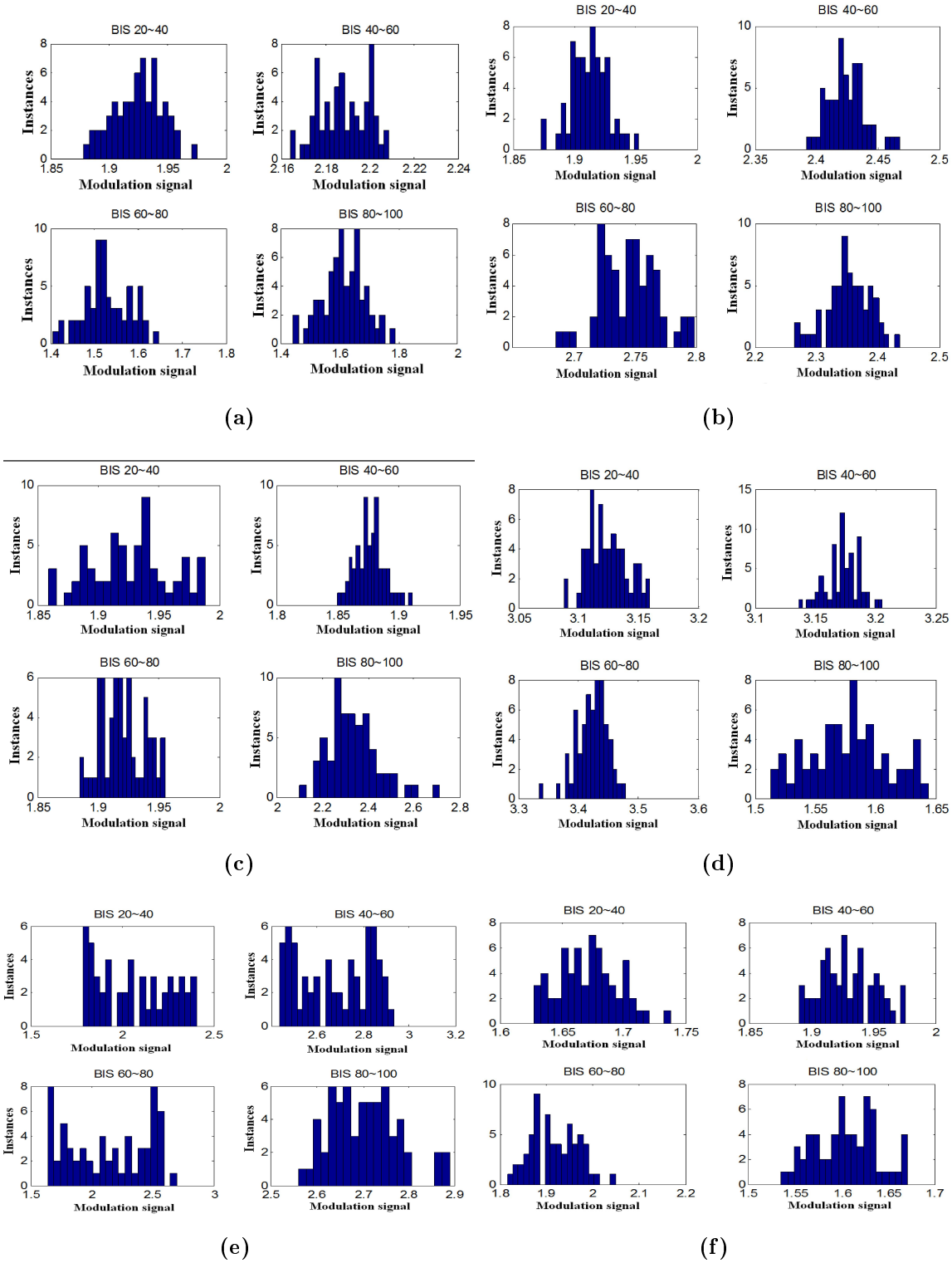

Figure 4.18 The variation of entropy and BIS during time in second scenario. (a) Patient 12,(b) Patient 13, (c) Patient 14, (d) Patient 17, (e) Patient 23, (f) Patient 24.

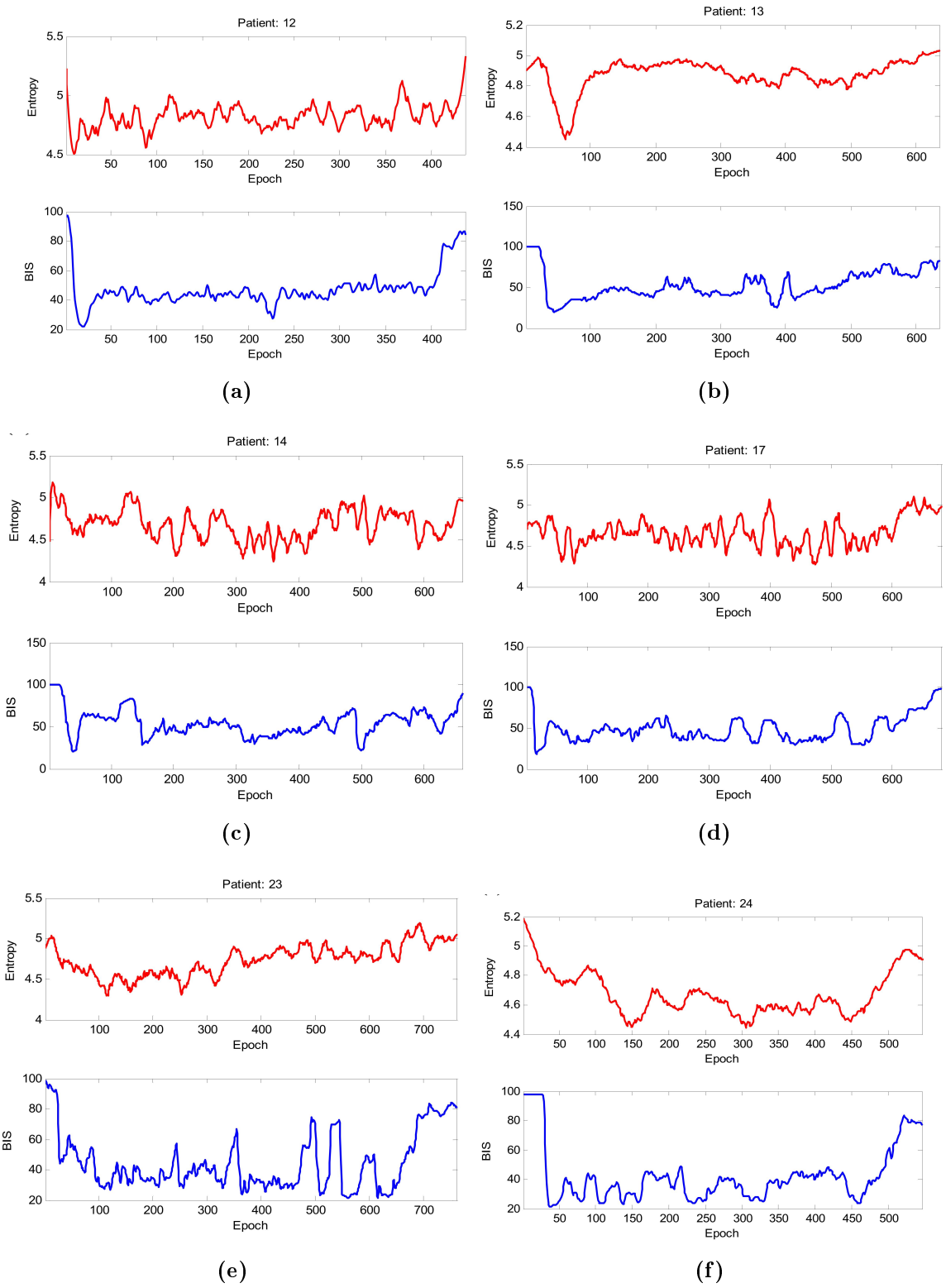

Figure 4.19 The variation of entropy and BIS during time in second scenario. (a) Patient 12, (b) Patient 13, (c) Patient 14, (d) Patient 17, (e) Patient 23, (f) Patient 24.

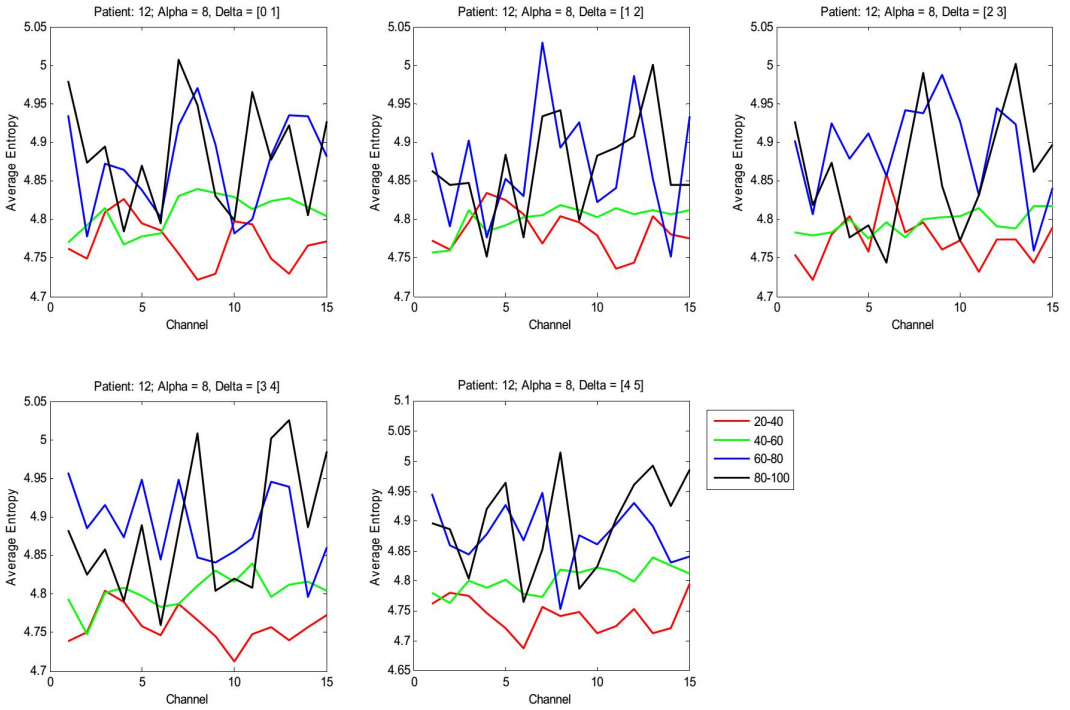
Patient: 12; Alpha = 8, Delta = [0 1]
Patient: 12; Alpha = 8, Delta = [1 2]
Patient: 12; Alpha = 8, Delta = [2 3]
Patient: 12; Alpha = 8, Delta = [3 4]
Patient: 12; Alpha = 8, Delta = [4 5]
Average Entropy
Channel
20-40
40-60
60-80
80-100

(a)

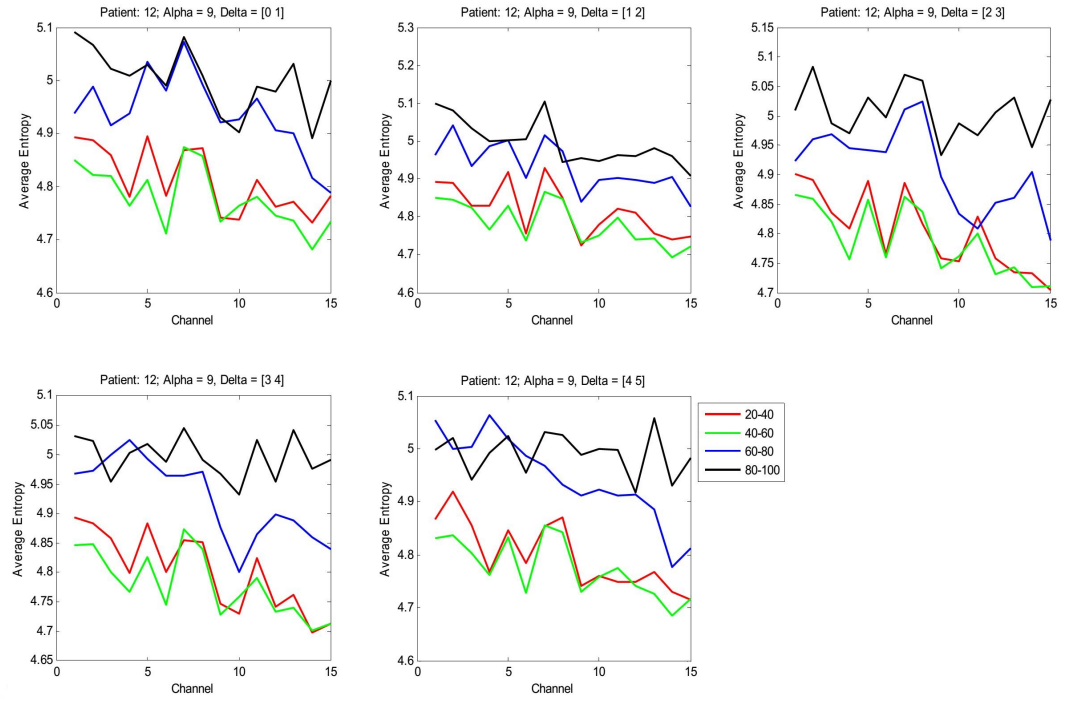
Patient: 12; Alpha = 9, Delta = [0 1]
Patient: 12; Alpha = 9, Delta = [1 2]
Patient: 12; Alpha = 9, Delta = [2 3]
Patient: 12; Alpha = 9, Delta = [3 4]
Patient: 12; Alpha = 9, Delta = [4 5]
Average Entropy
Channel
20-40
40-60
60-80
80-100

(b)

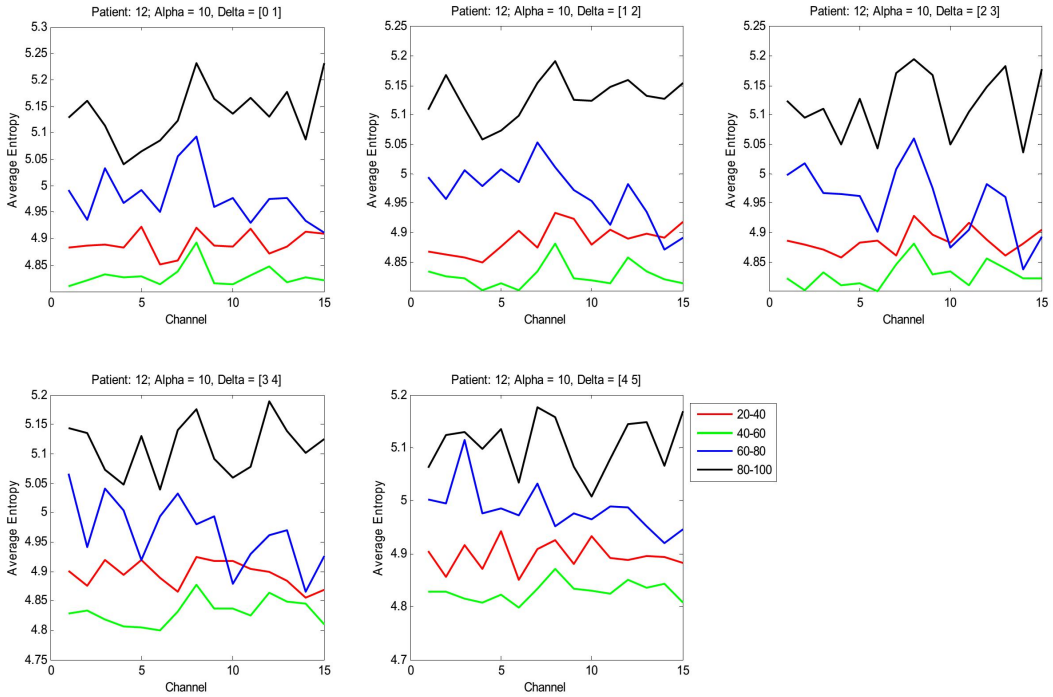
Patient: 12; Alpha = 10, Delta = [0 1]
Patient: 12; Alpha = 10, Delta = [1 2]
Patient: 12; Alpha = 10, Delta = [2 3]
Patient: 12; Alpha = 10, Delta = [3 4]
Patient: 12; Alpha = 10, Delta = [4 5]
Average Entropy
Channel
20-40
40-60
60-80
80-100

(c)

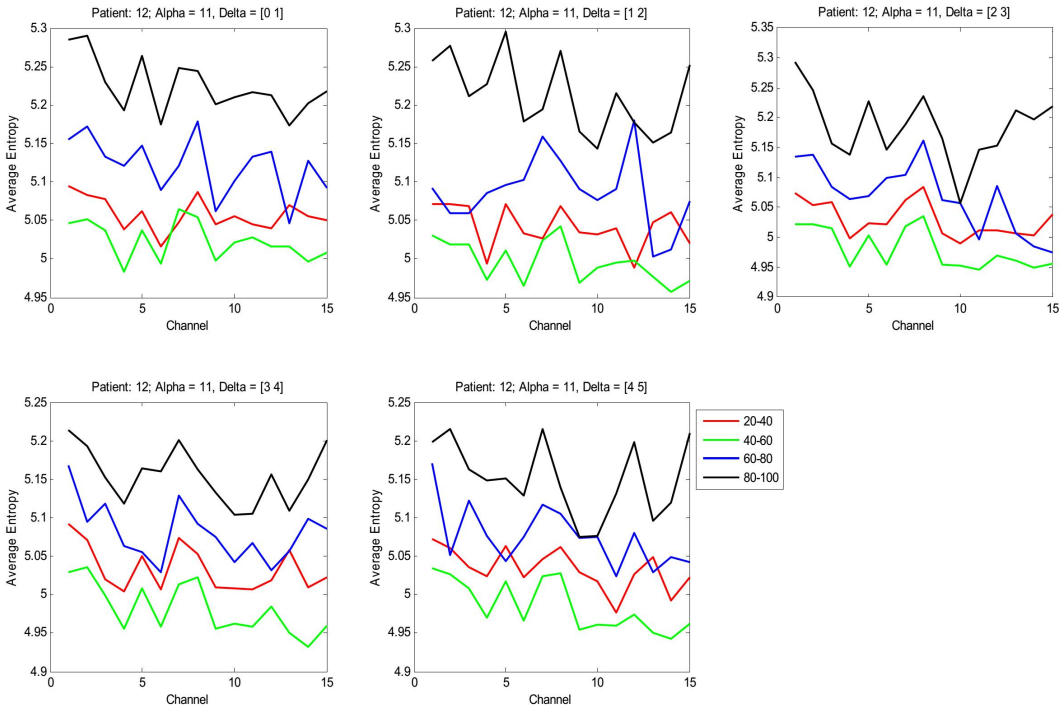
Patient: 12; Alpha = 11, Delta = [0 1]
Patient: 12; Alpha = 11, Delta = [1 2]
Patient: 12; Alpha = 11, Delta = [2 3]
Patient: 12; Alpha = 11, Delta = [3 4]
Patient: 12; Alpha = 11, Delta = [4 5]
Average Entropy
Channel
20-40
40-60
60-80
80-100

(d)

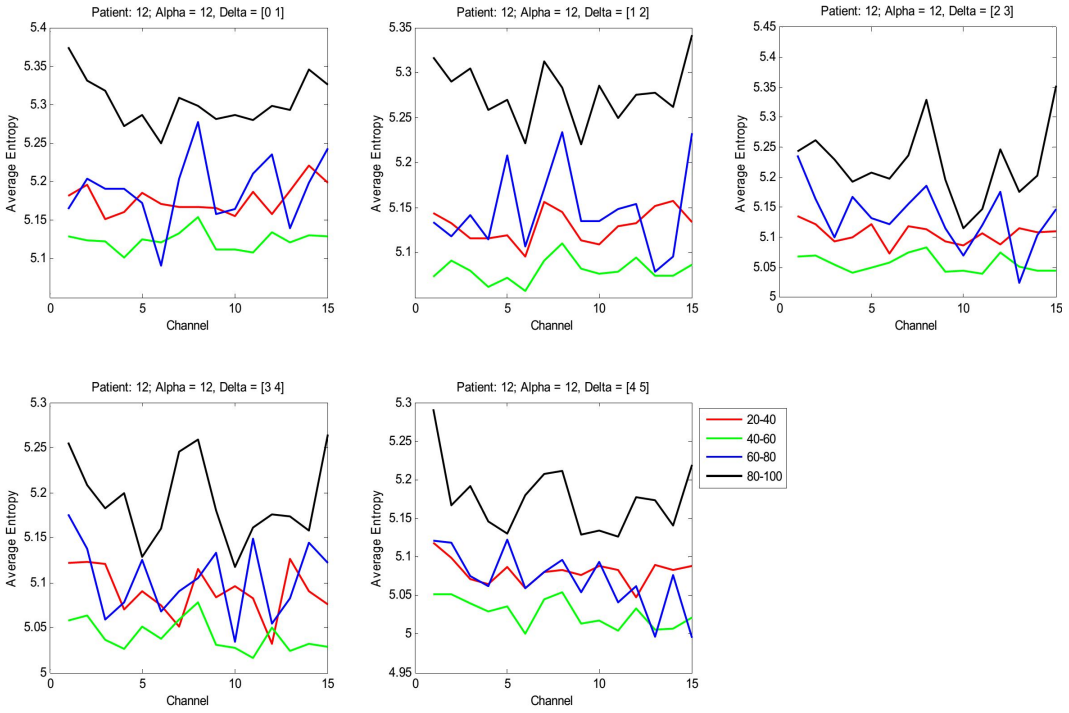

(e)

Figure 4.20 Average entropies of different BIS ranges for **patient 12**. In each sub-figure, for specific alpha sub-bands, results are shown for all delta sub-bands. (a) α = [8-9], (b) α = [9-10], (c) α = [10-11], (d) α = [11-12], (e) α = [12-13]

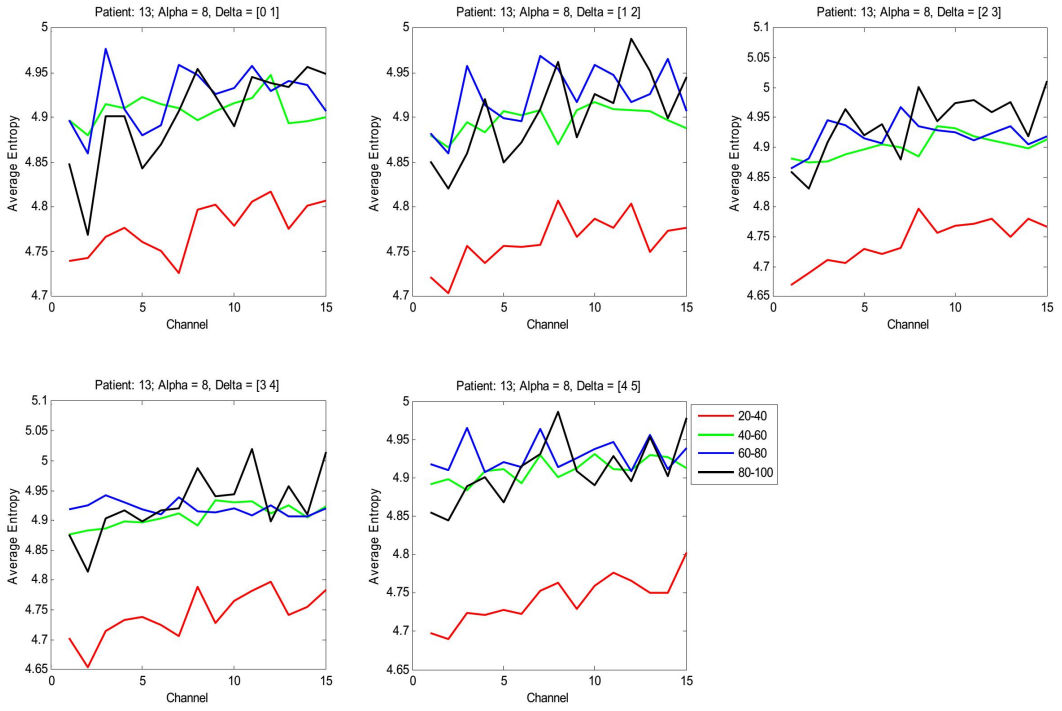
Patient: 13; Alpha = 8, Delta = [0 1]
Patient: 13; Alpha = 8, Delta = [1 2]
Patient: 13; Alpha = 8, Delta = [2 3]
Patient: 13; Alpha = 8, Delta = [3 4]
Patient: 13; Alpha = 8, Delta = [4 5]
Average Entropy
Channel
20-40
40-60
60-80
80-100

(a)

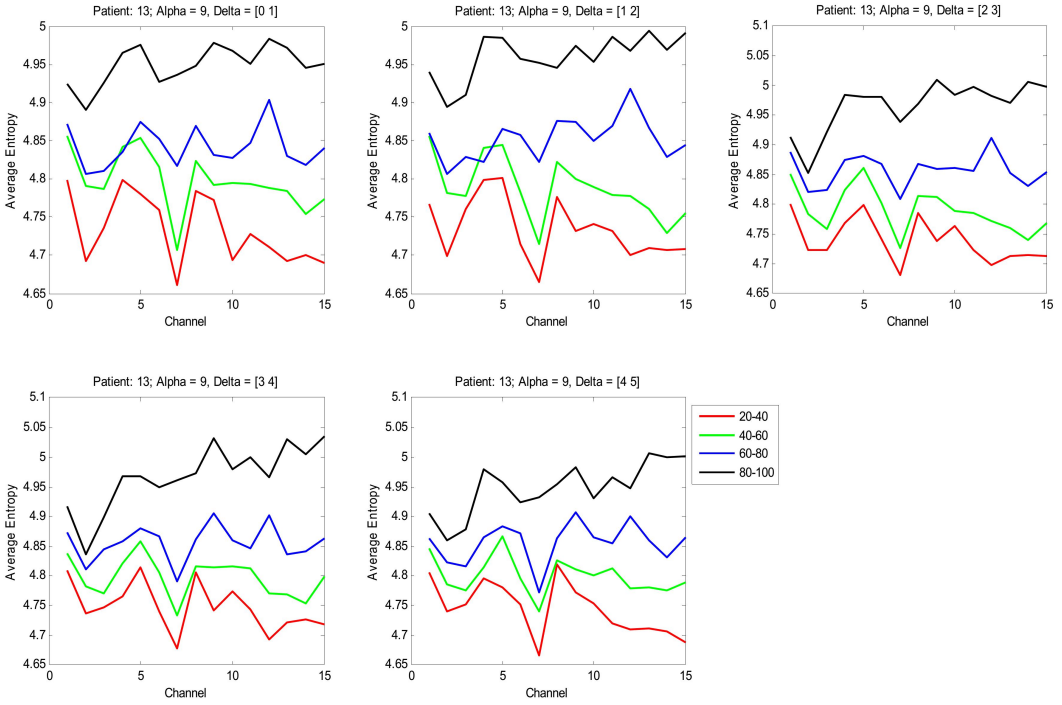
Patient: 13; Alpha = 9, Delta = [0 1]
Patient: 13; Alpha = 9, Delta = [1 2]
Patient: 13; Alpha = 9, Delta = [2 3]
Patient: 13; Alpha = 9, Delta = [3 4]
Patient: 13; Alpha = 9, Delta = [4 5]
Average Entropy
Channel
20-40
40-60
60-80
80-100

(b)

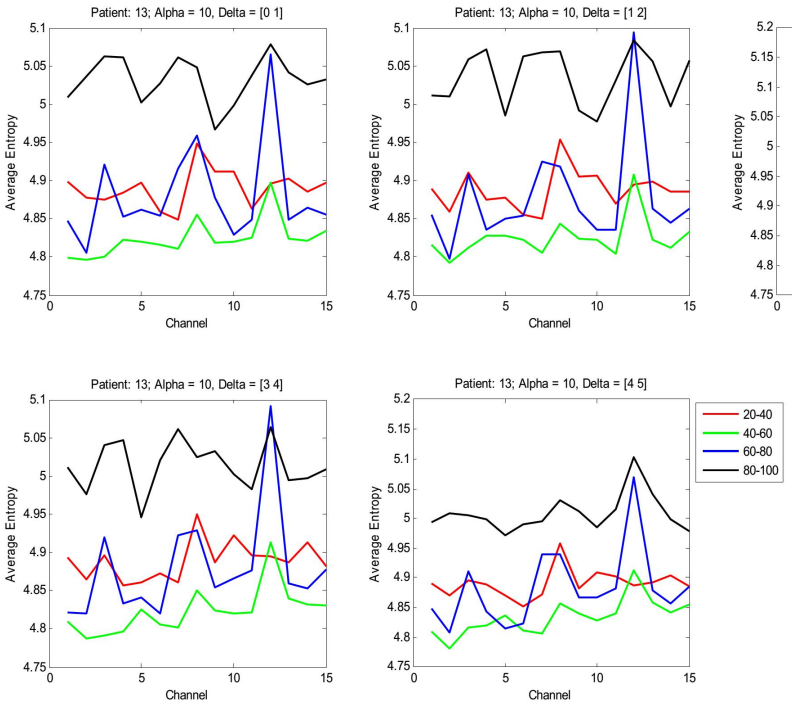
Patient: 13; Alpha = 10, Delta = [0 1]
Patient: 13; Alpha = 10, Delta = [1 2]
Patient: 13; Alpha = 10, Delta = [2 3]
Patient: 13; Alpha = 10, Delta = [3 4]
Patient: 13; Alpha = 10, Delta = [4 5]
Average Entropy
Channel
20-40
40-60
60-80
80-100

(c)

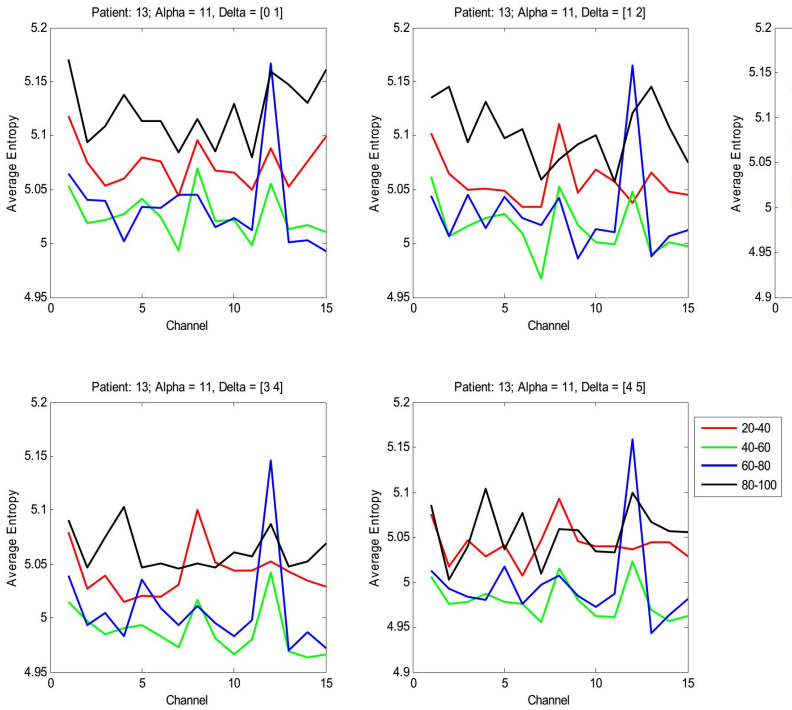
Patient: 13; Alpha = 11, Delta = [0 1]
Patient: 13; Alpha = 11, Delta = [1 2]
Patient: 13; Alpha = 11, Delta = [2 3]
Patient: 13; Alpha = 11, Delta = [3 4]
Patient: 13; Alpha = 11, Delta = [4 5]
Average Entropy
Channel
20-40
40-60
60-80
80-100

(d)

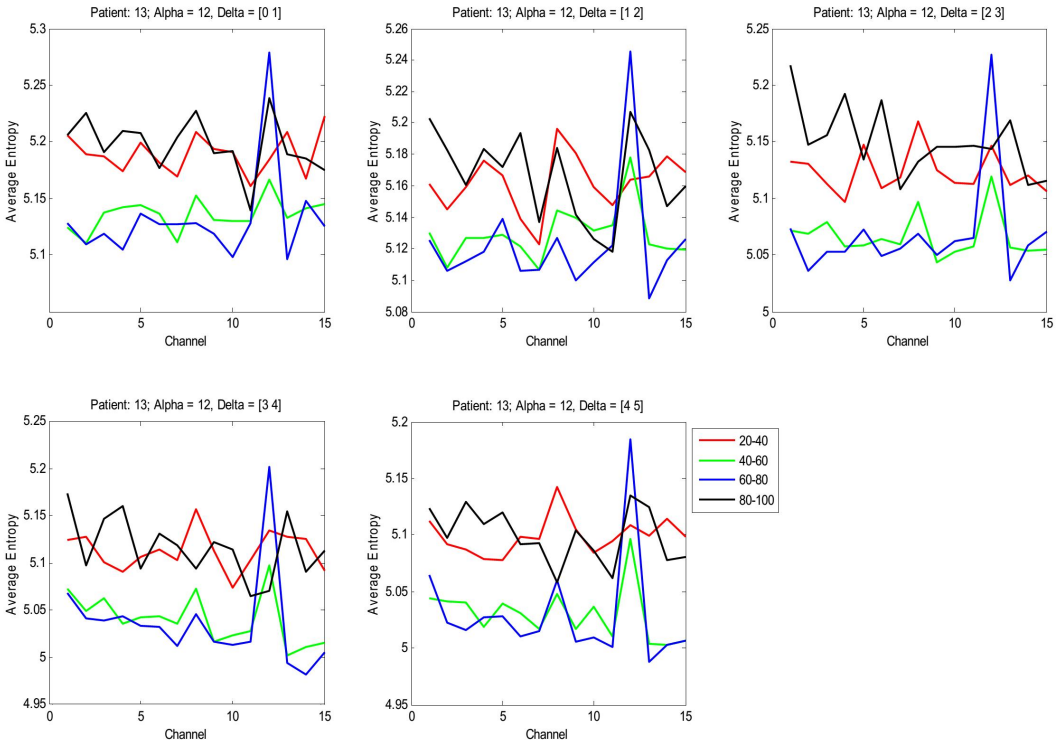

(e)

Figure 4.21 Average entropies of different BIS ranges for **patient 13**. In each sub-figure, for specific alpha sub-bands, results are shown for all delta sub-bands. (a) α = [8-9], (b) α = [9-10], (c) α = [10-11], (d) α = [11-12], (e) α = [12-13]

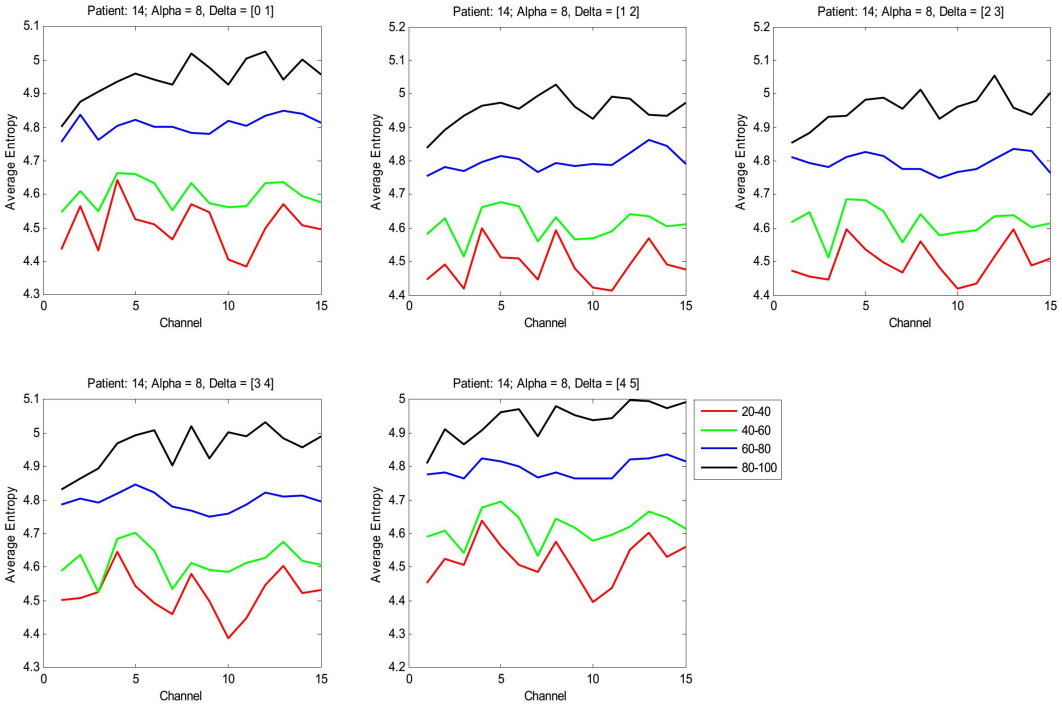
Patient: 14; Alpha = 8, Delta = [0 1]
Patient: 14; Alpha = 8, Delta = [1 2]
Patient: 14; Alpha = 8, Delta = [2 3]
Patient: 14; Alpha = 8, Delta = [3 4]
Patient: 14; Alpha = 8, Delta = [4 5]
Average Entropy
Channel
20-40
40-60
60-80
80-100

(a)

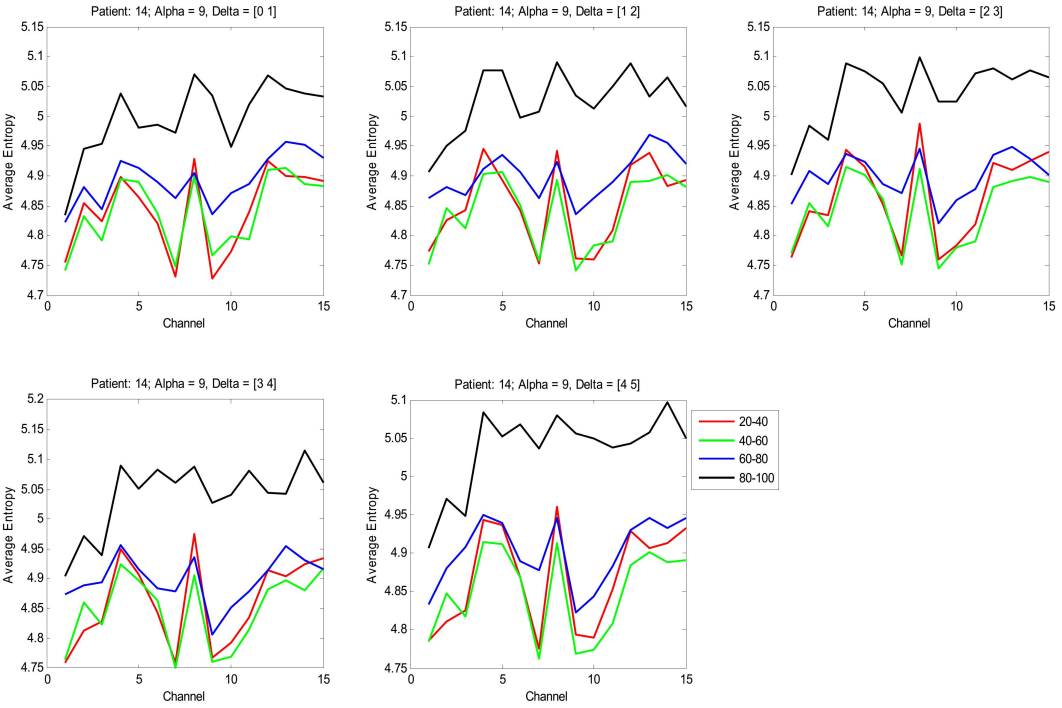
Patient: 14; Alpha = 9, Delta = [0 1]
Patient: 14; Alpha = 9, Delta = [1 2]
Patient: 14; Alpha = 9, Delta = [2 3]
Patient: 14; Alpha = 9, Delta = [3 4]
Patient: 14; Alpha = 9, Delta = [4 5]
Average Entropy
Channel
20-40
40-60
60-80
80-100

(b)

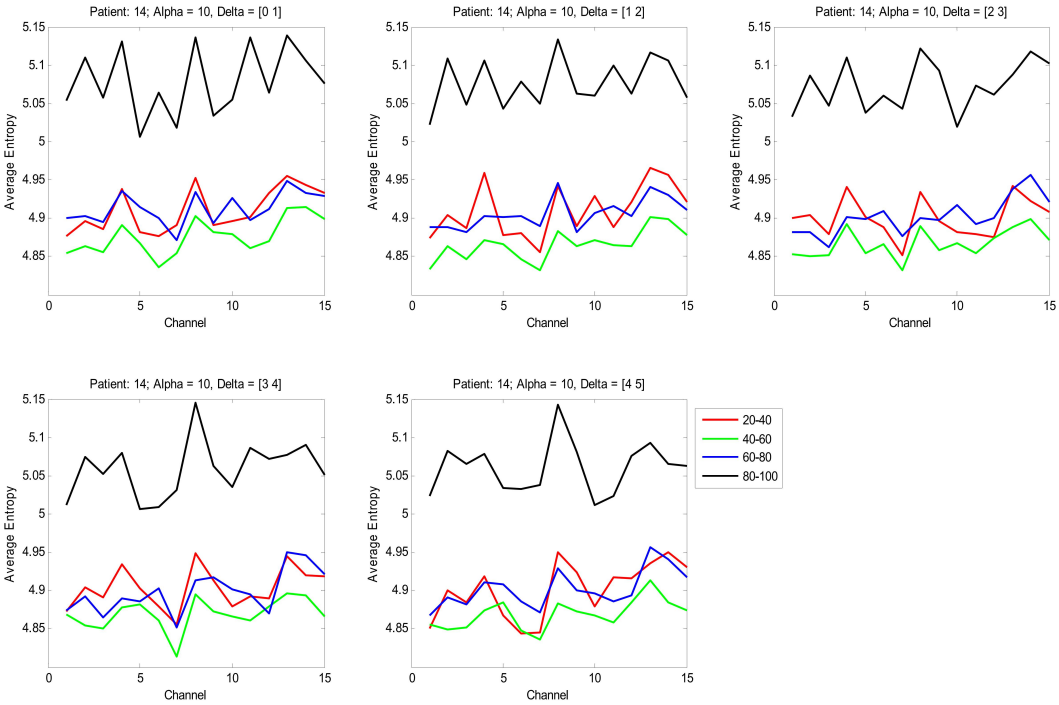
Patient: 14; Alpha = 10, Delta = [0 1]
Patient: 14; Alpha = 10, Delta = [1 2]
Patient: 14; Alpha = 10, Delta = [2 3]
Patient: 14; Alpha = 10, Delta = [3 4]
Patient: 14; Alpha = 10, Delta = [4 5]
Average Entropy
Channel
20-40
40-60
60-80
80-100

(c)

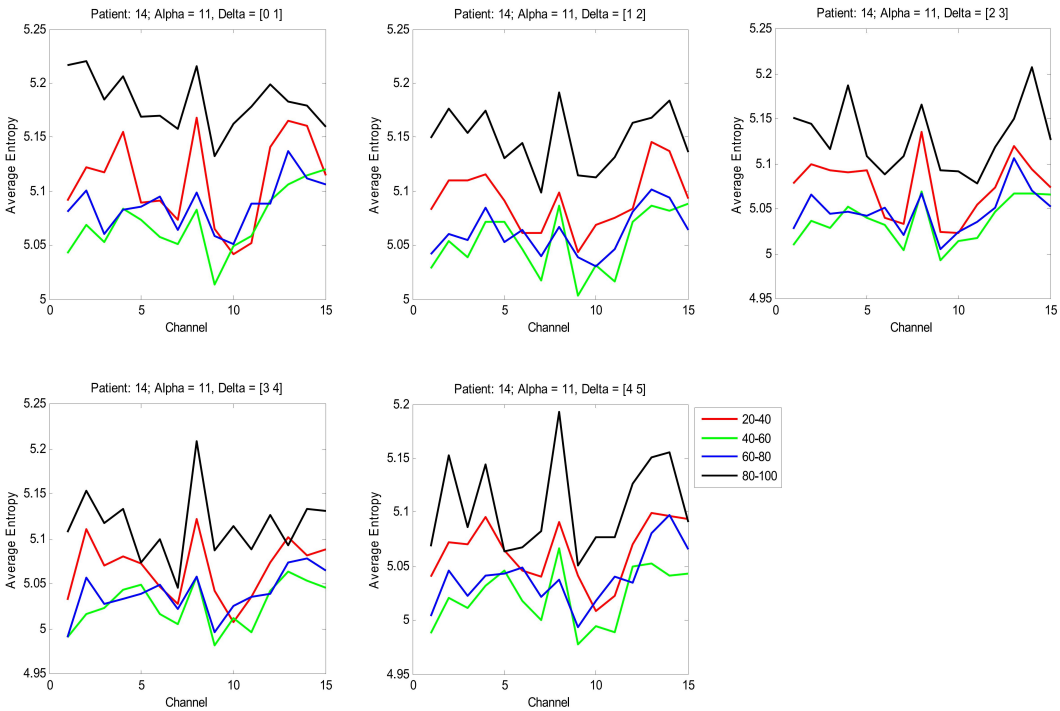
Patient: 14; Alpha = 11, Delta = [0 1]
Patient: 14; Alpha = 11, Delta = [1 2]
Patient: 14; Alpha = 11, Delta = [2 3]
Patient: 14; Alpha = 11, Delta = [3 4]
Patient: 14; Alpha = 11, Delta = [4 5]
Average Entropy
Channel
20-40
40-60
60-80
80-100

(d)

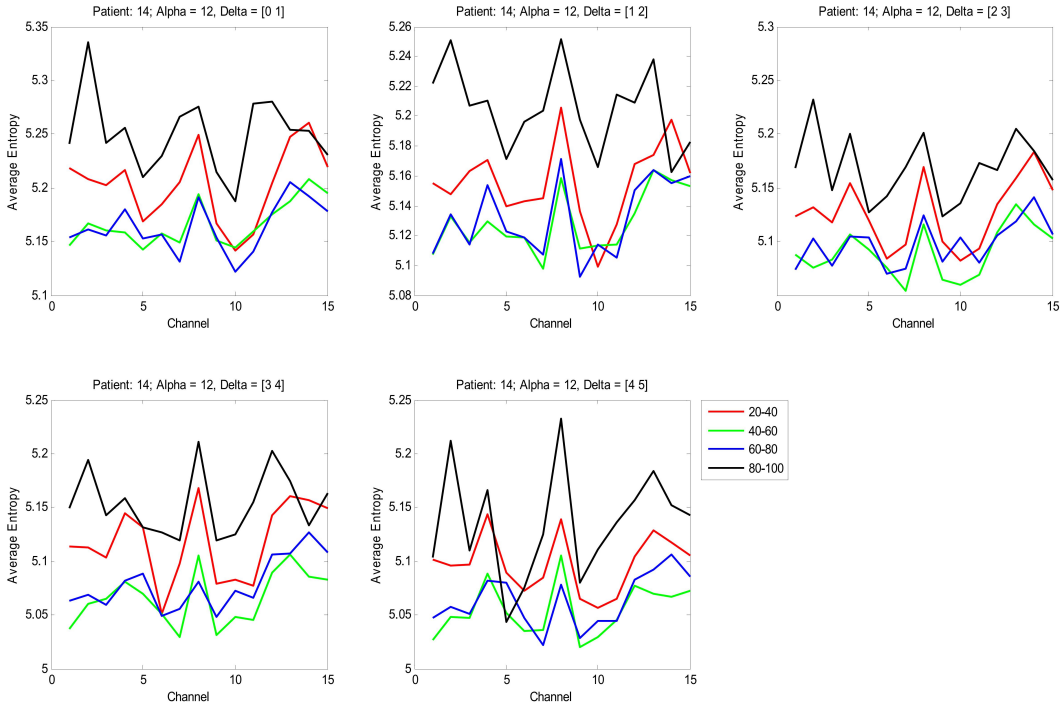

(e)

Figure 4.22 Average entropies of different BIS ranges for **patient 14**. In each sub-figure, for specific alpha sub-bands, results are shown for all delta sub-bands. (a) α = [8-9], (b) α = [9-10], (c) α = [10-11], (d) α = [11-12], (e) α = [12-13]

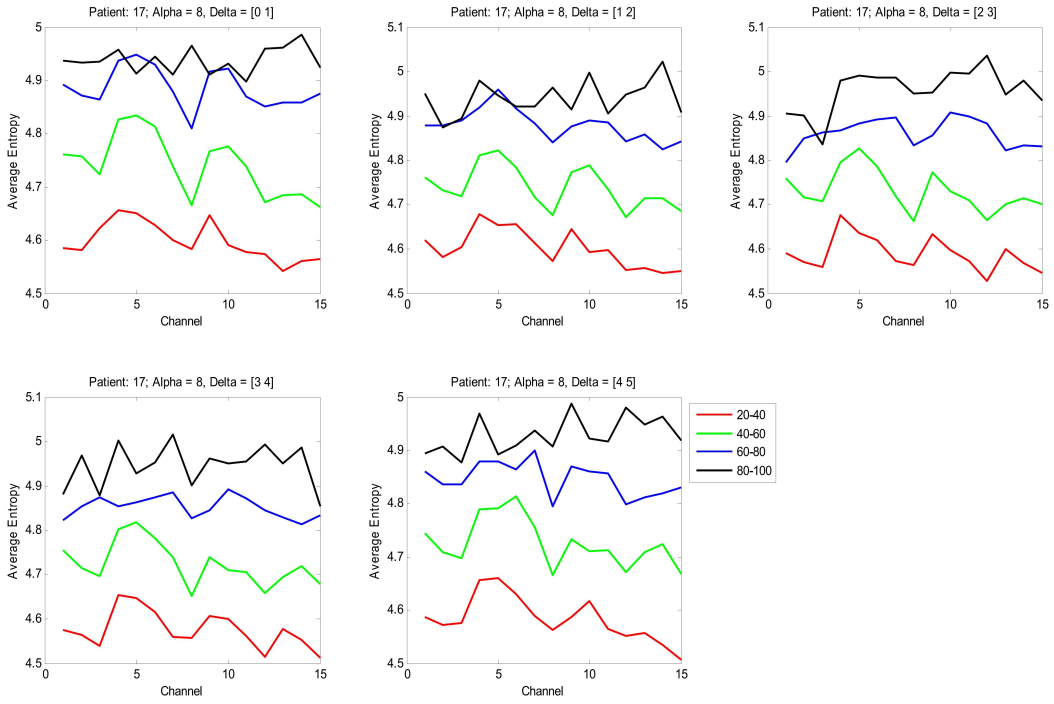
Patient: 17; Alpha = 8, Delta = [0 1]
Patient: 17; Alpha = 8, Delta = [1 2]
Patient: 17; Alpha = 8, Delta = [2 3]
Patient: 17; Alpha = 8, Delta = [3 4]
Patient: 17; Alpha = 8, Delta = [4 5]
Average Entropy
Channel
20-40
40-60
60-80
80-100

(a)

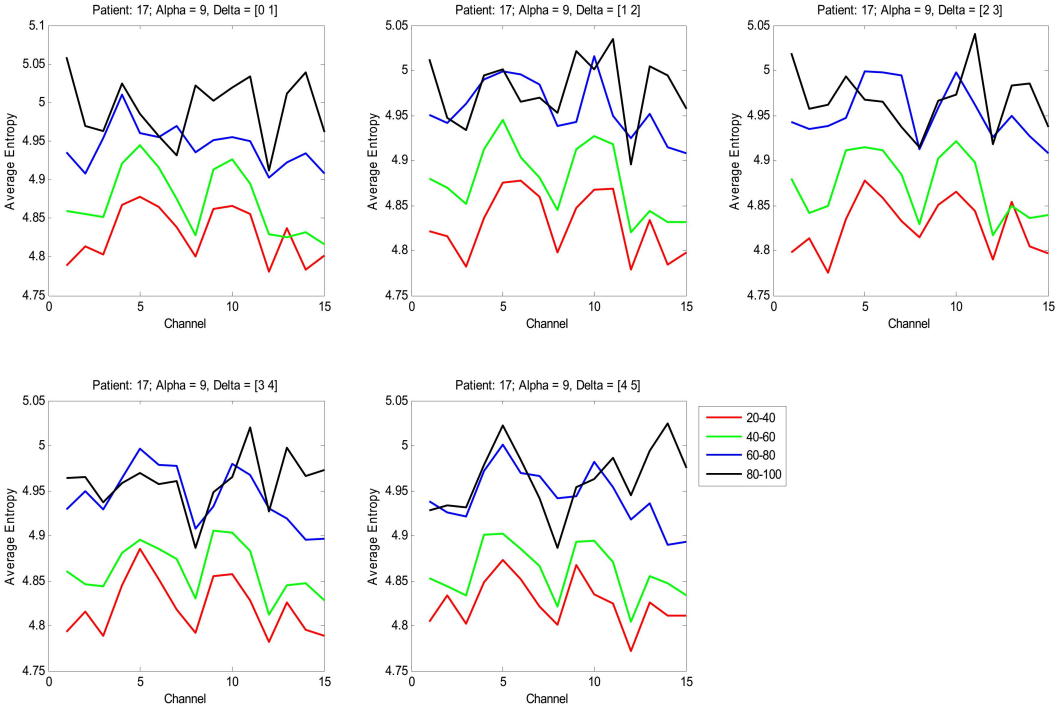
Patient: 17; Alpha = 9, Delta = [0 1]
Patient: 17; Alpha = 9, Delta = [1 2]
Patient: 17; Alpha = 9, Delta = [2 3]
Patient: 17; Alpha = 9, Delta = [3 4]
Patient: 17; Alpha = 9, Delta = [4 5]
Average Entropy
Channel
20-40
40-60
60-80
80-100

(b)

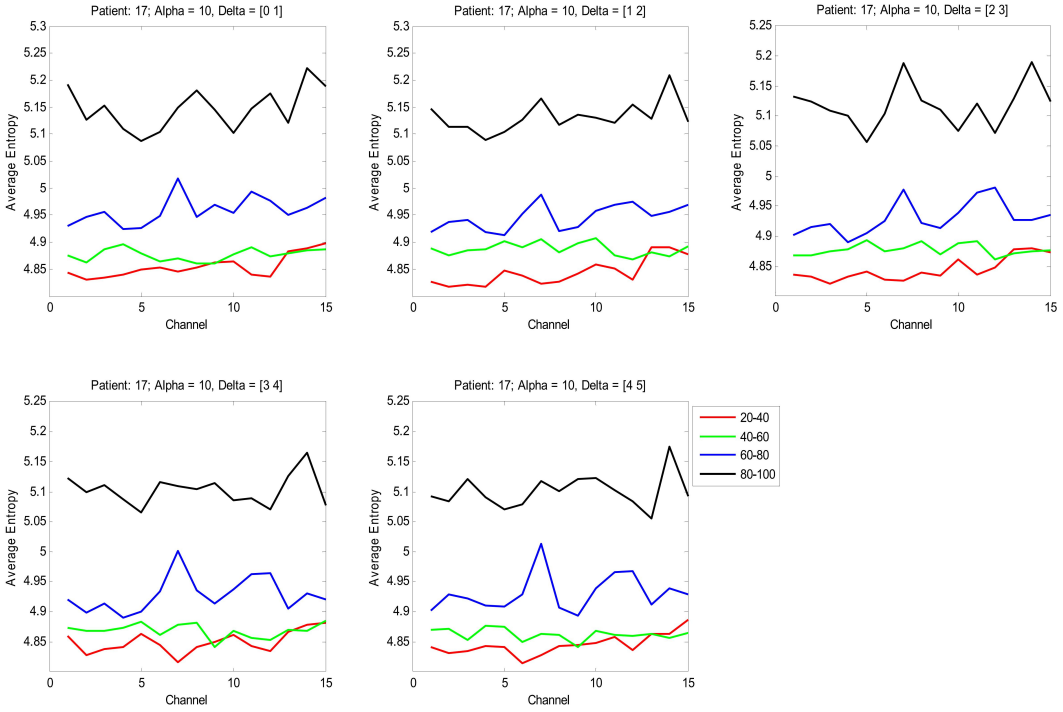
Patient: 17; Alpha = 10, Delta = [0 1]
Patient: 17; Alpha = 10, Delta = [1 2]
Patient: 17; Alpha = 10, Delta = [2 3]
Patient: 17; Alpha = 10, Delta = [3 4]
Patient: 17; Alpha = 10, Delta = [4 5]
Average Entropy
Channel
20-40
40-60
60-80
80-100

(c)

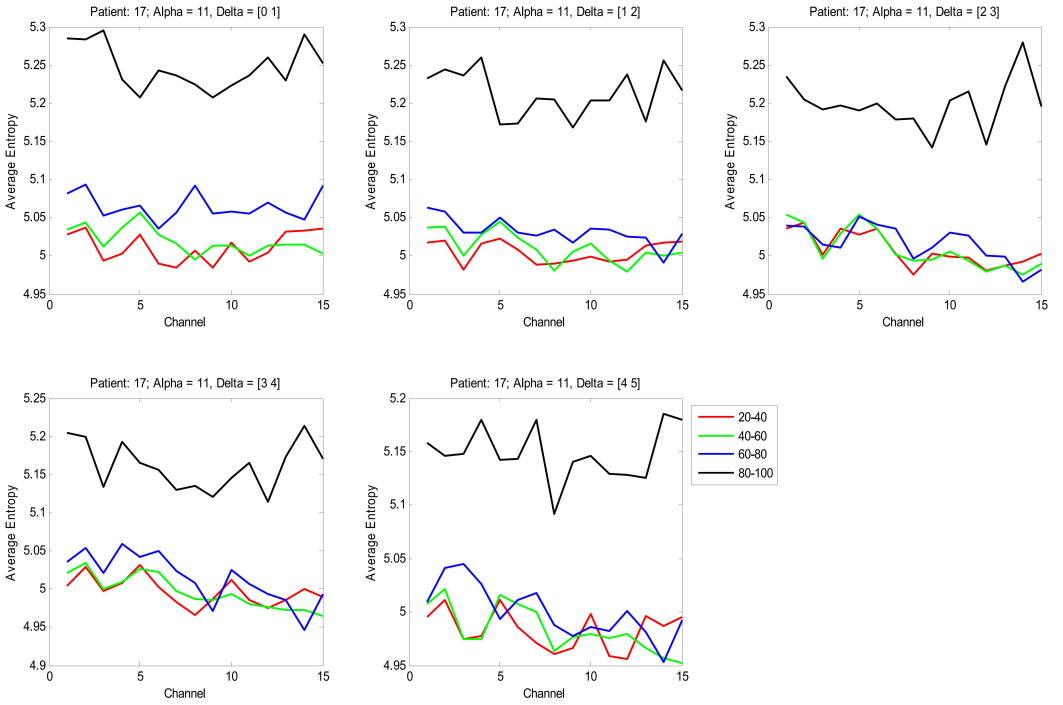
Patient: 17; Alpha = 11, Delta = [0 1]
Patient: 17; Alpha = 11, Delta = [1 2]
Patient: 17; Alpha = 11, Delta = [2 3]
Patient: 17; Alpha = 11, Delta = [3 4]
Patient: 17; Alpha = 11, Delta = [4 5]
Average Entropy
Channel
20-40
40-60
60-80
80-100

(d)

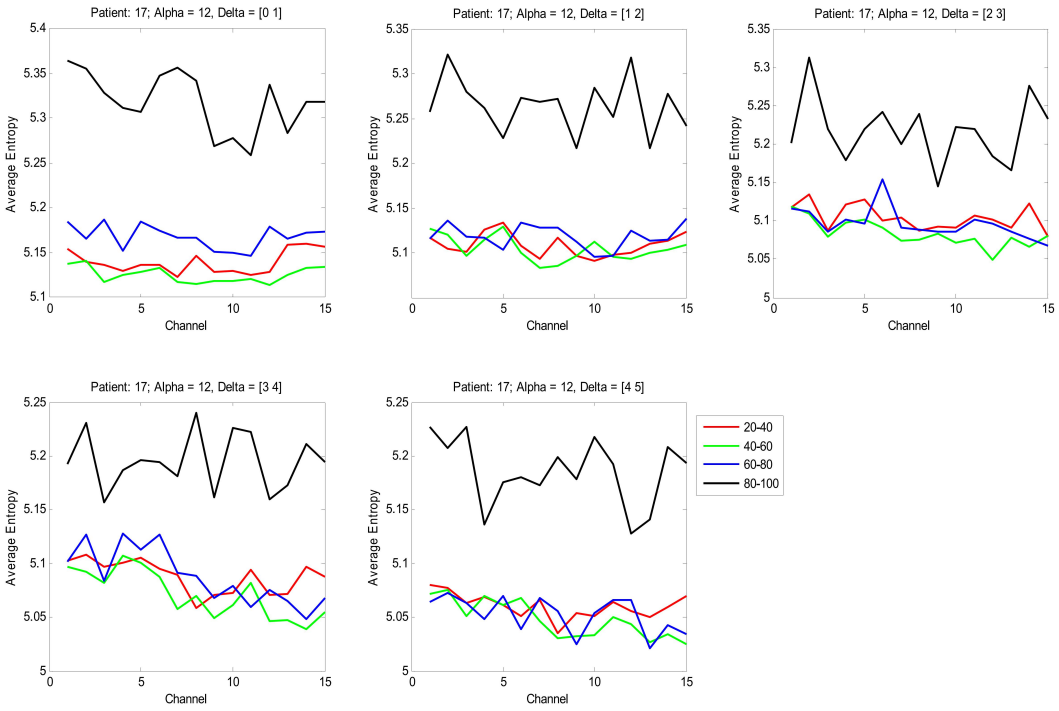

(e)

Figure 4.23 Average entropies of different BIS ranges for **patient 17**. In each sub-figure, for specific alpha sub-bands, results are shown for all delta sub-bands. (a) α = [8-9],(b) α = [9-10], (c) α = [10-11], (d) α = [11-12], (e) α = [12-13]

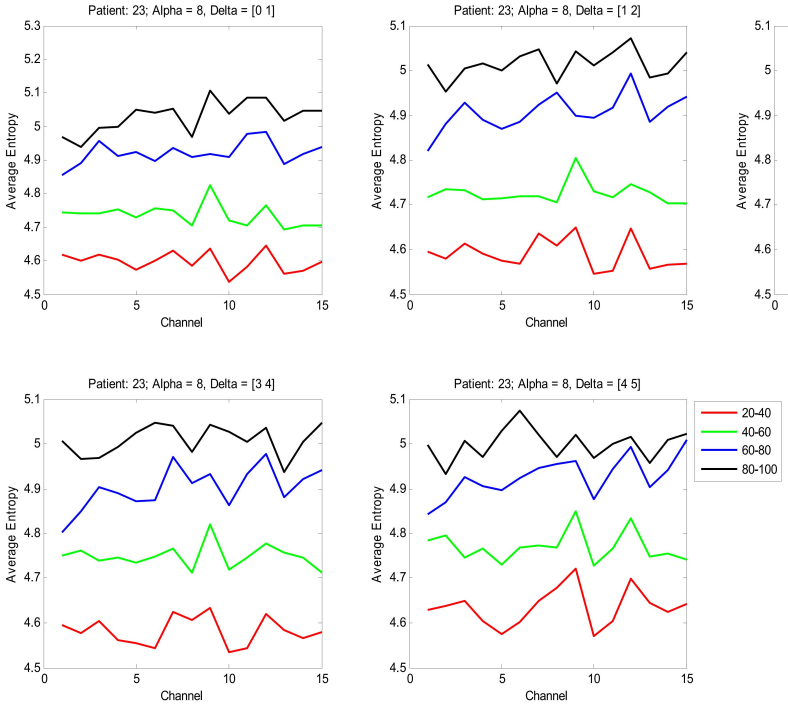
Patient: 23; Alpha = 8, Delta = [0 1]
Patient: 23; Alpha = 8, Delta = [1 2]
Patient: 23; Alpha = 8, Delta = [2 3]
Patient: 23; Alpha = 8, Delta = [3 4]
Patient: 23; Alpha = 8, Delta = [4 5]
Average Entropy
Channel
20-40
40-60
60-80
80-100

(a)

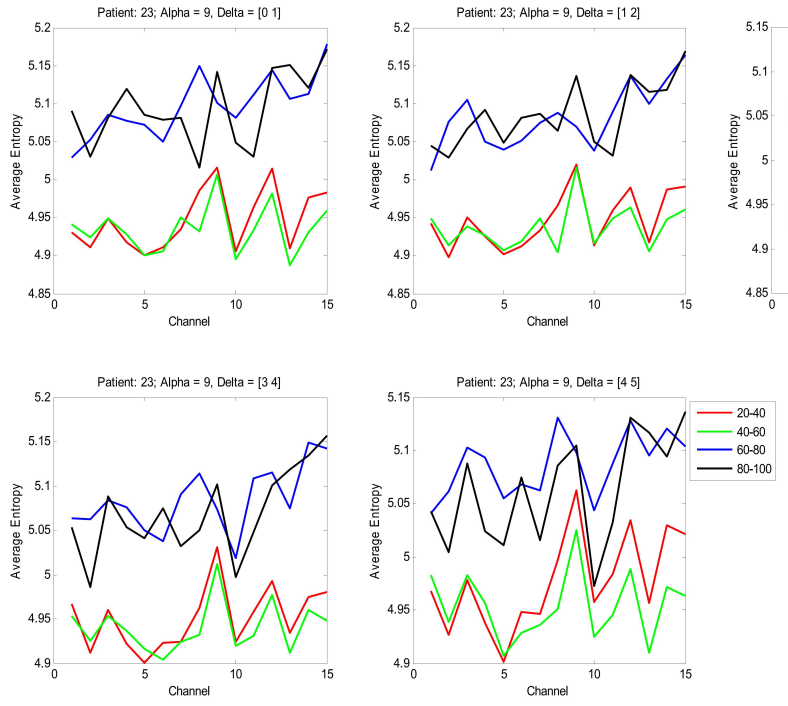
Patient: 23; Alpha = 9, Delta = [0 1]
Patient: 23; Alpha = 9, Delta = [1 2]
Patient: 23; Alpha = 9, Delta = [2 3]
Patient: 23; Alpha = 9, Delta = [3 4]
Patient: 23; Alpha = 9, Delta = [4 5]
Average Entropy
Channel
20-40
40-60
60-80
80-100

(b)

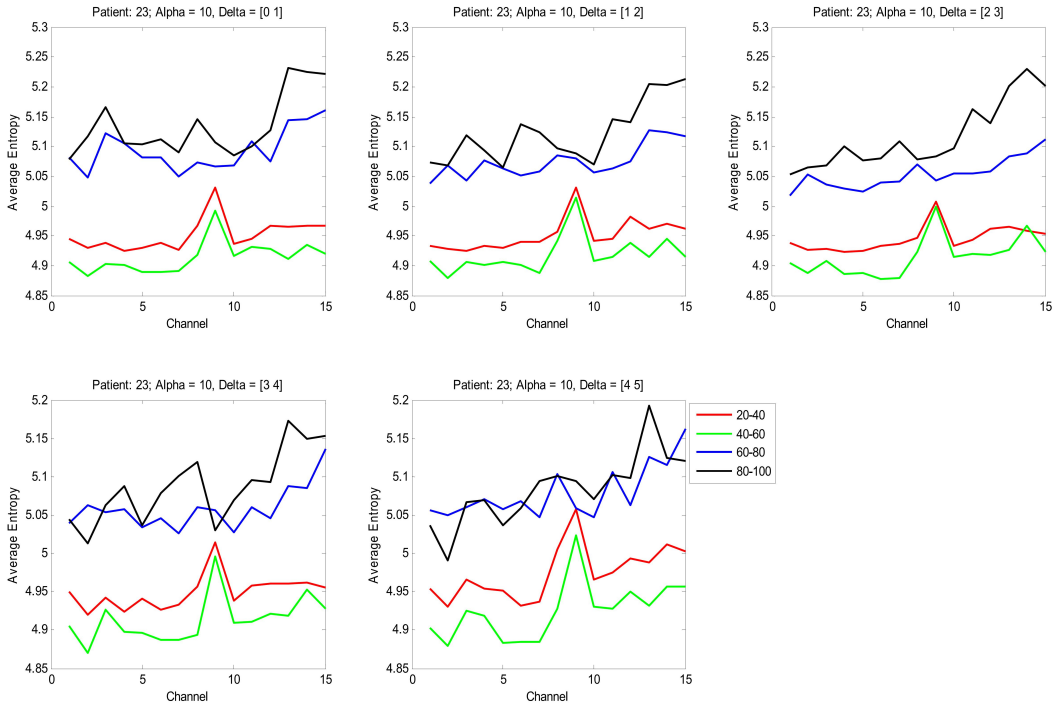
Patient: 23; Alpha = 10, Delta = [0 1]
Patient: 23; Alpha = 10, Delta = [1 2]
Patient: 23; Alpha = 10, Delta = [2 3]
Patient: 23; Alpha = 10, Delta = [3 4]
Patient: 23; Alpha = 10, Delta = [4 5]
Average Entropy
Channel
20-40
40-60
60-80
80-100

(c)

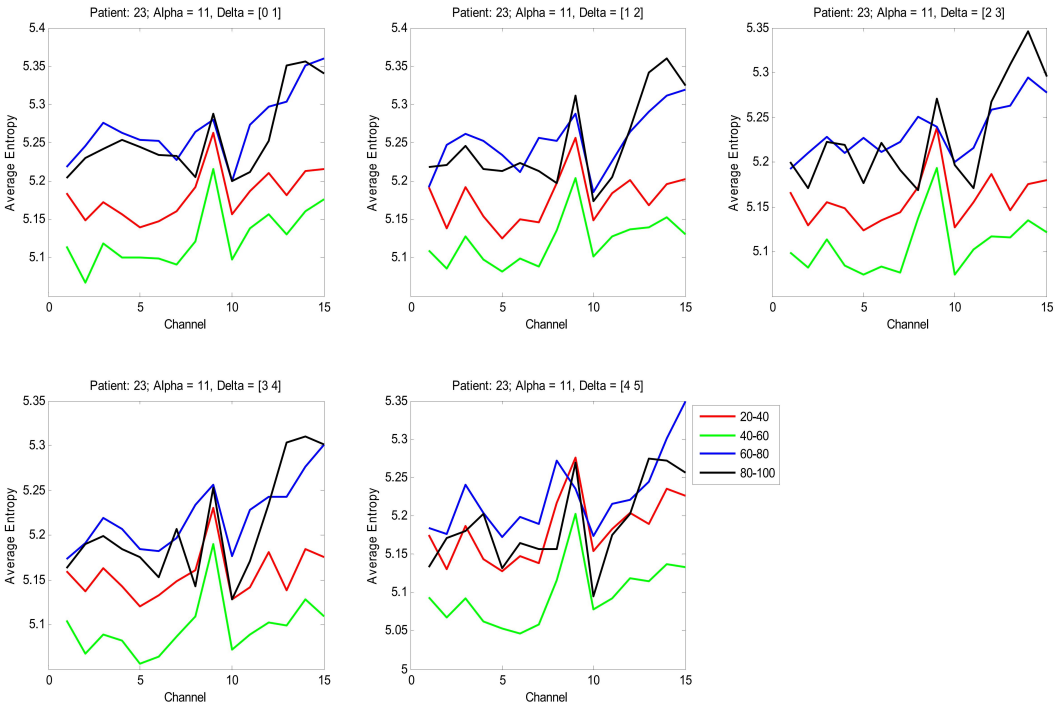
Patient: 23; Alpha = 11, Delta = [0 1]
Patient: 23; Alpha = 11, Delta = [1 2]
Patient: 23; Alpha = 11, Delta = [2 3]
Patient: 23; Alpha = 11, Delta = [3 4]
Patient: 23; Alpha = 11, Delta = [4 5]
Average Entropy
Channel
20-40
40-60
60-80
80-100

(d)

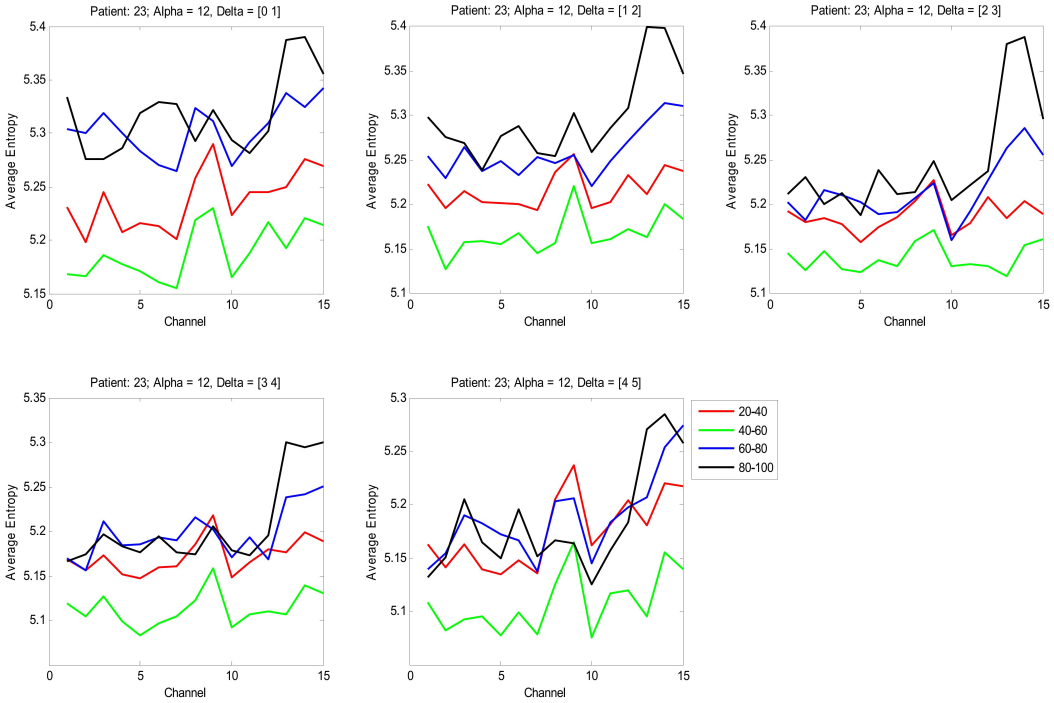

(e)

Figure 4.24 Average entropies of different BIS ranges for **patient 23**. In each sub-figure, for specific alpha sub-bands, results are shown for all delta sub-bands. (a) α = [8-9],(b) α = [9-10], (c) α = [10-11], (d) α = [11-12], (e) α = [12-13]

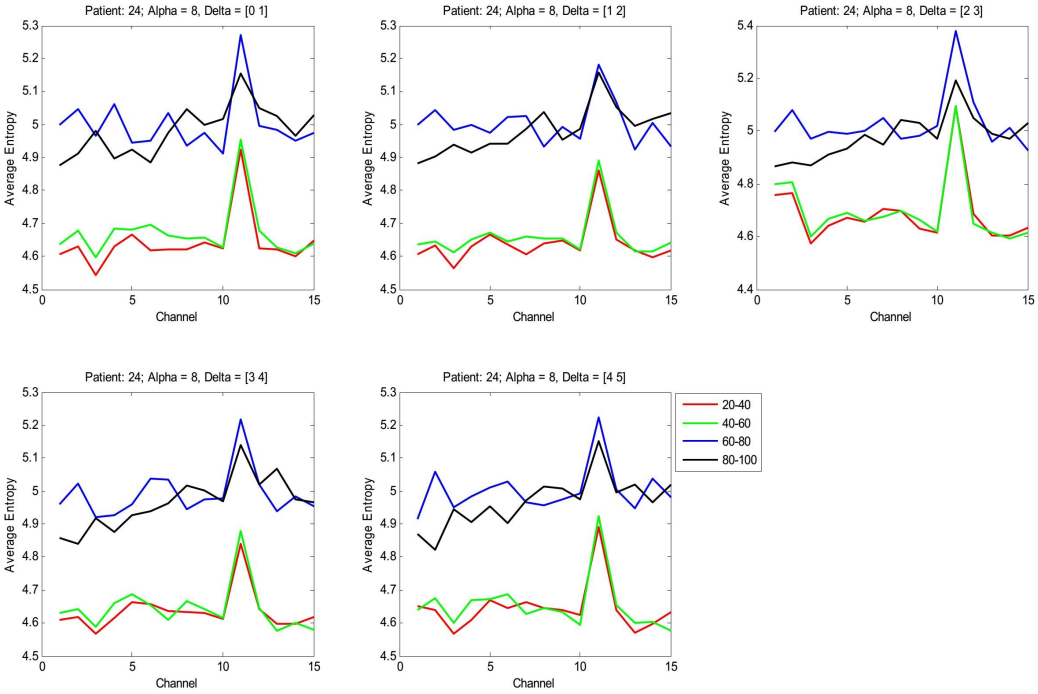
Patient: 24; Alpha = 8, Delta = [0 1]
Patient: 24; Alpha = 8, Delta = [1 2]
Patient: 24; Alpha = 8, Delta = [2 3]
Patient: 24; Alpha = 8, Delta = [3 4]
Patient: 24; Alpha = 8, Delta = [4 5]
Average Entropy
Channel
20-40
40-60
60-80
80-100

(a)

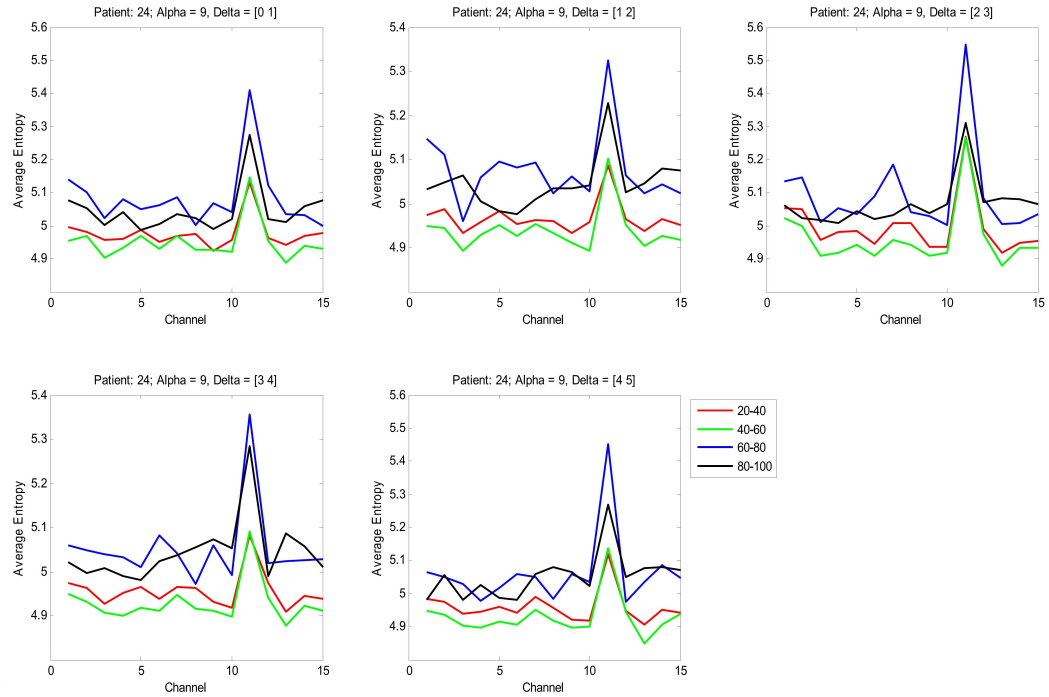
Patient: 24; Alpha = 9, Delta = [0 1]
Patient: 24; Alpha = 9, Delta = [1 2]
Patient: 24; Alpha = 9, Delta = [2 3]
Patient: 24; Alpha = 9, Delta = [3 4]
Patient: 24; Alpha = 9, Delta = [4 5]
Average Entropy
Channel
20-40
40-60
60-80
80-100

(b)

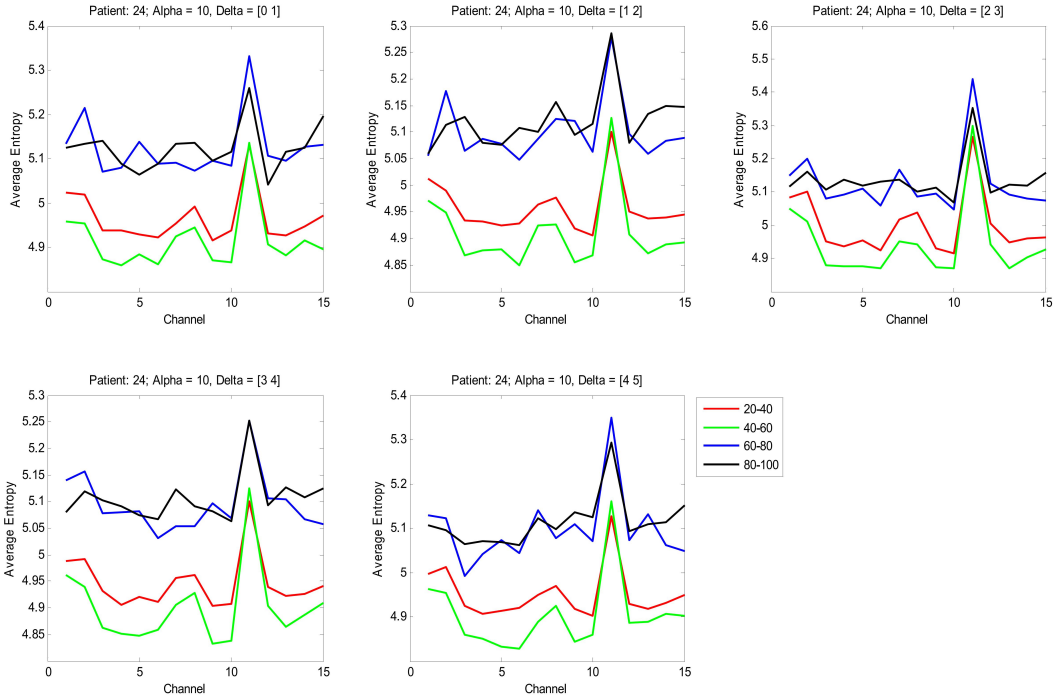
Patient: 24; Alpha = 10, Delta = [0 1]
Patient: 24; Alpha = 10, Delta = [1 2]
Patient: 24; Alpha = 10, Delta = [2 3]
Patient: 24; Alpha = 10, Delta = [3 4]
Patient: 24; Alpha = 10, Delta = [4 5]
Average Entropy
Channel
20-40
40-60
60-80
80-100

(c)

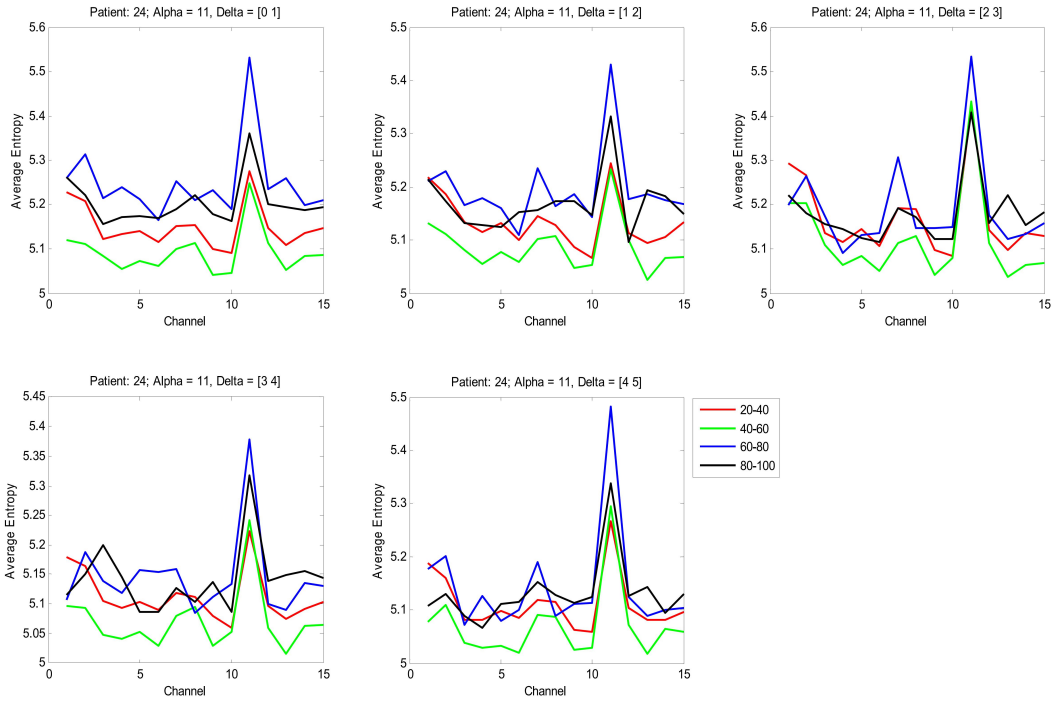
Patient: 24; Alpha = 11, Delta = [0 1]
Patient: 24; Alpha = 11, Delta = [1 2]
Patient: 24; Alpha = 11, Delta = [2 3]
Patient: 24; Alpha = 11, Delta = [3 4]
Patient: 24; Alpha = 11, Delta = [4 5]
Average Entropy
Channel
20-40
40-60
60-80
80-100

(d)

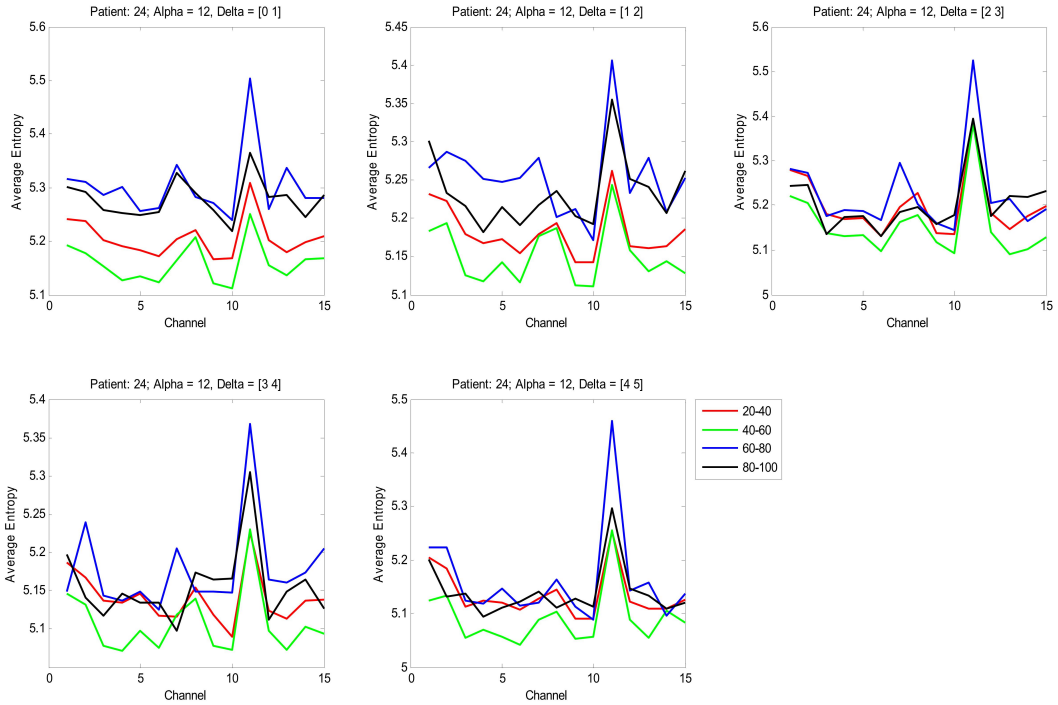

(e)

Figure 4.25 Average entropies of different BIS ranges for **patient 24**. In each sub-figure, for specific alpha sub-bands, results are shown for all delta sub-bands. (a) α = [8-9],(b) α = [9-10], (c) α = [10-11], (d) α = [11-12], (e) α = [12-13]

In the following Tables, the channels that have modulation effect among alpha and delta sub-bands for patients are shown. In some cells, "All (E. x)" was written, it means that all channels have modulation effect except channel/channels x.

Table 4.6
Channels that have modulation effect in different patients in third scenario

Patient	Alpha	Delta				
		0 - 1	**1 - 2**	**2 - 3**	**3 - 4**	**4 - 5**
12	7.5 - 8.5	1, 7, 15	8, 10, 11, 13	1, 2, 13, 15	8, 12, 13, 15	4, 5, 11, 12, 13, 14, 15
	8.5 - 9.5	—	9	13	10	11
	9.5 - 10.5	—	—	—	—	—
	10.5 - 11.5	7	—	—	—	—
	11.5 - 12.5	—	—	—	12	—
13	7.5 - 8.5	8, 15	12, 13, 15	4, 5, 6, 8, 13, 14, 15	8	15
	8.5 - 9.5	All	All (E. 4)	All	All	All
	9.5 - 10.5	—	—	—	—	—
	10.5 - 11.5	—	—	—	—	—
	11.5 - 12.5	—	—	—	—	—
14	7.5 - 8.5	All	All	All	All	All
	8.5 - 9.5	5, 6, 7, 9, 13	10, 14	1	1, 2, 3, 6	1, 2
	9.5 - 10.5	—	—	—	—	—
	10.5 - 11.5	10, 11	—	—	—	—
	11.5 - 12.5	—	10	—	—	—
17	7.5 - 8.5	1, 2, 3, 8, 12, 13, 14, 15	1, 8, 10, 12, 13, 14, 15	All (E. 3)	All (E. 3,15)	All
	8.5 - 9.5	1, 2, 8, 9, 10, 11, 14, 15	1, 9, 11, 13, 13, 15	1, 2, 3, 4, 11, 14, 15	1, 2, 11, 13, 14, 15	5, 11, 12, 13, 14, 15
	9.5 - 10.5	1, 2, 3, 4, 5, 6, 7, 11, 12	All (E. 13, 14)	All (E. 12, 13, 14, 15)	1, 2, 3, 4, 5, 6, 7, 8, 11, 12	1, 2, 3, 4, 5, 6, 7, 8, 12
	10.5 - 11.5	1, 2, 3, 4, 5, 6, 7, 9, 11, 12	1, 2, 3, 4, 5, 6, 7, 9, 10	8	1, 6, 7, 8	1, 6, 7, 8, 9, 11, 12
	11.5 - 12.5	—	1, 10	—	—	—
23	7.5 - 8.5	All	All	All	All	All
	8.5 - 9.5	1, 4	1, 5, 6, 7	—	—	—
	9.5 - 10.5	—	—	—	—	14
	10.5 - 11.5	—	—	—	—	—
	11.5 - 12.5	—	—	—	—	—
24	7.5 - 8.5	3, 8, 9, 10, 12, 13, 14, 15	8, 12, 13, 14, 15	8, 9, 13	8, 9	8, 13
	8.5 - 9.5	—	—	—	—	—
	9.5 - 10.5	—	—	—	—	—
	10.5 - 11.5	—	—	—	—	—
	11.5 - 12.5	—	—	—	—	—

Now, the channels that had modulation effect in specific frequency ranges in all patients are shown. The term "Y (E. X)" means that in all patients except patient X, the channel Y has modulation effect in the specified frequency range.

Table 4.7
Channels that have modulation effect in all patients in third scenario

		Delta				
		0 - 1	1 – 2	2 - 3	3 - 4	4 - 5
Alpha	7.5 - 8.5	15 (E. 24)	8 (E. 13), 12 (E. 12), 15 (E. 12)	8 (E. 12), 15 (E. 24)	8	15 (E. 24)
	8.5 - 9.5	—	—	—	—	—
	9.5 - 10.5	—	—	—	—	—
	10.5 - 11.5	—	—	—	—	—
	11.5 - 12.5	—	—	—	—	—

As seen, only the channel 8 at the frequency range (7.5-8.5) Hz and (3-4) Hz has modulation in different BIS ranges. In Figure 4.26, the mean and standard deviation of the entropy of the channel 8 in the specified ranges is presented.

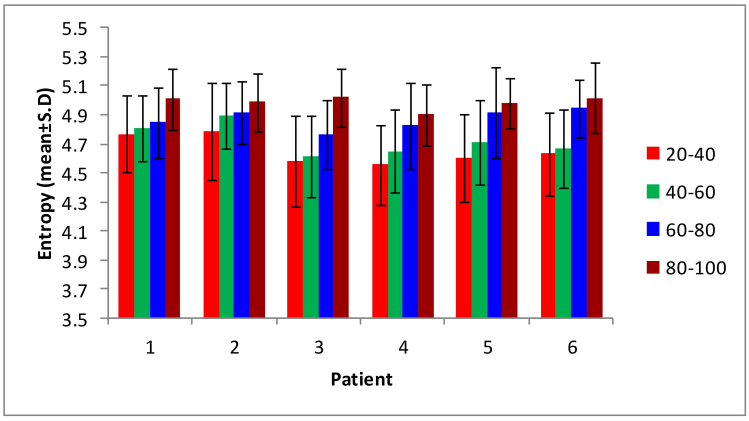

Figure 4.26 Mean and standard deviation of entropy of modulation signal between delta sub-band [3-4] Hz and alpha sub-band [8 9] obtained in channel 8 (T7) for different BIS intervals in third scenario

In Figure 4.27, the histogram of modulated signal for different BIS ranges are shown.

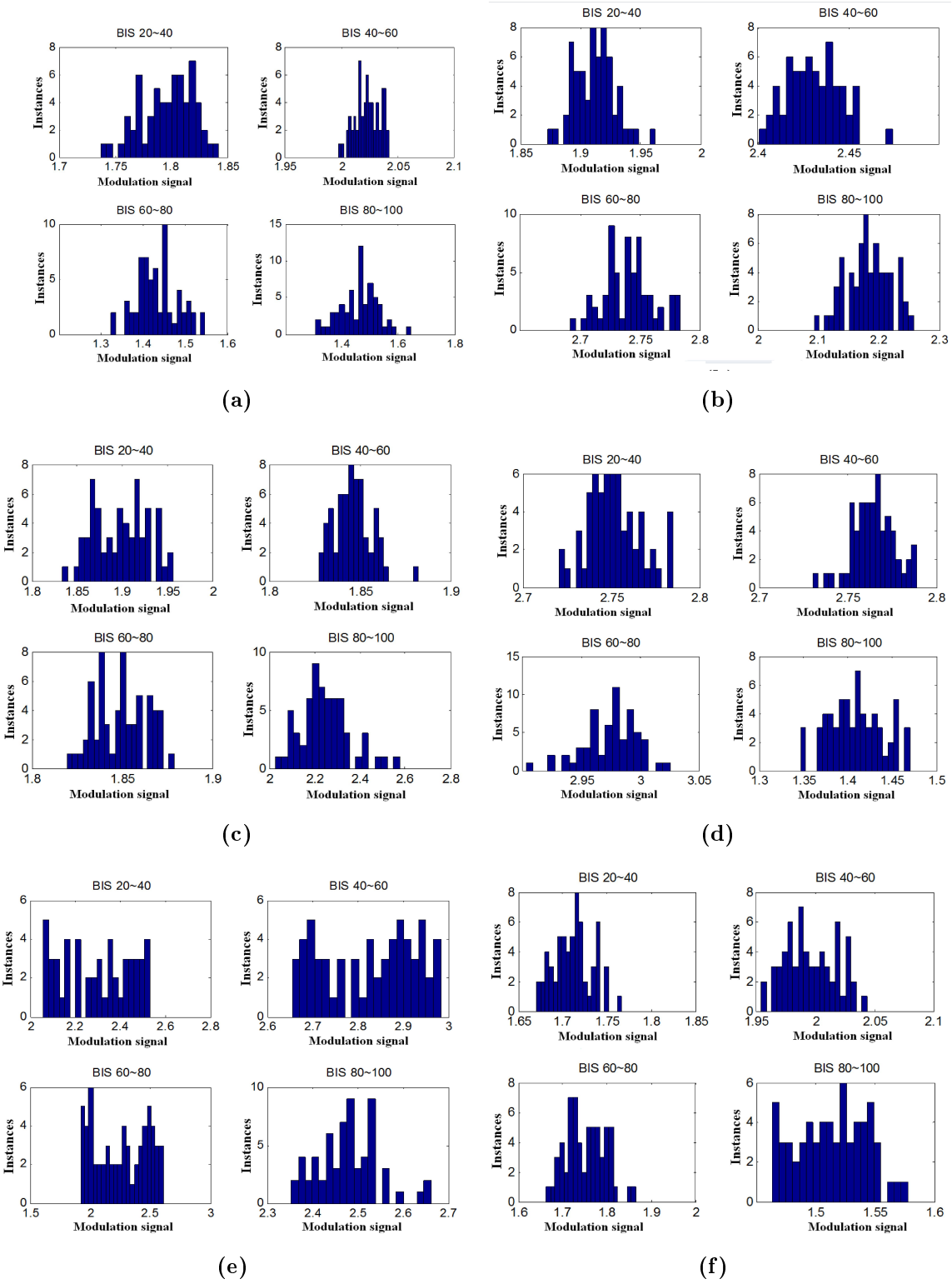

Figure 4.27 The histogram related to the different BIS ranges in third scenario: (a) Patient 12, (b) Patient 13, (c) Patient 14, (d) Patient 17, (e) Patient 23, (f) Patient 24.

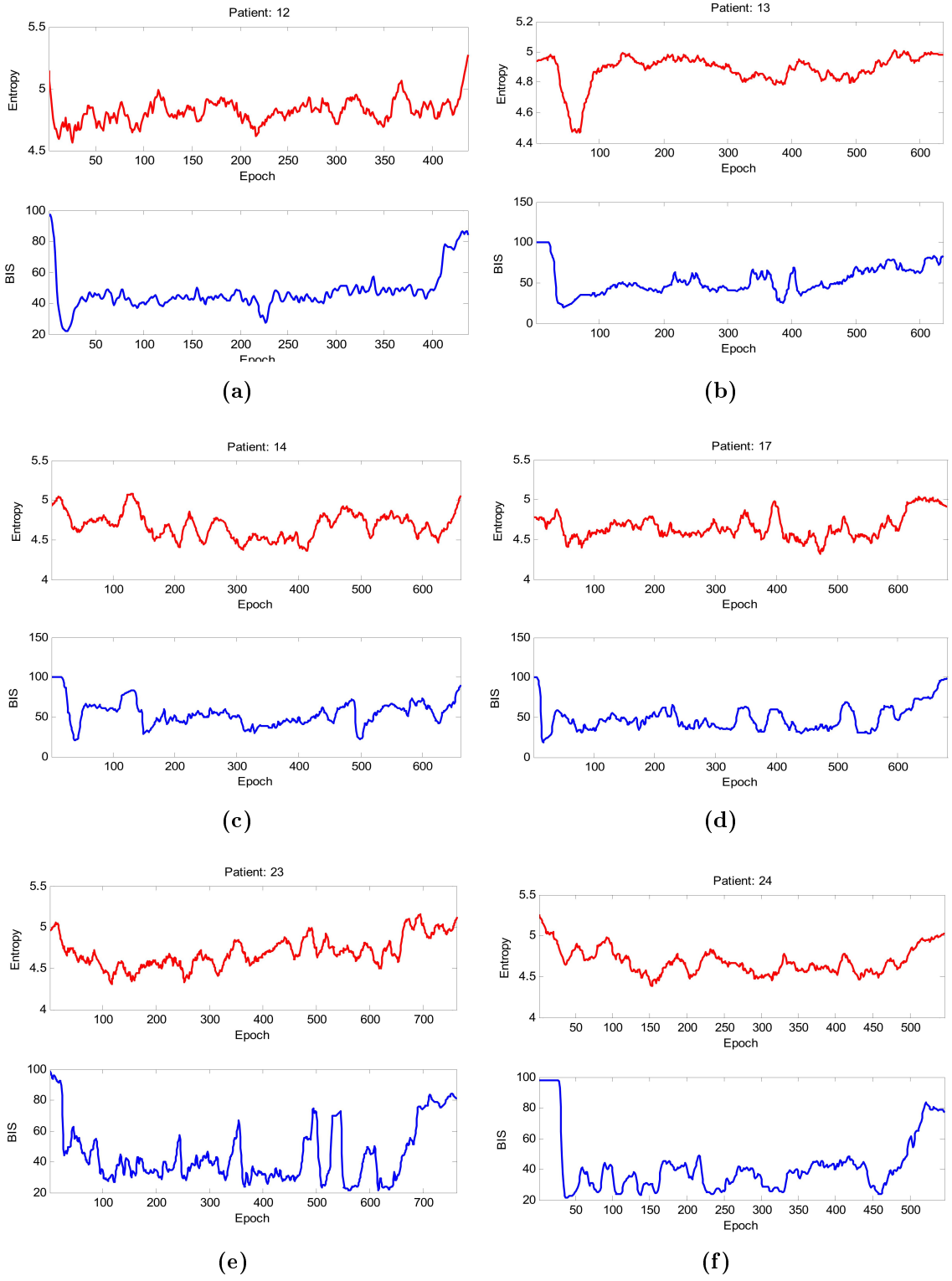

Figure 4.28 The variation of entropy and BIS during time in third scenario: (a) Patient 12, (b) Patient 13, (c) Patient 14, (d) Patient 17, (e) Patient 23, (f) Patient 24.

Variations of entropy of modulation at (7.5-8.5) Hz and delta (3-4) Hz in channel 8 for different epochs are shown. As seen, the variations in the entropy follow the variations in the BIS, and entropy increases when BIS increases, and vice versa.

In the following, the results of Mann-Whitney U test in the BIS intervals are shown in Table 4.8.

Table 4.8
Results of Mann-Whitney Test for third scenario, $h = 1$ denotes BIS ranges have different distributions, while $h = 0$ indicates they have same distributions

BIS ranges	**Test Result**	**Patient**						
		12	**13**	**14**	**17**	**23**	**24**	**Overall**
R_a, R_b	h (p)	0 (0.25)	1 (0.0066)	0 (0.21)	1 (5.9e-05)	1 (0.00036)	0 (0.26)	1 (5.4e-21)
R_a, R_c	h (p)	0 (0.31)	1 (0.0017)	1 (2.7e-07)	1 (1.7e-14)	1 (2.1e-15)	1 (1.58e-9)	1 (1.6e-51)
R_a, R_d	h (p)	0 (0.0042)	1 (7.4e-05)	1 (1.4e-14)	1 (1.2e-10)	1 (3.4e-18)	1 (9.1e-13)	1 (4.1e-63)
R_b, R_c	h (p)	0 (0.53)	0 (0.33)	1 (4.4e-09)	1 (3.1e-08)	1 (1.1e-07)	1 (2.4e-08)	1 (1.5e-20)
R_b, R_d	h (p)	1 (0.0051)	1 (0.0022)	1 (6.1e-19)	1 (1.2e-06)	1 (6.6e-11)	1 (5.1e-11)	1 (5.1e-43)
R_c, R_d	h (p)	0 (0.067)	1 (0.013)	1 (1.2e-10)	0 (0.36)	0 (0.28)	0 (0.071)	1 (1.3e-12)

5. DISCUSSION

This dissertation was done to evaluate DOA in order to prevent awareness during general anesthesia and its serious complications with Propofol intravenous anesthetic agent. As the final target effects of all general anesthetic drugs are brain, consequently we chose an especial EEG based approach that has high sensitivity and accuracy for determination of DOA.

Due to the non-stationary nature of EEG signals, wavelet transforms have become powerful tools in capturing dynamic patterns [65]. Blanco et al.'s study on EEG time-frequency analysis showed that noisy signals contaminated by muscle artifacts can be precisely filtered out with wavelets without modifying the pattern of the remnant ones [65].

Wavelet analysis is helpful in finding hidden frequency information in the signal. In addition, it enables a 3- representation of the signal: amplitude, frequency, and time [62, 66]. However, it is important to note that the significance of the wavelet analysis is still dependent on the choice of the mother wavelet used. For these specifications in this dissertation, we studied the phase coupling between δ and α sub-bands in spontaneous EEG signals using Morlet continuous complex wavelet transform analysis to find an accurate formula to prevent awareness during general anesthesia.In order to calculate modulation effect, delta and alpha bands were partitioned into smaller sub-bands through three different scenarios.

In the first scenario, we partitioned delta band into three sub-bands; VSD, SD, and FD with frequency covering in the range (0.1-0.5) Hz, (0.7-1.7) Hz, and (2-4) Hz, respectively. Whole of the alpha band was considered as one sub-band in the range (8-13) Hz.This partitioning is the same as approach that was used by B. Molaee-Ardekan et al [53]. After obtaining modulated signals (Figure 4.1) between δ and α sub-bands in order to compare the calculated entropy with corresponding

recorded BIS, the BIS values of each epoch were averaged based on Figures 4.2 and 4.7 As seen in Table 4.1 the modulation effect between alpha and slow delta sub-bands were observed in more channels especially in channel 9(C3) which was seen in all studied patients. In Figures 4.8 and 4.9,mean and standard deviation of the entropy of EEG epoches, and the histogram of modulation signal were shown that there were coordination between BIS ranges and corresponding entropy of modulation signal of slow delta and alpha sub-bands in channel 9 in all patients except in patient 5 (Pt 23). Patient 5 was awake during operating period in spite of her BIS index which was 23, because of her physiologic variability. Results of Mann-Whitney Test for first scenario (Table 4.2)illustrate that entropies of the different BIS intervals come from different distributions which indicate that proposed method can be used to measure DOA.

In this scenario we find out that single channel C_3 may be used to record EEG signals instead of using Fp and F_7 simultaneously. The advantages of our method are being economical,ease of usage and omitting unwanted FEMG.It also can be inferred that the processing method with wavelet approach has better performance in all DOA levels.While Ardakani et al [53] have concluded that there is no single delta sub-band with the best performance in different DOA levels. This difference can be originated from the following factors as: Selected EEG signal processing method,EEG electrode montage method and the used intravenous anesthetic agents instead of inhalational agent which was used by Ardakani et al.

In second and third scenarios delta and alpha bands are partitioned innovatively into five sub-bands with 1 Hz bandwidth. In both scenarios, the edge frequencies of delta sub-bands are located at integer frequencies. In this manner, different delta sub-bands are (0- 1) Hz, (1- 2) Hz, (2 -3]) Hz, (3- 4) Hz, and (4 -5) Hz. Difference between second and third scenarios is in the edge frequencies of sub-bands of alpha band. In second scenario, edge frequencies of alpha sub-bands are located at integer frequencies including:(8- 9) Hz, (9- 10) Hz, (10- 11) Hz, (11- 12) Hz, and (12 -13) Hz.

In third scenario, the center frequencies of alpha sub-bands are located at integer frequencies too. But edge frequencies are at the middle of two consecutive integers.

Therefore, alpha sub-bands are (7.5- 8.5) Hz, (8.5- 9.5) Hz, (9.5- 10.5) Hz, (10.5- 11.5) Hz, (11.5-12.5) Hz.

Second and third procedures are similar to ones that introduced in the first scenario. The average entropies of BISs related to different alpha and delta sub-bands are shown in Figures from 4.11 to 4.16. By analyzing these Figures, the channels which have modulation effect among alpha and delta sub-bands are identified. As seen in Table 4.4, there is phase modulation among alpha and delta sub-bands at ranges (8-9) Hz and (3-4) Hz, respectively in all patients in channel 8 (T_7). In Figure 4.17, the average and standard deviation of entropy in different DOA levels in channel 8 for all patients are presented. As seen, the average entropy increases as BIS increases. Patient 5(Pt 23) similar to first scenario is exceptional for her physiological variation. As can be observed, at Figure 4.19, the variations in entropy follow the variations in BIS values, and when entropy increases, BIS also increases, and vice versa.

As presented in result section the best modulation effect between alpha and slow delta sub-bands were observed in channel 9(C3) at first scenario butin the second and third scenarios the best modulation effect between alpha and slow delta sub-bands were observed in channel 8 (T_7) I think this difference in quality of recorded phase coupling between delta and alpha sub-bands between scenarios is related to physiologic origin of emitted signal.

Third scenario and its results are the same as second scenario but it has modulation in channel 8 for different BIS ranges at frequency ranges (7.5-8.5) Hz and (3-4) Hz.According to Figure 4.28, entropy variations follow BIS variations, and when entropy increases, BIS also increases, and vice versa.

The BIS values from 0 to 100 are segmented into four ranges, R_a (20-40), R_b (40-60), R_c (60-80), and R_d (80-100). We did not consider the interval 0-20, since the number of epochs whose relative BIS belonging to this range, was very low. The average entropy for all BIS intervals were calculated for all channels and all possible modulations between α and δ sub-bands. For each patient, Mann-Whitney test was

performed for all possible pairs of entropies related to R_a, R_b, R_c and R_d where the significance level was set to 0.05. The results were presented in Table 5.1. As it can be average entropy at various BIS intervals have significant differences.It indicates that the proposed method can be used to measure the DOA with high accuracy.

Our findings in this study can be employed in the physiologically-based mean-field modeling of brain electrical activities in general anesthesia. Modulation of alpha band oscillations concurrently by delta bands activities is a characteristic of the EEG that, to our knowledge, has not been considered yet in mean-field models designed for EEG signals in anesthesia [67–69]. However, recently the switching behavior of neural populations to UP and DOWN states in the delta frequency range, which may trigger the modulation of alpha oscillations, and its possible underlying mechanisms have been addressed without studying the relation between slow and fast components of EEG signals [70–72]. Mechanisms, which make relations between slow and fast EEG components, still need to be better characterized, and to be modeled mathematically in mean-field models.

Some limitations in performing this study include:

a) Electromagnetic and electric interferences of the devices which are used in operating room such as electrocutery devices.

b) The patient head Movement due to surgical and anesthesiology personnel interventions.

c) Time changing on EEG electrodes which changes the impedance of skin surface because of precipitation and or drying the special gel of electrodes consequently deterioration of signal quality especially in long duration surgeries.

As an idea for future works, we can suggest to introduce pattern recognition approach to classify the epochs. We can split the range of BIS index i.e., 0$\sim$100 to different ranges. Clearly, in this case, efficient features must be extracted from each epoch to have better classification performance. Some epochs from each range are

Table 5.1
Results of Mann-Whitney Test for **third scenario**, h = 1 denotes BIS ranges have different distributions, while h = 0 indicates they have same distribution

BIS ranges	Scenario	Test Result	Patient						
			12	13	14	17	23	24	Overall
R_a, R_b	First	$h\ (p)$	0 (0.51)	0 (0.33)	1 (0.011)	1(0.0025)	0 (0.081)	0 (0.36)	1(2.9e-14)
	Second	$h\ (p)$	0 (0.075)	1 (0.0022)	0 (0.078)	1(3.3e-05)	0 (0.052)	1 (0.048)	1(4.1e-18)
	Third	$h\ (p)$	0 (0.25)	1 (0.0066)	0 (0.21)	1(5.9e-05)	1(0.00036)	0 (0.26)	1(5.4e-21)
R_a, R_c	First	$h\ (p)$	1(0.0011)	1(0.00011)	1 (5.1e-08)	1(7.1e-06)	0 (0.78)	1(9.3e-10)	0 (0.33)
	Second	$h\ (p)$	0 (0.13)	1 (0.0011)	1 (8.1e-07)	1(4.1e-14)	1(7.4e-14)	1(1.4e-10)	1(1.1e-45)
	Third	$h\ (p)$	0 (0.31)	1 (0.0017)	1 (2.7e-07)	1(1.7e-14)	1(2.1e-15)	1(1.58e-9)	1(1.6e-51)
R_a, R_d	First	$h\ (p)$	1(6.9e-07)	1 (7.5e-05)	1 (7.7e-07)	1(1.2e-10)	0 (0.16)	1(4.5e-12)	1(4.6e-09)
	Second	$h\ (p)$	1(0.0055)	1 (1.1e-05)	1 (1.3e-12)	1(4.9e-10)	1(7.1e-14)	1(4.6e-15)	1(7.4e-58)
	Third	$h\ (p)$	1(0.0042)	1 (7.4e-05)	1 (1.4e-14)	1(1.2e-10)	1(3.4e-18)	1(9.1e-13)	1(4.1e-63)
R_b, R_c	First	$h\ (p)$	1(0.0023)	1 (0.0023)	1(1.31e-05)	1 (0.027)	0 (0.39)	1(1.5e-08)	1(5.4e-16)
	Second	$h\ (p)$	0 (0.38)	0 (0.49)	1 (2.5e-07)	1(7.2e-08)	1(5.7e-09)	1(3.7e-08)	1(7.7e-19)
	Third	$h\ (p)$	0 (0.53)	0 (0.33)	1 (4.4e-09)	1(3.1e-08)	1(1.1e-07)	1(2.4e-08)	1(1.5e-20)
R_b, R_d	First	$h\ (p)$	1(8.6e-09)	1(0.00022)	1 (5.2e-05)	1(1.1e-07)	0 (0.61)	1(9.9e-11)	1(3.3e-29)
	Second	$h\ (p)$	1(0.0065)	1(0.00076)	1 (1.1e-16)	1(2.9e-06)	1(1.6e-09)	1(5.1e-12)	1(9.8e-40)
	Third	$h\ (p)$	1(0.0051)	1 (0.0022)	1 (6.1e-19)	1(1.2e-06)	1(6.6e-11)	1(5.1e-11)	1(5.1e-43)
R_c, R_d	First	$h\ (p)$	0 (0.058)	0 (0.22)	0 (0.099)	1(3.3e-05)	0 (0.36)	0 (0.56)	1(4.5e-09)
	Second	$h\ (p)$	0 (0.11)	1 (0.0036)	1 (3.5e-09)	0 (0.37)	0 (0.52)	0 (0.31)	1(1.6e-11)
	Third	$h\ (p)$	0 (0.067)	1 (0.013)	1 (1.2e-10)	0 (0.36)	0 (0.28)	0 (0.071)	1(1.3e-12)

used to train the classifier, and then classifier can be used to classify the incoming epochs to one of previously predefined ranges. Artificial neural networks, support vector machines (SVM) and other classifiers can be tested and from them efficient classifier can be chosen.

6. CONCLUSION

In this study, a new method for DOA measurement based on Morlet Complex CWT was presented. Delta and alpha bands were partitioned into five one Hz bandwidth sub-bands. DOA was measured using Entropy of MS among them in different channels. Obtained results in terms of mean of different BIS ranges showed that MS between (3- 4) Hz and (8- 9) Hz sub-bands in channel 8 achieves the best results in DOA measurement. Mann-Whitney U test also showed that average entropy at various BIS intervals have significant difference which show the proposed method can be used to measure DOA with high accuracy.We suggest in the future in another study to be investigated, the possibility of doing this study by recording the EEG data from a single C_3 or T_7 channel instead 10-20 multi-channel standard in both total intravenous and inhalational anesthesia to generalize using this method as standard anesthesia monitoring.

REFERENCES

1. Fishbeinn, M., *The New illustrated medical and health encyclopedia*, New York: H S Stuttman Co, 1970.

2. Sebel, P. S., T. A. Bowdle, M. M. Ghoneim, I. J. Rampil, R. E. Padilla, T. J. Gan, and K. B. Domino, "The incidence of awareness during anesthesia: a multicenter united states study," *Anesthesia & Analgesia*, Vol. 99, no. 3, pp. 833–839, 2004.

3. Sandin, R. H., G. Enlund, P. Samuelsson, and C. Lennmarken, "Awareness during anaesthesia: a prospective case study," *The Lancet*, Vol. 9205, pp. 707–711, 2000.

4. Rani, D. D., and S. Harsoor, "Depth of general anaesthesia monitors," *Indian J Anaesth*, Vol. 56, no. 5, pp. 437–441, 2012.

5. Myles, P. S., "Prevention of awareness during anaesthesia," *Best Pract Res Clin Anaesthesiol*, Vol. 21, no. 3, pp. 345–355, 2007.

6. Zanatta, P., S. M. Benvenuti, E. Bosco, F. Baldanzi, C. Longo, D. Palomba, V. Salandin, and C. Sorbara, "Intraoperative neurophysiological monitoring of the afferent pain pathway in cardiac surgery patients," *Clinical Neurophysiology*, Vol. 122, no. 10, pp. 2093–2099, 2011.

7. Bruhn, J., P. Myles, R. Sneyd, and M. Struys, "Depth of anaesthesia monitoring: what's available, what's validated and what's next?," *British journal of anaesthesia*, Vol. 97, no. 1, pp. 85–94, 2006.

8. y Ye, S., J. m Park, J. h Kim, J. h Jung, A. y Jeon, I. c Kim, J. m Son, K. g Nam, S. w Baik, and J. h Ro, "Development for the evaluation index of an anesthesia depth using the bispectrum analysis," *International Journal of Biological and Medical Sciences*, Vol. 4, pp. 67–70, 2009.

9. Glass, P. S., and I. J. Rampil, "Automated anesthesia: Fact or fantasy?," *International Journal of Biological and Medical Sciences*, Vol. 95, no. 1, pp. 1–2, 2011.

10. Kent, C. D., and K. B. Domino, "Depth of anesthesia," *Current Opinion in Anesthesiology*, Vol. 22, no. 6, pp. 782–787, 2009.

11. Alkire, M. T., A. G. Hudetz, and G. Tononi, "Consciousness and anesthesia," *Science*, Vol. 322, no. 5903, pp. 876–880, 2008.

12. Musizza, B., and S. Ribaric, "Monitoring the depth of anaesthesia," *Sensors*, Vol. 10, no. 12, pp. 10896–10935, 2010.

13. Khan, M. F., K. Samad, F. Shamim, and H. Ullah, "Awareness during anesthesia–an update," *Middle East journal of anesthesiology*, Vol. 19, no. 4, p. 723, 2008.

14. Ghoneim, M. M., and R. B. Weiskopf, "Awareness during anesthesia," *Anesthesiology*, Vol. 92, no. 2, p. 597, 2000.

15. Moerman, N., B. Bonke, and J. Oosting, "Awareness and recall during general anesthesia: Facts and feelings," *Anesthesiology*, Vol. 79, no. 3, pp. 454–464, 1993.

16. Schwender, D., H. Kunze-Kronawitter, P. Dietrich, S. Klasing, H. Forst, and C. Madler, "Conscious awareness during general anaesthesia: patients' perceptions, emotions, cognition and reactions," *British journal of anaesthesia*, Vol. 80, no. 2, pp. 133–139, 1998.

17. Ghoneim, M. M., R. I. Block, M. Haffarnan, and M. J. Mathews, "Awareness during anesthesia: risk factors, causes and sequelae: a review of reported cases in the literature," *Anesthesia & Analgesia*, Vol. 108, no. 2, pp. 527–535, 2009.

18. Aitkenhead, A., "The pattern of litigation against anaesthetists," *British journal of anaesthesia*, Vol. 73, no. 1, pp. 10–21, 1994.

19. Grover, V., and N. Bharti, "Measuring depth of anaesthesia-an overview on the currently available monitoring systems," in *Indian Anaesthetists' Forum*, Vol. 9, pp. 1–32, 2008.

20. Trillo-Urrutia, L., S. Fernandez-Galinski, and J. Castano-Santa, "Awareness detected by auditory evoked potential monitoring," *British journal of anaesthesia*, Vol. 91, no. 2, pp. 290–292, 2003.

21. Sinha, P. K., and T. Koshy, "Monitoring devices for measuring the depth of anaesthesia-an overview," *Indian Journal of Anaesthesia*, Vol. 51, no. 5, p. 365, 2007.

22. Miller, R. D., *Miller's Anesthesia, 7th ed.*, Elsevier Health Sciences, 2010.

23. Abeles, M., and M. H. Goldstein, "Multispike train analysis," in *Proceedings of the IEEE*, Vol. 65 of *5*, pp. 762–773, 1997.

24. Webster, J. G., *Medical instrumentation: application and design, 4th ed.*, John Wiley & Sons, 2009.

25. Lotte, F., *Study of electroencephalographic signal processing and classification techniques towards the use of brain-computer interfaces in virtual reality applications.* PhD thesis, Insa De Rennes, France, 2009.

26. Sirois, J. E., Q. Lei, E. M. Talley, C. Lynch, and D. A. Bayliss, "The task-1 two-pore domain k+ channel is a molecular substrate for neuronal effects of inhalation anesthetics," *The Journal of Neuroscience*, Vol. 20, no. 17, pp. 6347–6354, 2000.

27. Mashour, G. A., S. A. Forman, and J. A. Campagna, "Mechanisms of general anesthesia: from molecules to mind," *Best Practice & Research Clinical Anaesthesiology*, Vol. 19, no. 3, pp. 349–364, 2005.

28. Mashour, G. A., "Integrating the science of consciousness and anesthesia," *Anesthesia & Analgesia*, Vol. 103, no. 4, pp. 975–982, 2006.

29. Schneider, G., and P. Sebel, "Monitoring depth of anaesthesia," *European Journal of Anaesthesiology (EJA)*, Vol. 14, pp. 21–28, 1997.

30. Mahla, M. E., "The electroencephalogram in the operating room," in *Seminars in Anesthesia, Perioperative Medicine and Pain*, Vol. 16, pp. 3–13, WB Saunders, 1997.

31. Constant, I., R. Seeman, and I. Murat, "Sevoflurane and epileptiform eeg changes," *Pediatric Anesthesia*, Vol. 15, no. 4, pp. 266–274, 2005.

32. Afrasiabi, S., R. Boostani, S. Koochaki, and F. Zand, "Presenting an effective eeg-based index to monitor the depth of anesthesia," in *Artificial Intelligence and Signal Processing (AISP), 2012 16th CSI International Symposium on: 2012*, pp. 5557–562, IEEE for Engineering in Medicine and Biology Society, 2012.

33. Johansen, J. W., and P. S. Sebel, "Development and clinical application of electroencephalographic bispectrum monitoring," *Anesthesiology*, Vol. 93, no. 5, pp. 1336–1344, 2000.

34. Rampil, I. J., "A primer for eeg signal processing in anesthesia," *Anesthesiology*, Vol. 89, no. 4, pp. 980–1002, 1998.

35. Luginbuhl, M., S. Wuthrich, S. Petersen-Felix, A. Zbinden, and T. Schnider, "Different benefit of bispectal index (BIS^{TM}) in desflurane and propofol anesthesia," *Acta anaesthesiologica scandinavica*, Vol. 47, no. 2, pp. 165–173, 2003.

36. Schneider, G., S. Schoniger, and E. Kochs, "Does bispectral analysis add anything but complexity? bis sub-components may be superior to bis for detection of awareness," *British journal of anaesthesia*, Vol. 93, no. 4, pp. 596–597, 2004.

37. Hall, J., and G. Lockwood, "Bispectral index: comparison of two montages," *British journal of anaesthesia*, Vol. 80, no. 3, pp. 342–344, 1998.

38. Tempe, D. K., and L. Satyanarayana, "Editorial i is there any alternative to the bispectral index monitor?," *British journal of anaesthesia*, Vol. 92, no. 1, pp. 1–3, 2004.

39. Schultz, B., A. Schultz, and U. Grouven, "Sleeping stage based systems (narcotrend), new aspects of high technology in medicine 2000," *British journal of anaesthesia*, pp. 285–291, 2000.

40. Pilge, S., R. Zanner, G. Schneider, J. Blum, M. Kreuzer, and E. F. Kochs, "Time delay of index calculation: analysis of cerebral state, bispectral, and narcotrend indices," *Anesthesiology*, Vol. 104, no. 3, pp. 488–494, 2006.

41. Mashou, G. A., ed., *Consciousness, awareness, and anesthesia*, Cambridge University Press, 2010.

42. Schneider, G., W. Nahm, E. Kochs, P. Bischoff, C. Kalkman, H. Kuppe, and C. Thornton, "Quality of perioperative AEP-variability of expert ratings," *British journal of anaesthesia*, Vol. 91, no. 6, pp. 905–908, 2003.

43. Messner, M., U. Beese, J. Romstock, M. Dinkel, and K. Tschaikowsky, "The bispectral index declines during neuromuscular block in fully awake persons," *Anesthesia & Analgesia*, Vol. 97, no. 2, pp. 488–491, 2003.

44. Jameson, L. C., and T. B. Sloan, "Using eeg to monitor anesthesia drug effects during surgery," *Journal of clinical monitoring and computing*, Vol. 20, no. 6, pp. 445–472, 2006.

45. Schwartz, R. S., E. N. Brown, R. Lydic, and N. D. Schiff, "General anesthesia, sleep, and coma," *New England Journal of Medicine*, Vol. 363, no. 27, pp. 2638–2650, 2010.

46. Voss, L., and J. Sleigh, "Monitoring consciousness: the current status of eeg-based depth of anaesthesia monitors," *Best Practice & Research Clinical Anaesthesiology*, Vol. 21, no. 3, pp. 313–325, 2007.

47. Franks, N., "General anaesthesia: from molecular targets to neuronal pathways of sleep and arousal," *Nature Reviews Neuroscience*, Vol. 9, no. 5, pp. 370–386, 2008.

48. Steriade, M., "Grouping of brain rhythms in corticothalamic systems," *Neuroscience*, Vol. 137, no. 4, pp. 1087–1106, 2006.

49. Steriade, M., A. Nunez, and F. Amzica, "The slow (< 1 hz) oscillation in reticular thalamic and thalamocortical neurons: scenario of sleep rhythm generation in interacting thalamic and neocortical networks," *The Journal of Neuroscience*, Vol. 13, no. 8, pp. 3284–3299, 1993.

50. Steriade, M., F. Amzica, and D. Contreras, "Synchronization of fast (30-40 hz) spontaneous cortical rhythms during brain activation," *The Journal of Neuroscience*, Vol. 16, no. 1, pp. 392–417, 1996.

51. Fell, J., H. Elfadil, J. Roschke, W. Bur, P. Klaver, C. Elger, and G. Fernandez, "Brief communication human scalp recorded sigma activity is modulated by slow eeg oscillations during deep sleep," *International Journal of Neuroscience*, Vol. 112, no. 7, pp. 893–900, 2002.

52. Molle, M., L. Marshall, S. Gais, and J. Born, "Grouping of spindle activity during slow oscillations in human non-rapid eye movement sleep," *The Journal of Neuroscience*, Vol. 22, no. 24, pp. 10941–10947, 2002.

53. Molaee-Ardekani, B., M. B. Shamsollahi, O. Tirel, B. Vosoughi-Vahdat, E. Wodey, and L. Senhadji, "Investigation of the modulation between eeg alpha waves and slow/fast delta waves in children in different depths of desflurane anesthesia," *Irbm*, Vol. 31, no. 1, pp. 55–56, 2010.

54. Benoit, O., A. Daurat, and J. Prado, "Slow (0.7-2 hz) and fast (2-4hz) delta components are differently correlated to theta, alpha and beta frequency bands during nrem sleep," *Clinical Neurophysiology*, Vol. 111, no. 12, pp. 2103–2106, 2000.

55. Sanei, S., and J. A. Chambers, *EEG signal processing*, John Wiley & Sons, 2008.

56. Addison, P. S., *The Illustrated Wavelet Transform Handbook: Introductory Theory and Applications in Science, Engineering, Medicine, and Financel*, Bristol, UK: Institute of Physics Publishing, 2002.

57. Vetterli, M., and J. Kovacevic, *Wavelets and subband coding*, New Jersey USA: Prentice Hall PTR Englewood Cliffs, 1995.

58. Kingsbury, N., "Complex wavelets for shift invariant analysis and filtering of signals," *Applied and computational harmonic analysis*, Vol. 10, no. 3, pp. 234–253, 2001.

59. Sun, Z., and C. Chang, "Structural damage assessment based on wavelet packet transform," *Journal of structural engineering*, Vol. 128, no. 10, pp. 1354–1361, 2002.

60. Nason, G. P., and B. W. Silverman, *Wavelets and statistics: The stationary wavelet transform and some statistical applications*, Springer, 1995.

61. Teolis, A., *Computational signal processing with wavelets*, Springer, 1998.

62. Akin, M., "Comparison of wavelet transform and FFT methods in the analysis of EEG signals," *Journal of Medical Systems*, Vol. 26, no. 3, pp. 241–247, 2002.

63. Shannon, C. E., "A mathematical theory of communication," *ACM SIGMOBILE Mobile Computing and Communications Review*, Vol. 5, no. 1, pp. 3–55, 2001.

64. Gibbons, J. D., and S. Chakraborti, *Nonparametric statistical inference*, Springer, 2011.

65. Blanco, S., A. Figliola, R. Q. Quiroga, O. Rosso, and E. Serrano, "Time-frequency analysis of electroencephalogram series. III. wavelet packets and information cost function," *Physical Review E*, Vol. 57, no. 1, p. 932, 1998.

66. Young, C. K., and J. J. Eggermont, "Coupling of mesoscopic brain oscillations: recent advances in analytical and theoretical perspectives," *Progress in neurobiology*, Vol. 89, no. 1, pp. 61–78, 2009.

67. Bojak, I., and D. Liley, "Modeling the effects of anesthesia on the electroencephalogram," *Physical Review E*, Vol. 71, no. 4, p. 041902, 2005.

68. Foster, B. L., I. Bojak, and D. T. Liley, "Population based models of cortical drug response: insights from anaesthesia," *Cognitive neurodynamics*, Vol. 2, no. 4, pp. 283–296, 2008.

69. Steyn-Ross, M. L., D. A. Steyn-Ross, and J. W. Sleigh, "Modelling general anaesthesia as a first-order phase transition in the cortex," *Progress in biophysics and molecular biology*, Vol. 85, no. 2, pp. 369–385, 2004.

70. Molaee-Ardekani, B., L. Senhadji, M. B. Shamsollahi, B. Vosoughi-Vahdat, and E. Wodey, "Brain activity modeling in general anesthesia: enhancing local mean-field models using a slow adaptive firing rate," *Physical Review E*, Vol. 76, no. 4, p. 041911, 2007.

71. Wilson, M. T., M. Barry, J. N. J. Reynolds, E. J. W. Hutchison, and D. A. Steyn-Ros, "Characteristics of temporal fluctuations in the hyperpolarized state of the cortical slow oscillation," *Physical Review E*, Vol. 77, no. 6 pt 1, p. 061908, 2008.

72. Hutt, A., and A. Longtin, "Effects of the anesthetic agent propofol on neural populations," *Cognitive neurodynamics*, Vol. 4, no. 1, pp. 37–59, 2010.

73. Blanco, S., R. Q. Quiroga, O. Rosso, and S. Kochen, "Time-frequency analysis of electroencephalogram series," *Physical Review E*, Vol. 51, no. 3, p. 2624, 1995.